NASA CR135136
R76AEG597

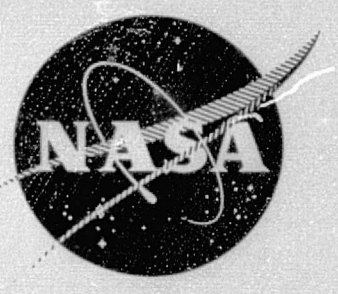

STUDY OF UNCONVENTIONAL AIRCRAFT ENGINES DESIGNED FOR LOW ENERGY CONSUMPTION

by

R. E. Neitzel
R. Hirschkron
R. P. Johnston

GENERAL ELECTRIC COMPANY

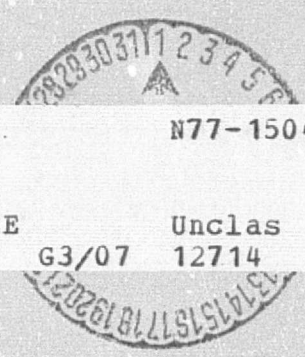

Prepared For

National Aeronautics and Space Administration

NASA Lewis Research Center

NAS3-19519

1. Report No.	2. Government Accession No.	3. Recipient's Catalog No.
NASA CR135136		

4. Title and Subtitle	5. Report Date
STUDY OF UNCONVENTIONAL AIRCRAFT ENGINES DESIGNED FOR LOW ENERGY CONSUMPTION	December, 1976
	6. Performing Organization Code
7. Author(s)	8. Performing Organization Report No.
R.E. Neitzel, R. Hirschkron, and R.P. Johnston	R76AEG597
	10. Work Unit No.
9. Performing Organization Name and Address	11. Contract or Grant No.
General Electric Company Aircraft Engine Group Cincinnati, Ohio 45215	NAS3-19519
	13. Type of Report and Period Covered
12. Sponsoring Agency Name and Address	Contractor Report
National Aeronautics and Space Administration Washington, D.C. 20546	14. Sponsoring Agency Code

15. Supplementary Notes

Project Manager, Gerald Knip, Wind Tunnel and Flight Division
NASA Lewis Research Center, Cleveland, Ohio 44135

16. Abstract

A study of unconventional engine cycle concepts, which may offer significantly lower energy consumption than conventional subsonic transport turbofans, is described herein. In Task I of the study a number of unconventional engine concepts were identified and parametrically studied to determine their relative fuel-saving potential. Based on results from these studies, regenerative, geared, and variable-boost turbofans, and combinations thereof, were selected along with advanced turboprop cycles for further evaluation and refinement in Task II. Preliminary aerodynamic and mechanical designs of these unconventional engine configurations were conducted and mission performance was compared to a conventional, direct-drive turbofan reference engine. In Task III consideration was given to the unconventional concepts, and their state-of-readiness for application, and areas of needed technology advancement were identified.

17. Key Words (Suggested by Author(s))	18. Distribution Statement
Unconventional Engine Cycles Subsonic Transports Improved Fuel Consumption Advanced Technolgoy	Unclassified - Unlimited

19. Security Classif. (of this report)	20. Security Classif. (of this page)	21. No. of Pages	22. Price*
UNCLASSIFIED	UNCLASSIFIED	154	

* For sale by the National Technical Information Service, Springfield, Virginia 22151

TABLE OF CONTENTS

TABLE OF CONTENTS (Concluded)

LIST OF ILLUSTRATIONS

LIST OF ILLUSTRATIONS (Continued)

LIST OF ILLUSTRATIONS (Concluded)

LIST OF TABLES

LIST OF TABLES (Continued)

LIST OF TABLES (Continued)

LIST OF TABLES (Concluded)

SECTION 1.0

SUMMARY

The overall objective of this study was to identify and evaluate unconventional designs with the potential for reducing energy consumption of subsonic transport engines and assist, thereby, in selecting the direction of future technology development.

Task I of this study involved the selection of promising engine concepts and evaluating them on a parametric basis. The systems considered were:

- Heat-exchanger cycles
  - Regeneration, postturbine and interturbine
  - Intercooling, with and without regeneration
  - Reheat combined with regeneration
- Novel engine arrangements
  - Geared turbofans, various arrangements
  - High bypass turbofans, fixed and variable pitch
  - Variable-boost concept, high cycle pressure ratio at cruise but not at takeoff.
- Turboprops
  - High disc-loading propellers
  - Shrouded propeller

The approach taken was to conduct preliminary cycle-variation studies for each concept in order to select reasonable design cases for evaluating the potential improvement in energy consumption and possible impact upon aircraft economics. These evaluations were conducted by estimating changes in the major engine characteristics (sfc, weight, price, and maintenance costs), on an installed basis, relative to an advanced-technology turbofan of conventional arrangement. The effect of these changes on the fuel usage and direct operating cost of an advanced-technology, 0.8 Mach number transport were then determined.

As a result of the Task I evaluation, the engines shown below were selected for more detailed analysis and evaluation during Task II. The cycle data are for the 10,670 m (35,000 ft), Mach 0.8, maximum climb point except as noted.

- **Baseline Direct-Drive Turbofan**
  - Bypass ratio = 7
  - Fan pressure ratio = 1.71
  - Turbine temperature = 1375° C (2500° F)
  - Cycle pressure ratio = 38
  - Sea level standard takeoff T_{41} = 1430° C (2600° F)

- **Regenerative Turbofan**
  - Bypass ratio = 7
  - Fan pressure ratio = 1.55
  - Direct drive
  - Turbine temperature = 1485° C (2700° F)
  - Cycle pressure ratio = 32
  - Interturbine rotary regenerator
  - Sea level standard takeoff T_{41} = 1540° C (2800° F)

- **Geared Turbofan**
  - Bypass ratio = 10
  - Fan pressure ratio = 1.55
  - Baseline core design and cycle parameters

- **Geared Variable-Boost Turbofan**
  - Same as above except cycle pressure ratio = 45.5

- **Advanced Turboprop**
  - Bypass ratio >100
  - Fan pressure ratio = 1.03
  - Disc loading = 289,000 W/m^2 (36 hp/ft^2)
  - Baseline core design and cycle parameters

- **Variable-Boost Turboprop**
  - Same as above except cycle pressure ratio = 45.5

The baseline reference design used in this study was a direct-drive turbofan (bypass ratio = 7) selected as a result of previous studies of advanced technology engines under NASA contract NAS3-19201 (Reference 1). Except for the regenerative turbofan, core designs were the same for all engines; technology levels of other components were made consistent with what would be available, with appropriate development, for introduction of the engine into service in 1985.

A brief summary of conclusions resulting from this study is presented below.

1. Regeneration and other cycles involving heat exchangers did not show a payoff. Except for an interturbine location of the regenerator, the physical size of the heat exchanger for the cases

considered was large enough to degrade installed sfc (nacelle drag included) relative to the conventional reference turbofan. For the interturbine location of the regenerator, an advantage in installed sfc of 8% over the conventional turbofan and 3% over the geared turbofan was estimated; however, the installed weight was 80% higher than the conventional turbofan and no fuel-usage advantage was achieved.

2. Geared turbofans showed a 5% improvement in installed sfc and fuel usage when compared to the direct-drive reference turbofan with similar technology. A lower fan pressure ratio (1.55) and higher bypass ratio (10:1) combination was selected relative to that preferred for the direct-drive turbofan. This selection was based on a systems study of fuel usage and direct operating cost (DOC) trends for variations in fan pressure ratio. A small improvement in DOC (1/2%) was also estimated, the improvement in sfc having a somewhat greater effect than the installed weight and cost penalties of the higher bypass, geared turbofan. The improvement in fuel usage requires that further consideration be given to the geared turbofan.

3. Advanced, 0.8 Mach number turboprop engines, based on projected improvements in propeller efficiency (the 80% range) for high disc-loading designs, indicated the potential for a 13% improvement in installed sfc compared to the conventional reference turbofan and 8% over the geared turbofan. Although a 45% increase in propulsion system weight was estimated for the turboprop installation, the improvement in fuel usage was 15% over the direct-drive turbofan and 10% over the geared turbofan for a four-engine transcontinental aircraft.

   An improvement in DOC of 4% was calculated based on input received for propeller first cost and maintenance costs. This improvement is subject to uncertainties, however, and is particularly dependent upon the achievement of high efficiencies for a practical propeller design installed in an 0.8 Mach number aircraft without significant interference penalties. In any event, the potential improvement in fuel usage was large enough to warrent further consideration of advanced turboprops as an alternative to turbofan engines.

4. The variable-boost concept involved designing for a higher cycle pressure ratio (than would have been selected otherwise) at altitude cruise and desupercharging the core at takeoff to avoid the problem of designing mechanically for high pressures and temperatures at the compressor discharge. For the geared fan, an improvement in sfc of slightly over 1%, without a penalty in weight or cost relative to the nonvariable-boost geared cycle, was estimated when sized for constant cruise thrust. However, a 12% lower takeoff thrust was predicted for an engine sized at cruise, which means the concept would be advantageous only for applications where

cruise, rather than takeoff, establishes the engine size. Similar results would be obtained for the variable- versus nonvariable-boost turboprop. The concept appears appropriate for the higher bypass, geared turbofan and the turboprop (which have more takeoff thrust, relative to cruise, than the conventional reference turbofan engine).

Task III of this study involved recommendations of needed technology development for the three promising engine concepts identified in this study: the direct-drive, conventional turbofan used as reference (also presented in Reference 1), the geared turbofan, and the turboprop. Core technology, including variable-boost versions of these engines, can be common to all three and may therefore go ahead independent of the final selection of engine type. Except for the fan and low pressure turbine, turbofan engine and installation technology is applicable to both direct-drive and geared designs. The turboprop requires some major steps in technology, the basic propeller efficiency levels for practical 0.8 Mach number flight requiring initial attention.

SECTION 2.0

INTRODUCTION

As a result of the energy crisis in early 1973, ongoing studies of advanced subsonic transport turbofans within the General Electric Company were redirected to put major emphasis on reduced energy consumption. In addition, NASA contracted a program entitled "Study of Turbofan Engines Designed for Low Energy Consumption." The General Electric study was given the acronym STEDLEC and was completed in mid-1975 and reported upon in References 1 and 2; design and technology features with the potential for reducing fuel usage were identified and evaluated. The CF6 family of engines and all-new advanced engines, consistent with 1985 introduction into service, were considered. Emphasis was placed on achieving an improvement in aircraft economics, as well as fuel usage, in evaluating the results.

Based on cycle studies and the considerations given to payoff and risks of various advanced-technology features studied in STEDLEC, a specific advanced engine and nacelle were selected and carried through a preliminary design. The goals for this design were to obtain an improvement in installed sfc of 10% over a modern, high bypass engine now in production: the CF6-50C. In addition, goals were established of a 20% improvement in installed weight over a scaled CF6-50C, equivalent engine production cost, an improvement in maintenance costs, and compatibility with environmental requirements. The engine was designed to meet these goals, and the technology advances necessary to do so were identified as part of the STEDLEC contract effort.

The current study, described herein, was initiated in early 1975 to explore alternatives to the conventional turbofan for potential use in subsonic transports in the mid-1980's. This contract, entitled "Study of Unconventional Aircraft Engines Designed for Low Energy Consumption," was called U-STEDLEC, or SUAEDLEC, to distinguish it from the initial STEDLEC contract. The study was initiated primarily to explore the potential of regeneration and other novel cycles but was expanded to include unconventional engine arrangements such as geared turbofans. Projected improvements in propeller efficiency for a Mach 0.8 application indicated the turboprop to be a potential low sfc engine for subsonic transports; therefore, it was considered in the study. Hamilton Standard supplied, on a subcontract basis, the necessary data on the propeller, gearset, and associated systems for the turboprop. A description of the advanced propeller design concepts is presented in an AIAA paper by Rohrbach and Metzger (Reference 3).

To provide maximum continuity, the advanced technology turbofan identified in STEDLEC was used as a baseline from which U-STEDLEC engines were compared for fuel usage and economics. Evaluation procedures, except changes necessary for the turboprop evaluation, were kept the same. Technology utilized in the U-STEDLEC designs was made consistent with the baseline turbofan except for those items unique to the specific case under consideration.

SECTION 3.0

TASK I PARAMETRIC ANALYSIS

3.1 APPROACH

Various engine concepts have been proposed to improve fuel consumption beyond the reductions projected for an advanced, high bypass turbofan engine as studied under the STEDLEC program. The unconventional concepts considered in this study were drawn from suggestions and ideas from NASA, within General Electric, and other sources. After initial screening, several concepts were selected and grouped in broad categories for study:

- Heat-exchanger engines
- Unconventional arrangements
- Turboprops

In order to select specific cases for evaluation, limited parametric cycle studies were conducted to establish bare-engine sfc levels. Aerodynamic flowpath layouts were made of the more promising cases for the purpose of refining component-performance levels. Where the bare-engine sfc showed enough potential to warrant further consideration, installation layouts were made to define installed drag penalties. Weight, price, and maintenance data were then prepared for each of the promising concepts and a preliminary engine economic evaluation was conducted. Finally, the economic results were compared to the advanced conventional reference turbofan, in a commercial transport mission, to establish merit factors. Direct operating cost and fuel consumed were considered to be the primary figures of merit. Since the DOC includes fuel consumed as well as weight and price effects, it was used as a reference for configurations which showed reduced fuel consumption.

As a result of the Task I parametric analysis, several specific engines were selected for refined evaluation in Task II. It should be pointed out that some of the quantitative results obtained in the Task II studies differ from those presented in this section.

3.2 EVALUATION PROCEDURE: TURBOFANS

The procedure used in this evaluation consisted of establishing baseline-aircraft designs for transcontinental and intercontinental missions. These aircraft designs were identical to those developed for the "Study of Turbofan Engines Designed for Low Energy Consumption" (STEDLEC, Reference 1). They were based on structural and aerodynamic ground rules from the study reported in Reference 4. Key features of these aircraft designs are presented in

Table I; the evaluation procedure is outlined in Table II. Engine designs were carried out in a convenient size and then scaled to the mission by the scaling exponents tabulated; no corrections were made to installed sfc for size.

First, mission trade factors were determined for specified changes in each of the propulsion system characteristics. These mission trade factors, derived for the part-range/part-load average mission, are given in Table III. Prices and maintenance costs were kept at 1974 levels, without escalation, in order to keep the same base and comparable prices to the STEDLEC study initiated in 1974. In assessing the maintenance cost of an engine, the replacement rates and price of the major components were individually estimated and then totaled.

Second, changes in the propulsion system installed sfc, installed weight, price, and maintenance cost (relative to the baseline engine) were estimated for the propulsion system under consideration.

3.3 BASELINE ENGINE AND INSTALLATION

The baseline engine and installation used in this study is the advanced turbofan design developed as the result of optimization studies conducted during Task III of STEDLEC (Reference 1). A cross section of that engine is shown in Figure 1, and the mixed-flow installation is shown in Figure 2. The key design features of this engine are given in Tables IV and V. The engine is a direct-drive turbofan (bypass ratio = 7) with a cycle pressure ratio of 38:1 at maximum climb (altitude) and a turbine rotor inlet temperature of 1370° C (2500° F) at maximum climb and 1430° C (2600° F) at takeoff. Additional cycle data are presented in Table VI for the baseline engine.

The high pressure spool of the baseline engine is used in all the unconventional engines studied with the exception of the heat-exchanger cycles. Although different fans and low pressure turbines are specified for various unconventional engines, they are designed to a technology level consistent with the baseline engine. The mixed-flow installation is used for the turbofans with two exceptions: the variable-pitch fan and one heat-exchanger engine. These particular cycles used a separate-flow installation with structural and aerodynamic technology consistent with the baseline engine.

3.4 HEAT-EXCHANGER CYCLES

One group of concepts suggested for study was heat-exchange cycles. The basic intent of these concepts was to improve the overall thermal efficiency of the basic Brayton cycle. The following major cycle modifications were studied:

- Regeneration: Improved thermal efficiency of cycle by recovery of exhaust heat for reintroduction into combustor.

Table I. Baseline-Aircraft Characteristics.

Parameter	Transcontinental Trijet	Intercontinental Quadjet
Design Range km (nmi)	5,560 (3,000)	10,190 (5,500)
Design Payload, PAX	200	200
Cruise Altitude, m (ft)	10,670 (35,000)	10,670 (35,000)
Cruise Mach No.	0.80	0.80
TOGW kg (lbm)	101,200 (223,000)	145,100 (320,000)
SLS Takeoff F_n, N (lbf)	88,960 (20,000)	93,410 (21,000)
Wing Aspect Ratio	12	12
Average Cruise C_L	0.50	0.55
Average Cruise L/D	17	18

Table II. Evaluation Procedure.

- Constant Design Payload and Range, Variable Design Gross Weight
- Baseline Aircraft: 5560 km (3000 nmi), 200 PAX Trijet
  10,190 km (5500 nmi), 200 PAX Quadjet
- Baseline Engine: Direct-Drive Turbofan, 1.70 Pressure Ratio Fan, Mixed Flow with Advanced Technology
- Effects of Changes in Installed Engine Characteristics Determined for Each Variation Studied
- Effects of Engine Price Related to Production Cost in 1974 $
- Individual Part Replacement Rates Considered for Engine Maintenance Costs
- Engines Scaled to Thrust Required by Baseline Aircraft
  - Engine Scaling Exponents: Weight, 1.25; Price, 0.55
  - Installation Scaling Exponents: Weight, 1.10; Price, 0.80

Table III. Turbofan Mission Trade Factors, Average Mission.

Aircraft	Trijet		Quadjet	
Range, km (nmi)	1300 (700)		3700 (2000)	
Load Factor, %	55		55	
Fuel Cost $/m^3 (¢/gal)	79.2 (30)		118.9 (45)	
Change (per engine)	Δ DOC, %	Δ W_f, %	Δ DOC, %	Δ W_f, %
1% sfc	+0.39	+1.09	+0.71	+1.44
45.4 kg (100 lbm) Engine or Installation	+0.17	+0.26	+0.22	+0.31
$10,000 Engine Initial Price	+0.073	-	+0.060	-
$10,000 Engine Parts Price	+0.070	-	+0.065	-
$10,000 Installation Price	+0.073	-	+0.060	-
$1.0 Maintenance Cost/Flight-hr	+0.23	-	+0.24	-
$0.1 Maintenance Man-hr/Flight-hr	+0.50	-	+0.52	-

• 10,670 m (35,000 ft), Mach 0.8, +10° C (+18° F), Max. Climb

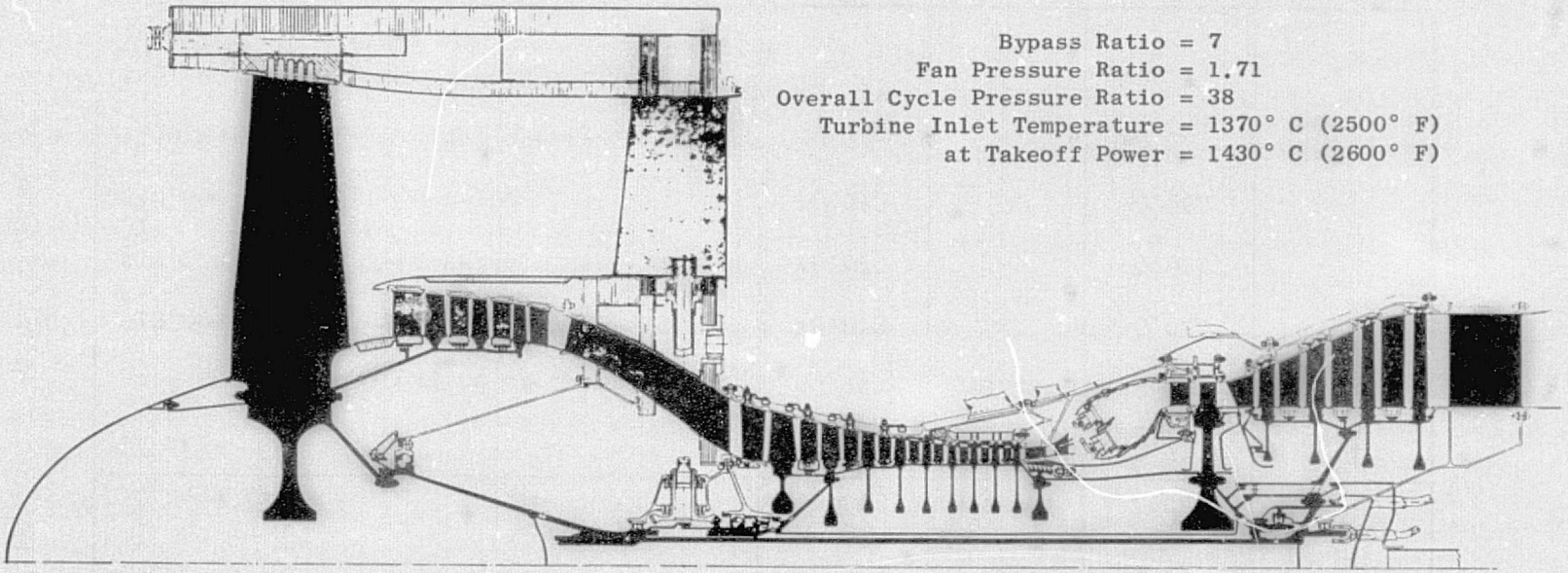

Bypass Ratio = 7
Fan Pressure Ratio = 1.71
Overall Cycle Pressure Ratio = 38
Turbine Inlet Temperature = 1370° C (2500° F)
at Takeoff Power = 1430° C (2600° F)

Figure 1. Baseline Engine.

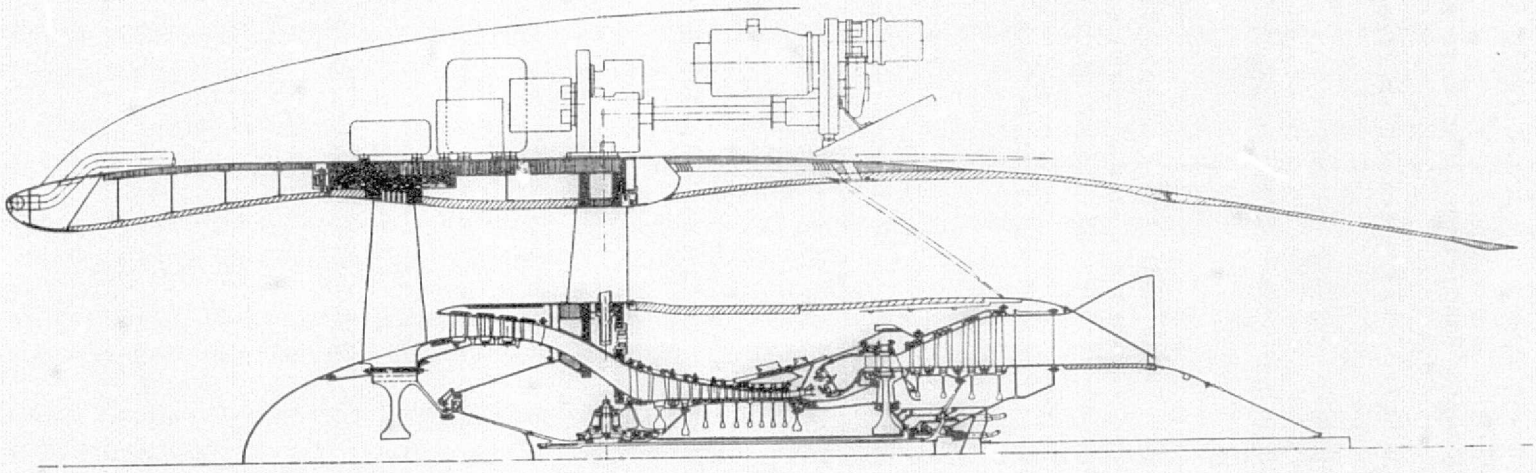

Figure 2. Advanced, Subsonic, Baseline-Turbofan Installation.

Table IV. Baseline-Turbofan, Advanced-Design Features.

Fan	Composite Blades High Tip Speed 494 m/sec (1620 ft/sec), 1.7 Pressure Ratio Composite Vane/Frame, Fan Case and Containment
Core Compressor	High $U_T/\sqrt{\theta}$, 523 m/sec (1715 ft/sec); 14:1 in 9 Stages Clearance Control Casing
Combustor	Double Dome for Low Emissions
High Pressure Turbine	Single Stage with 4:1 Pressure Ratio Active Clearance Control Features Advanced Ni-Base DS Blades with Film Impingement Cooling Ceramic Shrouds and Nozzle Bands
Low Pressure Turbine	High Aerodynamic Loading Advanced Ni-Base DS Blades - Stage 1 Cooled High Aspect Ratio and Increased Spacing on Rear Stages - Turbine Noise Reduction

Table V. Advanced Baseline-Turbofan Installation Design Features.

- Long Duct, Mixed Flow
- Composite Construction - Integrated with Fan Frame and Case
- High $D_{HL}/D_{Max.}$ Inlet and Pylon-Mounted Accessories
- Fan Stream Cascade-Type Reverser
- Bulk Absorber Inlet and Phased Fan Exhaust Treatment

Table VI. Baseline-Engine Cycle Definition.

Takeoff, Hot Day	Baseline Advanced Turbofan Trijet Mission Size
F_n, N (lbf)	88,975 (20,000)
T_{41} Turbine Rotor Inlet (Avg Cycle)	1427° C (2600° F)
10,670 m (35,000 ft), Mach 0.8: Aerodynamic Design Point	
Max. Climb F_n, N (lbf)	23,430 (5,265)
$W\sqrt{\theta}/\delta$, kg/sec (lbm/sec)	340 (755)
Fan Pressure Ratio	1.71
Booster Pressure Ratio (including Fan Hub)	2.75
Core Compression Ratio	14.0
Bypass Ratio	6.9
Overall Pressure Ratio	38
T_{41}, Turbine Rotor Inlet	1371° C (2500° F)
HPT Pressure Ratio	3.82
HPT Loading Parameter, $\overline{\psi}_p$	0.87
LPT Pressure Ratio	5.7
LPT Loading Parameter, $\overline{\psi}_p$	1.63
Mixing Effectiveness	0.75%

- Intercooling: Improved thermal efficiency by reducing work of Compression.

- Reheat: Improved specific output of the cycle by providing increased temperature at the low pressure turbine inlet.

- Turbine Air Cooling: Reduction of turbine cooling air temperature, thereby reducing quantity required.

Schematic representations of these cycles are presented in Figures 3 and 4. Parametric studies of these cycles, as well as combinations thereof, were conducted and a summary of results is presented in Table VII. Detailed discussion of each category follows.

3.4.1 Postturbine Regenerator

The postturbine regenerator extracts heat from the LP turbine discharge, via a heat exchanger, and returns it to the cycle ahead of the combustor reducing, thereby, the fuel required to reach a given turbine inlet temperature. Two types of heat exchangers were considered for use in this study: a fixed shell and tube type, and a rotary ceramic type. General arrangements of these heat exchangers are presented in Figures 5 and 6.

Parametric studies were conducted over a range of cycle pressure ratios and values of regenerator effectiveness for both fixed and rotary heat-exchanger types. Over a range of cycle pressure ratios (from 10 to 38), the bypass ratio varied from 6.5 to 7.7. Typical sfc and specific thrust trends are presented in Figure 7 for a fan pressure ratio of 1.65 (at max. climb) and a turbine inlet temperature of 1468° C (2675° F); the corresponding takeoff T_{41} = 1540° C (2800° F). These levels of turbine rotor inlet temperatures were selected based on previous in-house studies.

Based on a simple model, the benefit due to regeneration increases with the amount of heat recovered from LP turbine exhaust to compressor discharge. For a given turbine inlet temperature, the exhaust temperature increases with decreasing cycle pressure ratio, raising the heat-exchange potential but degrading the thermal efficiency of the basic cycle. The cycle pressure ratio for minimum sfc occurs at a balance point between these opposing trends at a pressure ratio lower than the unregenerated base cycle. Increasing heat-exchanger effectiveness tends to move this point to lower cycle pressure ratios, as seen in Figure 7. The reductions in specific thrust with increasing regenerator effectiveness result from the lower primary exhaust temperature.

Regenerator effectiveness values of 0.7 and 0.9, for the fixed and rotary respectively, were chosen as the maximum practical. The benefit of the high rotary effectiveness was in part offset by the leakage and carryover losses associated with this system. The leakage was past the regenerator seals, from the compressor discharge to the exhaust. The carryover was the

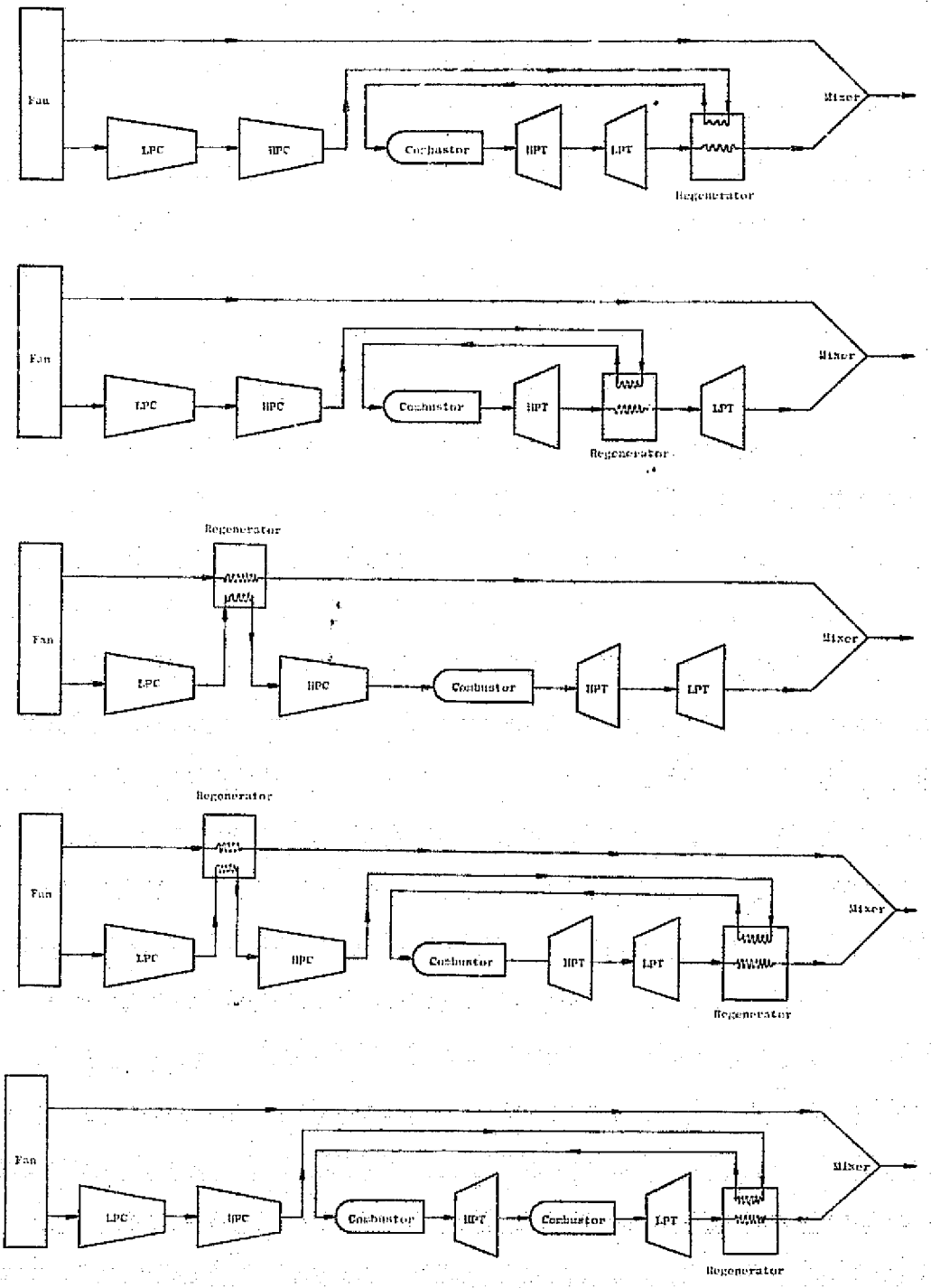

Figure 3. Heat Exchanger Cycles.

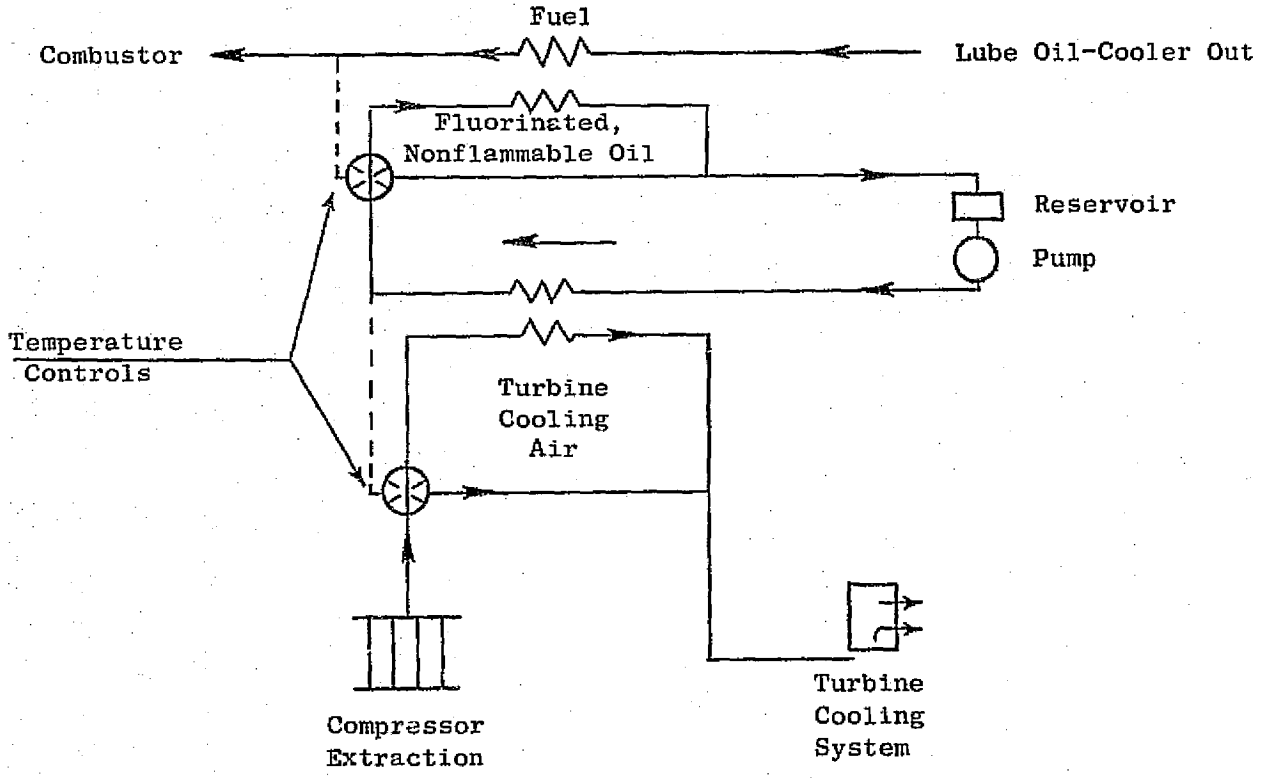

Figure 4. Turbine Cooling-Air Cooling Schematic.

Table VII. Summary of Regenerator Concepts Studied.

- 10,670 m (35,000 ft), Mach 0.8, +10° C (+18° F), Max. Climb

Concept	Range of Variables				Best Results Versus Advanced Turbofan (at same fan pressure ratio)			
	°C T_4 (°F)	Cycle Pressure Ratio	Fan Pressure Ratio	ϵ*	Δ%sfc	Δ%sfc$_I$	$\Delta F_n/W_2$	Comments
Postturbine Regenerator Shell and Tube	1430-1650 (2600-3000)	10-38	1.55-1.8	0.5-0.8	-4.0	+10	-2	• Large Drag and Weight Increases Offset Bare Engine sfc Reductions for Realistic Regenerators
Rotary	1430-1650 (2600-3000)	10-38	1.55-1.8	0.5-0.9	-4.0	+4	-2	
Intercooler Shell and Tube	1357-1579 (2475-2875)	25-70	1.55-1.8	0.5-1.0	-4.5		-10	• Benefit can be Utilized only in Ultrahigh Cycle P/P. • Large Installation Diameter Increase for Fan Duct Installation.
Regenerator/Intercooler	1357-1579 (2475-2875)	10-50	1.55-1.8	0.5-1.0	-4.0		-9.7	• Large Installation Diameter Increase. • No Benefit on Installation.
Regenerator/Reheat	1357-1468 (2425-2675)	10-50	1.65	0.5-0.8	-2.0		+2	• Complexity for Small Gain. • High Temperature LPT.
Interturbine Regenerator Rotary	1357-1579 (2475-2875)	10-40	1.55-1.7	0.8-0.9	-8.8	-6.8	-21.0	• Most Promising Potential Studied in Detail.

Note: T_{41} at Takeoff = T_{41} + 69° C (+125° F)

*ϵ = Effectiveness

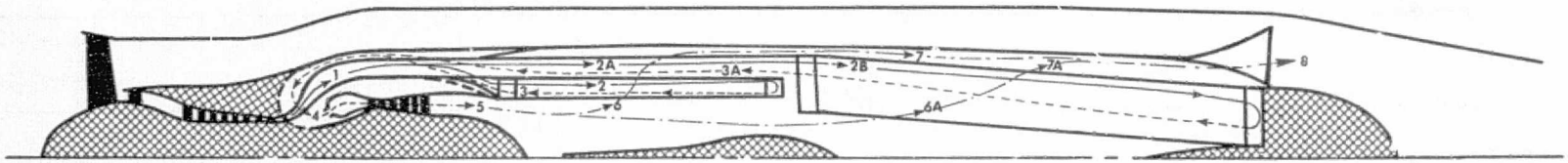

1: Compressor Discharge; Flow Splits

2: Portion of Compressor Discharge Flow Enters Forward Heat Exchanger

2A: Remainder of Compressor Discharge Flow

2B: Remainder of Compressor Discharge Flow Enters Aft Heat Exchanger

3: Compressor Discharge Flow Leaves Forward Heat Exchanger

3A: Compressor Discharge Flow Leaves Aft Heat Exchanger

4: Compressor Discharge Flow Enters Combustor, Then Turbine

5: Turbine Discharge Flow

6: Portion of Turbine Discharge Flow Enters Forward Heat Exchanger

6A: Remainder of Turbine Discharge Flow Enters Aft Heat Exchanger

7: Turbine Discharge Flow Leaves Forward Heat Exchanger

7A: Turbine Discharge Flow Leaves Aft Heat Exchanger

8: Turbine Discharge Mixes with Bypass Flow and Enters Nozzle

Figure 5. Fixed Postturbine Regenerator.

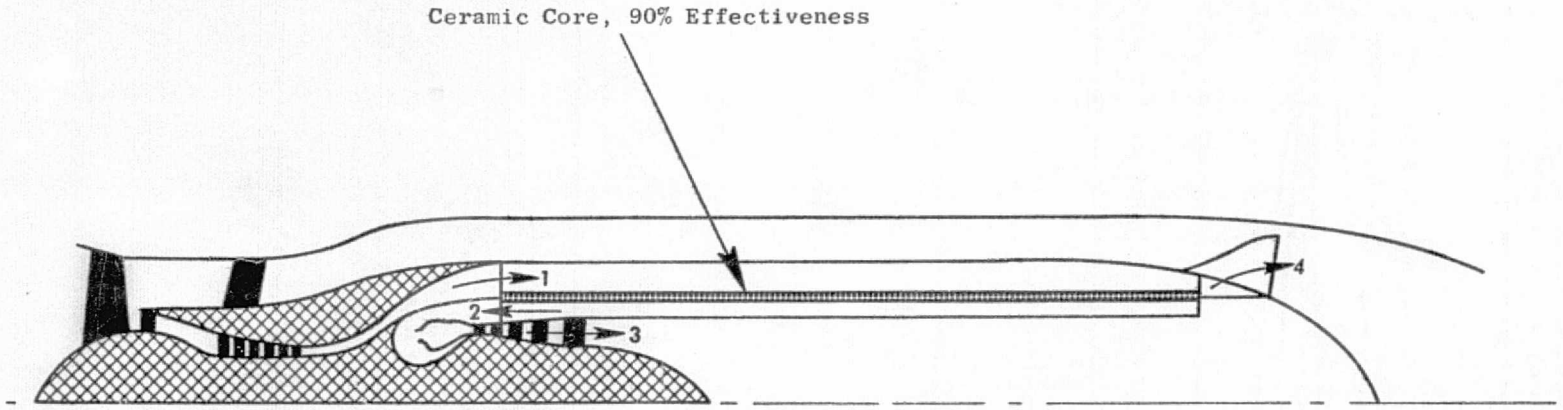

1: Compressor Discharge Enters Heat Exchanger
2: Compressor Discharge Leaves Heat Exchanger
3: Turbine Discharge Enters Heat Exchanger
4: Turbine Discharge Leaves Heat Exchanger

Figure 6. Rotary Regenerator Aft of Turbine.

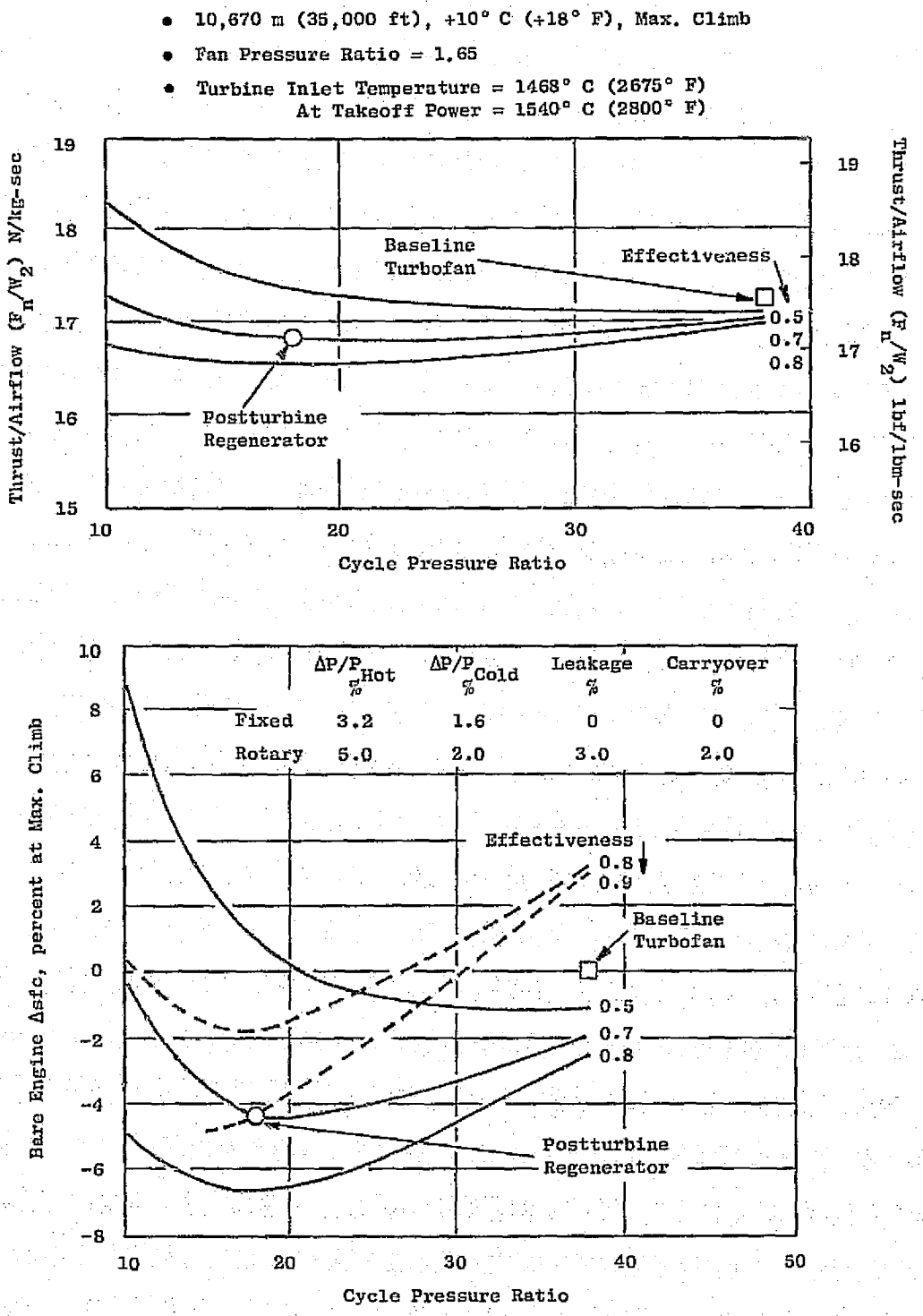

Figure 7. Postturbine Regenerator Cycle Trends.

mass of air trapped in the regenerator volume as the chambers were alternately exposed to high and low pressure supplies. For the purpose of this parametric analysis, the exact rotary configuration or hot/cold flow split was not necessary. Compared to the baseline turbofan engine, a maximum bare sfc improvement of approximately 4% was estimated for the above effectiveness levels. As shown on Figure 5 and 6, the physical size of the heat exchangers is extremely large, implying a significant installation drag. In fact, the 4% bare sfc advantage is changed to a 10 and 4% installed sfc penalty, for the fixed- and rotary-regenerator engines, respectively, due to installation drag. The results of these studies are presented in Table VIII.

Since no installed sfc benefit was achieved, study of this type of heat-exchanger cycle was not continued.

3.4.2 Interturbine Regenerator

In the interturbine regenerator, heat is removed between the HP turbine and LP turbine and returned to the engine ahead of the combustor. Relative to the postturbine regenerator, the heat is transferred from a higher temperature for a given turbine inlet temperature. The primary advantage of the cycle is that the density of the hot gas is considerably greater than in the postturbine regenerator; the increased gas density greatly reduces the size of the heat exchanger for a given heat-exchanger pressure loss. This reduction in size resulted in decreased carryover as well as reduced seal length and attendant leakage.

Parametric variations in turbine temperature, cycle pressure ratio, and effectiveness were exercised to optimize the sfc improvement. Figure 8 presents the results of this parametric study.

The sfc trend versus cycle pressure ratio is similar to that in the postturbine regenerator although minimum sfc occurs at a higher pressure ratio. Increasing turbine inlet temperature improves the sfc gain by providing a larger temperature difference between the HP turbine discharge and the compressor discharge but results in a lower specific thrust.

Two cycles, for comparative purposes, were chosen for further study: one with a design fan pressure ratio of 1.71 and the other 1.55; both having cycle pressure ratios of 32 and turbine inlet temperatures of 1540° C (2800° F). This temperature was considered a limit since it was felt that any further increases would require cooling of the regenerator ducting. The bypass ratio was adjusted to provide a core/fan exit velocity ratio of 1.2.

The interturbine regenerator configuration chosen is presented in Figure 9. The heat exchanger is a ceramic cylinder rotating about the engine axis and surrounding the core engine. The LP turbine is at a large diameter to eliminate the need for turning the hot gas inwards; it also allows a smaller number of LPT stages to be used for a given rpm. This configuration provides for a reasonably compact arrangement. Figure 10 presents a comparison of the

Table VIII. Postturbine Regenerator Results.

- 10,670 m (35,000 ft), Mach 0.8, +10° C (18° F), Max. Climb

Engine	Baseline Mixed Flow	Fixed Regenerator	Rotary Regenerator
Max. Climb T_{41}, ° C (° F)*	1370 (2500)	1370 (2500)	1370 (2500)
Max. Climb Cycle Pressure Ratio	38	18	18
Fan Pressure Ratio	1.71	1.71	1.71
Bypass Ratio	6.9	6.8	6.2
Booster Pressure Ratio	2.75	1.54	1.54
Core Pressure Ratio	14.0	11.8	11.8
Core Duct Pressure Loss, %	Base	+0.7	+0.07
Fan Duct Pressure Loss, %	Base	+1.05	+1.05
Regenerator Effectiveness	-	0.70	0.90
Cold $\Delta P/P$, %	-	3.2	2.0
Hot $\Delta P/P$, %	-	1.6	5.0
Carryover, %	-	-	3
Leakage, %	-	-	2
Bare sfc, Δ%	Base	-4	-4
F_n/W_2, Δ%	Base	+2	+2
Drag/F_n, %	4.5	+16.6	+12.4
Installed sfc, Δ%	Base	+10	+4

*T_{41} at Takeoff = T_{41} + 69° C (+125° F)

- 10,670 m (35,000 ft), Mach 0.8, +10° C (+18° F), Max. Climb
- Mixed Flow
- Fan Pressure Ratio = 1.65
- Rotary Regenerator Effectiveness = 1.90
- T_{41} at Takeoff = T_{41} + 69° C (+125° F)

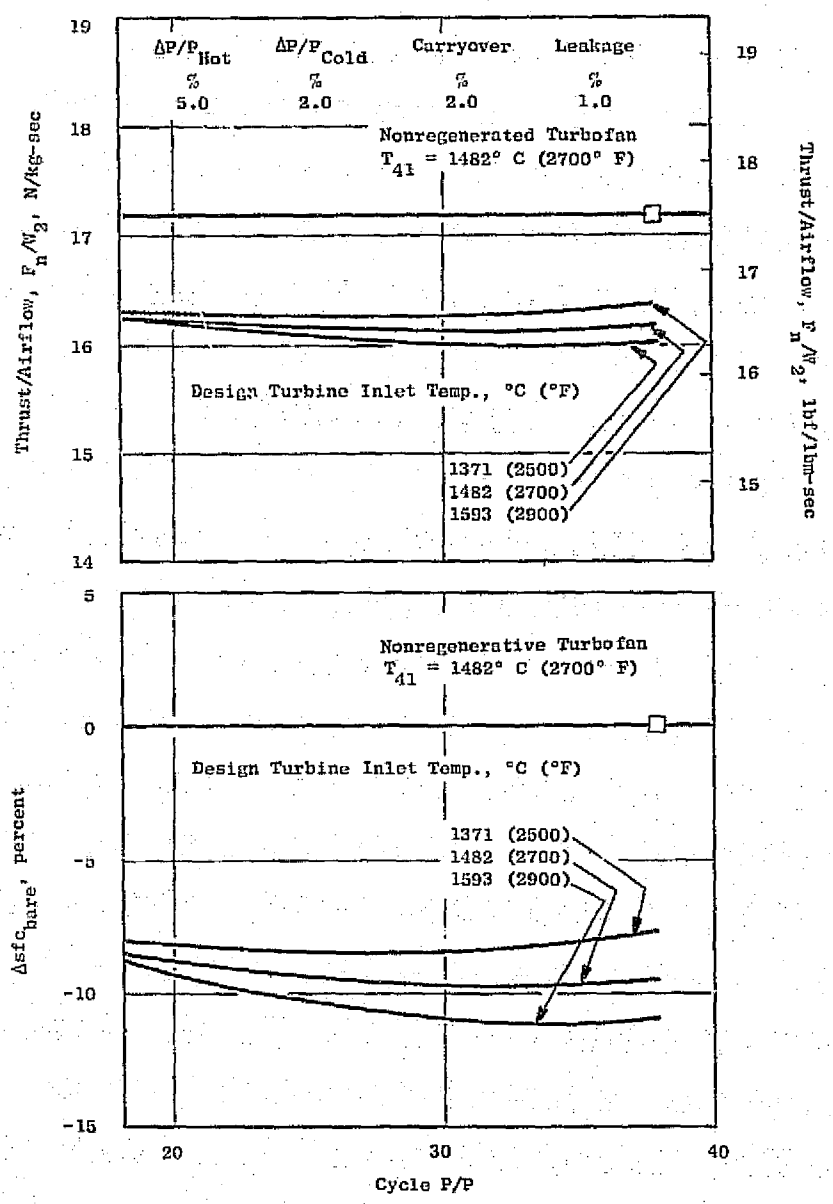

Figure 8. Interturbine Regenerator Cycle Parametric Trends.

• 10,670 m (35,000 ft), Mach 0.8, +10° C (+18° F), Max. Climb

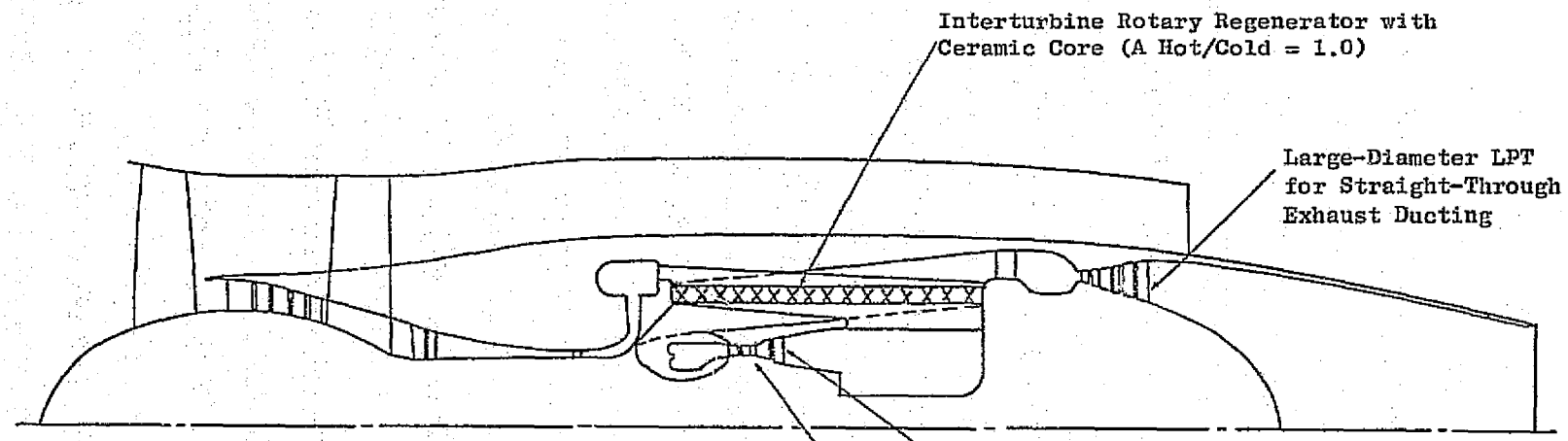

Bypass Ratio = 7
Fan Pressure Ratio = 1.55
Cycle Pressure Ratio = 32
Regenerator Efficiency = 0.9
Total Regenerator Pressure Loss = 8.4%
Turbine Inlet Temperature = 1480° C (2700° F)
at Takeoff Power = 1540° C (2800° F)

Figure 9. Interturbine Regenerative Turbofan.

- Scaled to Same Installed F_n: 20,640 N (4640 lbf)
- 10,670 m (35,000 ft), Mach 0.8, +10° C (+18° F), Max. Climb

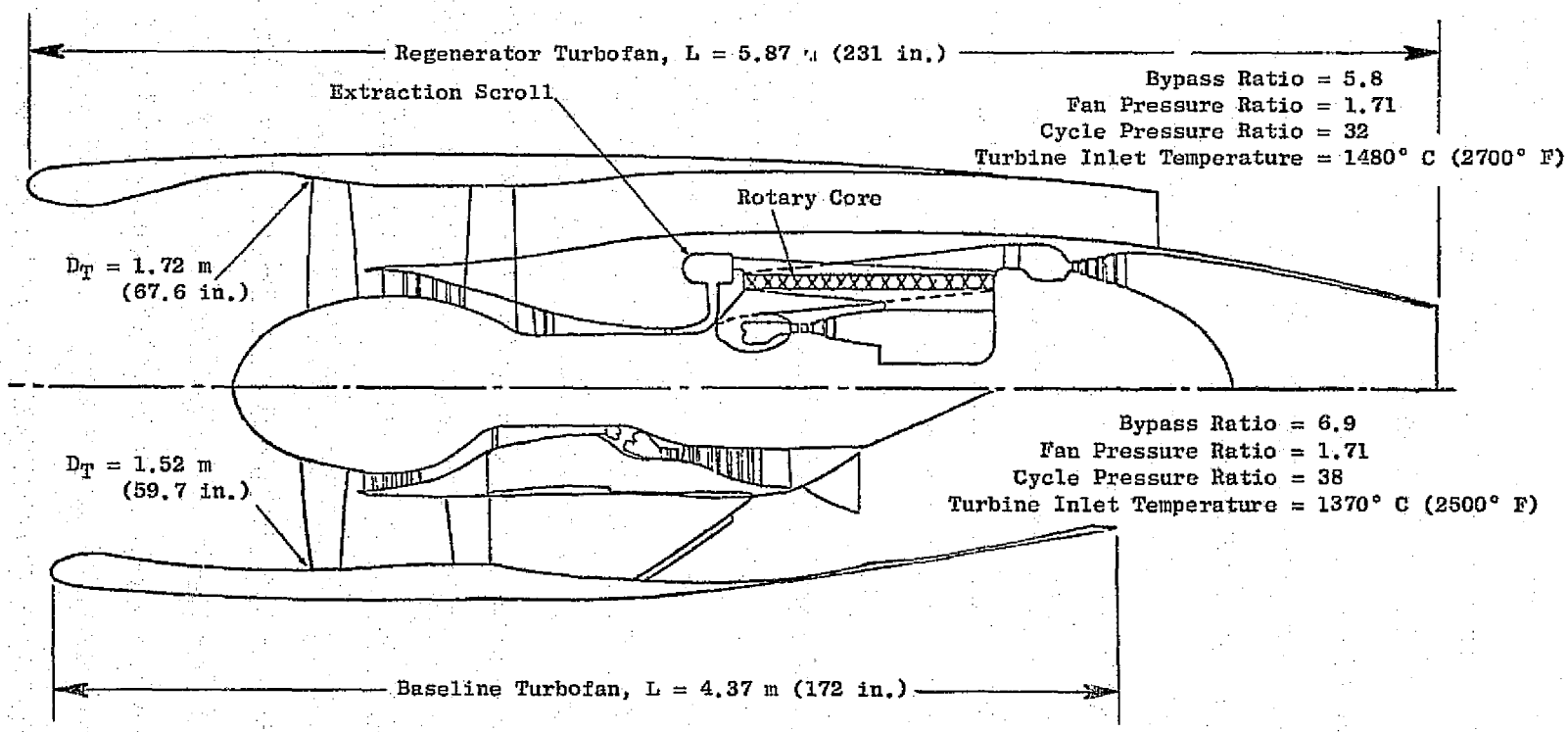

Figure 10. Interturbine Regenerator Vs. Baseline Turbofan.

interturbine regenerator scaled to the same installed thrust as the baseline reference turbofan.

Table IX presents a comparison of the interturbine-regenerator engines to the baseline reference turbofan in the mission size. The fan pressure ratio 1.71 and 1.55 cases have installed sfc improvements of 6.5% and 9.8%, respectively. In the Task II refined analysis, somewhat less improvement was estimated. An important item in this table is bypass ratio; for a fan pressure ratio of 1.71, the bypass ratio drops from 6.9 on the baseline turbofan to 5.8 on the regenerator engine as a result of the reduced LPT inlet temperature associated with cooling the HPT discharge in the regenerator. This implies a significant increase in core size and weight for a given fan size; the increased engine weight greatly reduces the fuel saving. A substantial fuel saving is indicated for the 1.55 pressure ratio cycle when compared to the 1.71 baseline, but much of this saving is a result of the improved propulsive efficiency of the lower fan pressure ratio and not thermal efficiency. The 1.55 fan pressure ratio engine was thought to be sufficiently interesting from the sfc standpoint to justify further study in Task II.

The interturbine regenerator concept was applied to a turboprop engine, but the sfc improvement, as tabulated in Table X, was reduced due to the high extraction of this cycle. This results in lower heat transfer in the exhaust compared with the turbofan; the regenerator, either interturbine or post-turbine, derives its benefit from this heat.

3.4.3 Intercooler

The objective of intercooling is to reduce the work of compression thereby making more output and energy available at the turbine. A side effect of intercooling is a reduction in compressor discharge temperature.

Parametric studies of cycles with intercoolers have shown that sfc improvements are possible only at exceptionally high pressure ratios. Since the use of an intercooler reduces the compressor discharge temperature for a given compression ratio, one barrier to engines with very high pressure ratios is removed. It does not, however, remove the mechanical design challenge of providing for very high pressures in the hot section of the engine. In addition, since the fan duct is used as the heat sink, it must increase in size; therefore, installation drag increases.

The results of typical parametric cycle studies of intercooling are presented in Figure 11. The best cycle pressure ratio for intercooling is very high, greater than 60:1 for the effectiveness levels and pressure drops chosen. At a pressure ratio of 38, the same as the baseline turbofan, there is an sfc increase due to the system pressure losses even at an effectiveness of 1.0.

Table IX. Interturbine Rotary Regenerator Results.

Engine	Baseline Turbofan	Regenerator			
Mission	Base	Trijet	Quadjet	Trijet	Quadjet
Fan P/"	1.71	1.71		1.55	
Cycle Pressure Ratio	38	32		32	
Takeoff T_{41}, ° C (° F)	1430 (2600)	1540 (2800)		1540 (2800)	
Bypass Ratio	6.9	5.8		7.0	
Installed sfc,* Δ%	Base	-6.5		-9.8	
Drag/F_n	4.9	7.0		7.3	
Δ Engine Weight, kg (lbm)	Base Base	962 (2120)	1021 (2250)	780 (1720)	826 (1820)
Δ Installed Weight, kg (lbm)	Base Base	182 (410)	197 (435)	186 (411)	197 (434)
Engine Price, Δ%	Base	48.1	40.2	48.1	40.2
Installed Price, Δ%	Base	+6.1	+5.1	+9.9	+8.2
DOC, Δ%	Base	+6.6	+5.9	+4.8	+2.7
W_f, Δ%	Base	-0.6	-0.9	-5.1	-6.8

*Max. Cruise

Table X. Regenerative Turboprop Vs. Turbofan.

- Transcontinental 5560 km (3000 nmi) Design

Engine	Turbofan		Turboprop	
Regenerator (Rotary Ceramic - Interturbine)	Without	With	Without	With
Fan/Prop Pressure Ratio	1.71	1.71	1.05	1.05
Takeoff, T_{41} - ° C (° F)	1430 (2600)	1540 (2800)	1430 (2600)	1540 (2800)
% sfc Installed 10,670 m (35,000 ft)/Mach 0.8	Base	-6.5	Base	-4.0
Cycle Pressure Ratio 10,670 m (35,000 ft)/Mach 0.8	38	32	38	32

• 10,670 m (35,000 ft), Mach 0.8

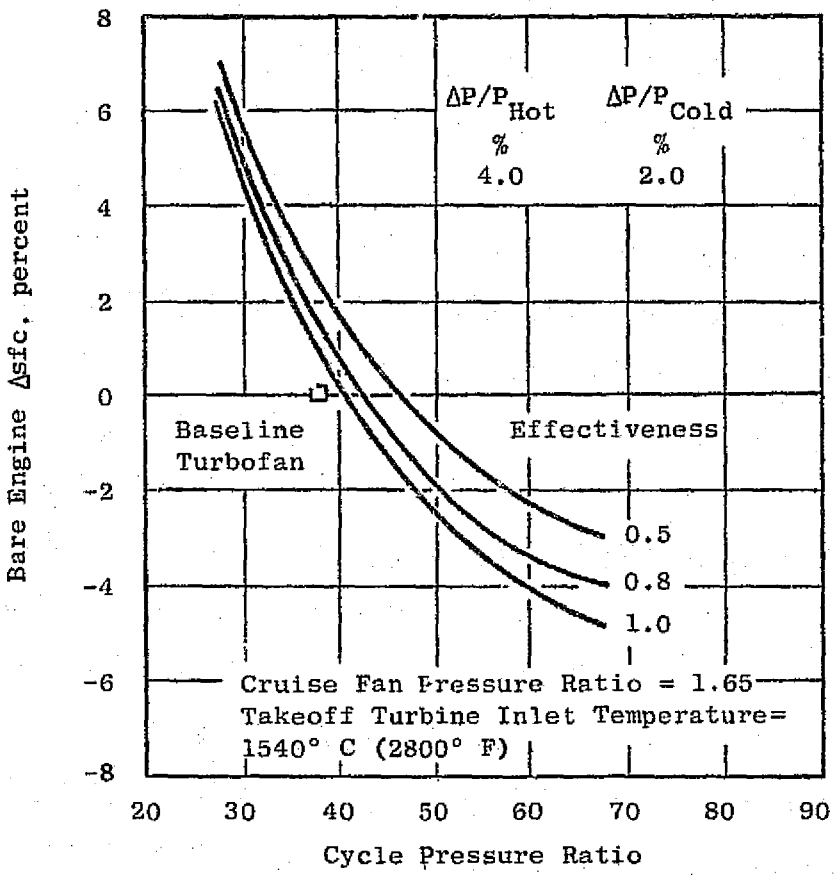

Figure 11. Core Compressor Inlet Intercooling: Cruise sfc Trends.

The effect of intercooling location was separately studied, and the core compressor inlet location was chosen because it results in the largest sfc improvement for a given regenerator effectiveness. Table XI gives a performance comparison for a specific intercooler cycle with the intercooling accomplished between the booster and the high pressure compressor. The intercooler cycle was dropped from the study because the 4% sfc reduction is too small to offset the obvious penalties of a very large intercooler plus the penalties of the larger engine required to make up a 10% specific thrust loss.

It became apparent from brief cycle studies that the sfc improvement of a combined regenerator/intercooler would not result in an improvement in sfc over the regenerator itself. Therefore further consideration of this item was dropped.

3.4.4 Regenerator/Reheat

Reheat by itself is not a concept to improve sfc, but it is worth consideration when combined with regeneration since it increases the amount of exhaust heat that can be recovered. For such a cycle, an advanced-technology reheat combustor was located between the high and low pressure turbines, as shown in the schematic of Figure 3. The typical parametric cycle sfc trends shown in Figure 12 illustrate that, for a larger reheat ΔT of 222° C (400° F), there is an sfc increase for a regenerator effectiveness of 0.8. This is primarily due to the increased cooling air required in the low pressure turbine. At a reheat ΔT of 111° C (200° F) and an effectiveness of 0.8, there is an sfc reduction of about 2% (at a P/P of approximately 20); this is less than obtained with the regenerator by itself. In principle, raising the interturbine temperature will increase the exhaust temperature and thus raise the regenerator potential. This ideal advantage is more than offset by the reheat combustor pressure losses and the turbine cooling penalties. In addition, there are great complexities in the reliable operation of a low pressure, low temperature-rise combustor at high efficiency.

The regenerator/reheat engine was therefore not considered further in this study.

3.4.5 Turbine Cooling-Air Cooling

The use of a heat exchanger for turbine cooling air, to allow its reduction, was briefly studied. The system shown schematically in Figure 4 can be applied to any of the advanced turbofan or turboprop engines. Fuel is the heat sink and a portion of the sfc improvement is due to the regenerative effect of adding the heat energy of the cooling air back into the cycle at the combustor.

The results of the evaluation are summarized in Table XII. About 0.3 to 0.4% fuel can be saved on the transcontinental mission by the application of

Table XI. Intercooler Cycle.

- 10,670 m (35,000 ft), Mach 0.8, +10° C (+18° F), Max. Climb

	Baseline Turbofan	Intercooled Turbofan
Fan Pressure Ratio	1.71	1.71
Cycle Pressure Ratio	38	60
Turbine Inlet Temp, ° C (° F)	1370 (2500)	1370 (2500)
Intercooler Effectiveness (Shell and Tube)	-	0.70
Intercooler Effectiveness	-	0.80
Fan Duct Δ P/P, %	-	2
Intercompressor (Booster) Δ P/P, %	-	4
Bare sfc, Δ%	Base	-4.5
F_n/W_2, Δ%	Base	-10

• 10,670 m (35,000 ft), Mach 0.8

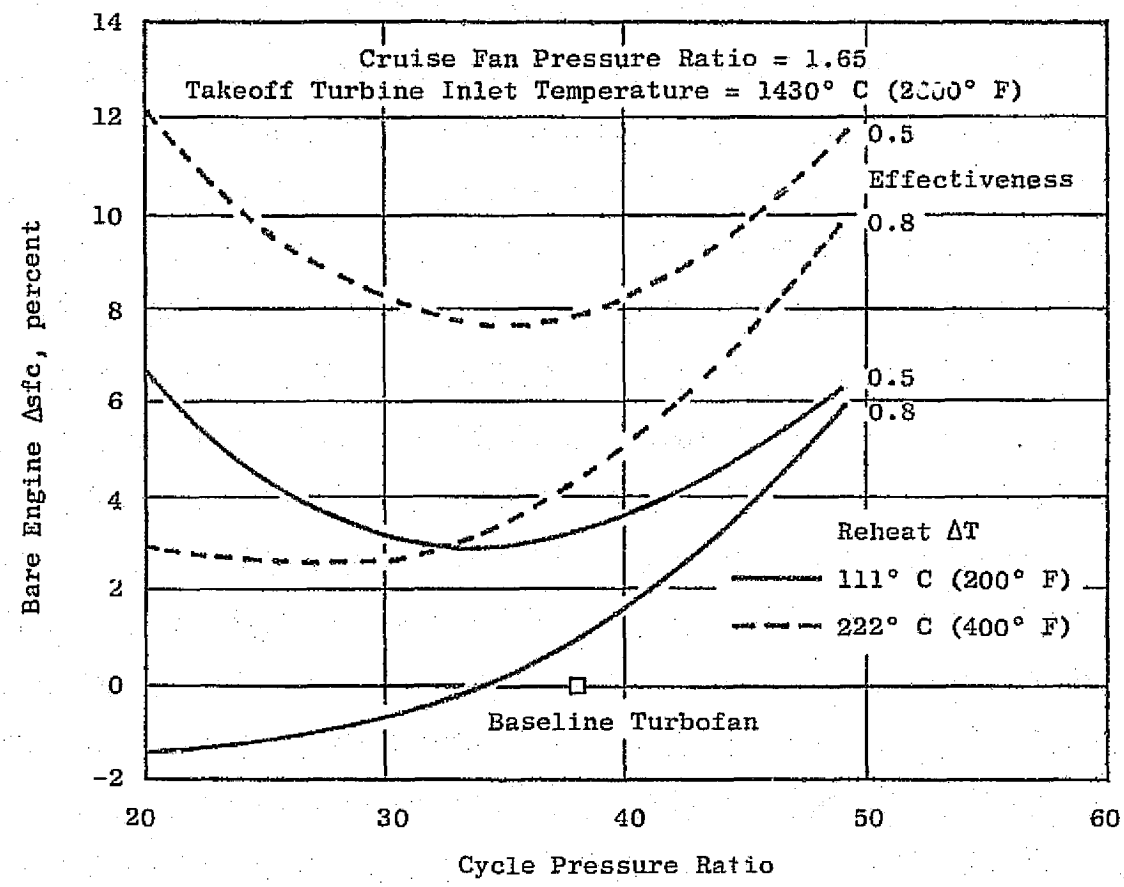

Figure 12. Postturbine Regenerator, with Reheat: Cruise sfc Trends.

the heat exchanger to either the HP or LP turbine cooling systems. It cannot be applied to both because of the limited heat capacity of the fuel.

Table XII. Turbine Cooling-Air Cooling.

- Can be Applied to any Advanced Turbofan or Turboprop
- Either HPT or LPT Cooling System
- Coolant Flow Savings Due to Lower Cooling Temperature by 100° C (180° F) to 128° C (230° F)
- Benefit of Regeneration to Fuel
- Fuel Saved: 0.3% to 0.4%
- DOC Reduction: <0.1%

3.5 NOVEL ARRANGEMENTS

The novel engine arrangements selected for study are: geared fans, both with counterrotating forward boosters and with aft high speed boosters; geared fans with aft high speed variable boosters; direct-drive, triple-spool turbofan; and geared, variable-pitch fan with aft high speed boosters. The results of this study, which are discussed in the following paragraphs, provided the basis for selecting the configurations for the Task II refined analysis.

All of the engines selected for parametric analysis in Task I are listed in Tables XIII and XIV with key features highlighted.

3.5.1 Geared Fans

A range of fan pressure ratios from 1.40 to 1.71 was chosen to determine where a geared fan would have the best payoff. Aft and forward locations of the boosters were investigated to determine their relative merits. A typical forward, counterrotating-booster design is shown in Figure 13; a typical aft-booster, geared-fan engine is shown in Figure 14.

The sfc versus fan pressure ratio trends are illustrated in Figure 15. The lower pressure ratios are favored for the geared turbofans, more so than for the direct-drive fans, due to the low pressure spool efficiency trends.

Table XIII. Geared-Fan Configuration Summary.

- Takeoff T_{41} = 1430° C (2600° F)
- Common Core Engine.

Item	Baseline Reference Turbofan	Novel Engine Arrangements					
Exhaust System Mixed/Separate	Mixed	Mixed	Mixed	Mixed	Separate	Mixed	Mixed
Fan Pressure Ratio	1.70	1.70	1.55	1.40	1.40	1.70	1.70
No. Spools	2	2	2	2	2	2	3
Booster Location	Aft	Front	Front	Front	Aft	Aft	Front
Variable Geometry	Booster Stator	Bleed Valve	Bleed Valve	Bleed Valve	Booster Stator	Booster Stator	Booster Turbine Vane
Fan Drive	Direct	Star Gear	Star Gear	Star Gear	Star Gear	Star Gear	Direct
Fan Pitch Angle	Fixed	Fixed	Fixed	Fixed	Variable	Fixed	Fixed
Cycle Pressure Ratio at Max. Climb	38	38	38	38	38	38	38

Table XIV. Novel Engine Arrangements: Cycle and Key Features.

Type	Baseline Turbofan Mixed Flow	Geared Fans Mixed Flow			Triple Spool Variable Boost Mixed Flow	Variable-Pitch Fan Separate Flow
Drive Type	Direct Drive	Geared			Direct Drive	Geared
Booster Arrangement	Aft	Counterrotating Forward Vs. Aft			Counterrotating Forward	Aft
Booster P/P	2.75	2.75			3.52	2.75
No. Spools	2	2			3	2
Max. Climb Fan Pressure Ratio	1.71	1.71	1.55	1.40	1.71	1.40
Max. Climb Overall Pressure Ratio	38	38 →			45	38
Max. Climb T_{41}, ° C (° F)	1370 (2500) →					
Core P/P at Max. Climb	14	14 →			13.3	14
Max. Climb Bypass Ratio	6.9	7.1	9.6	13.7	6.7	13.5
Takeoff T_{41}, ° C (° F)	1430 (2600) →					
Takeoff Overall Pressure Ratio	30 →					

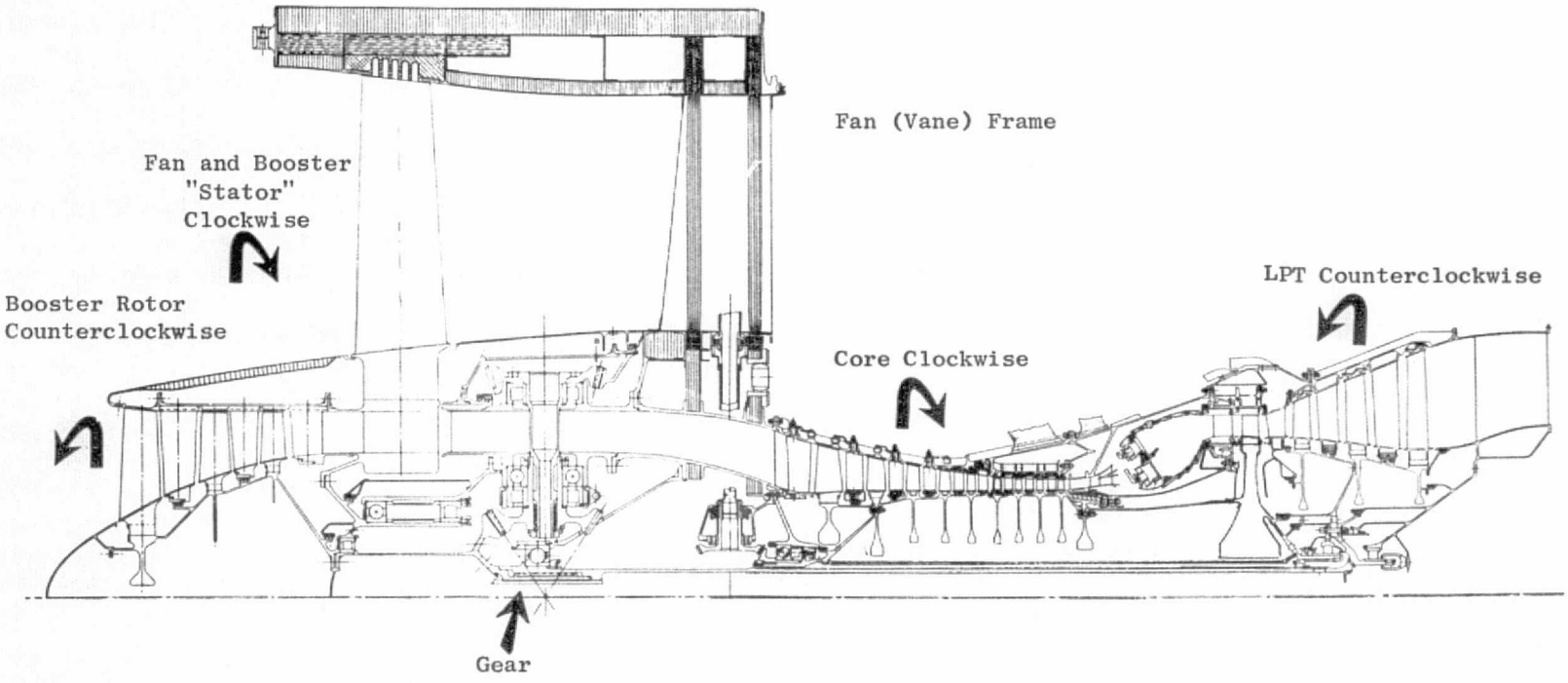

Figure 13. Geared Fan, Forward Counterrotating Booster.

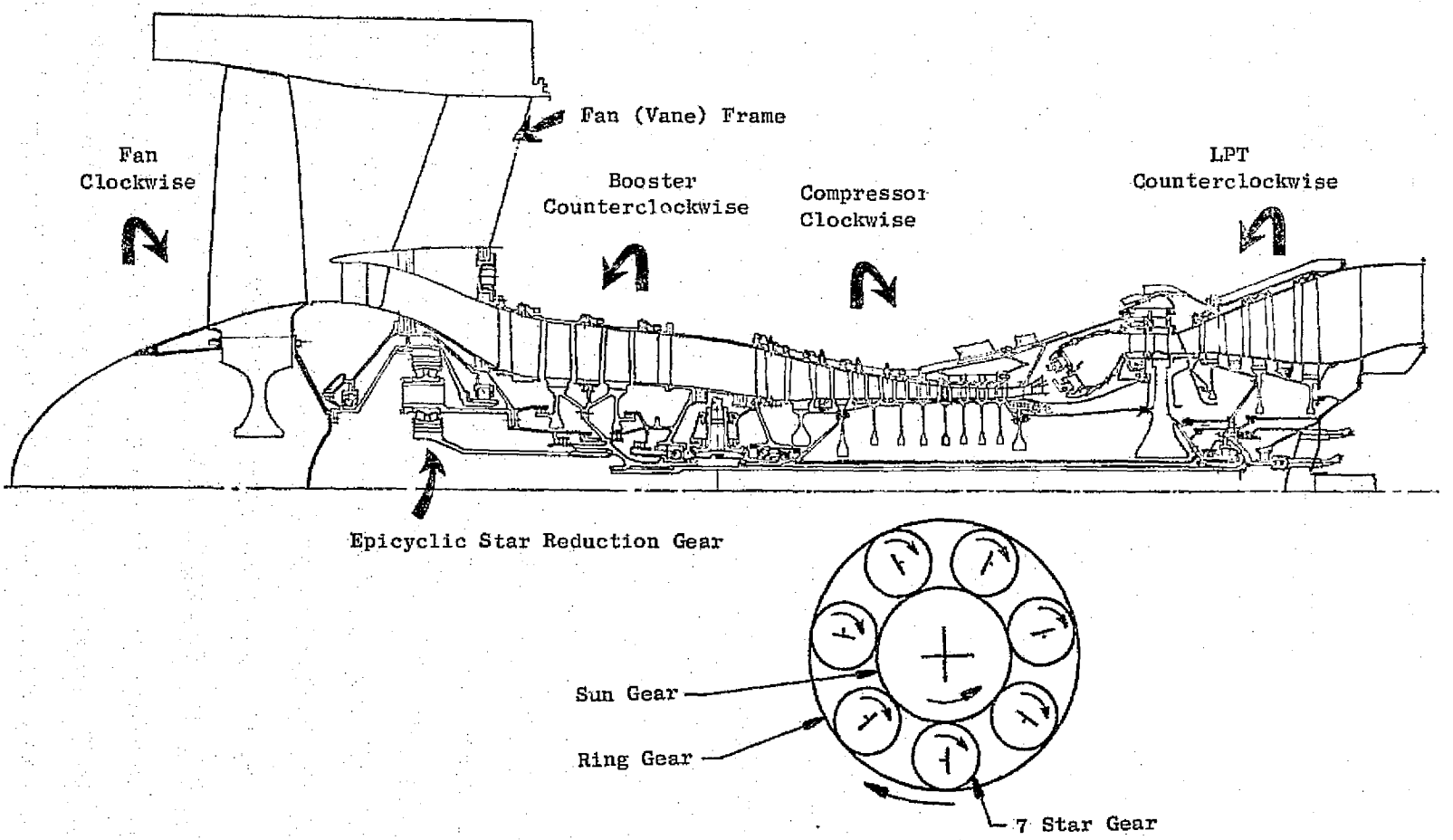

Figure 14. Geared Fan, Aft High Speed Boosters.

- 10,670 m (35,000 ft), Mach 0.8, +10° C (+18° F), 95% Max. Cruise

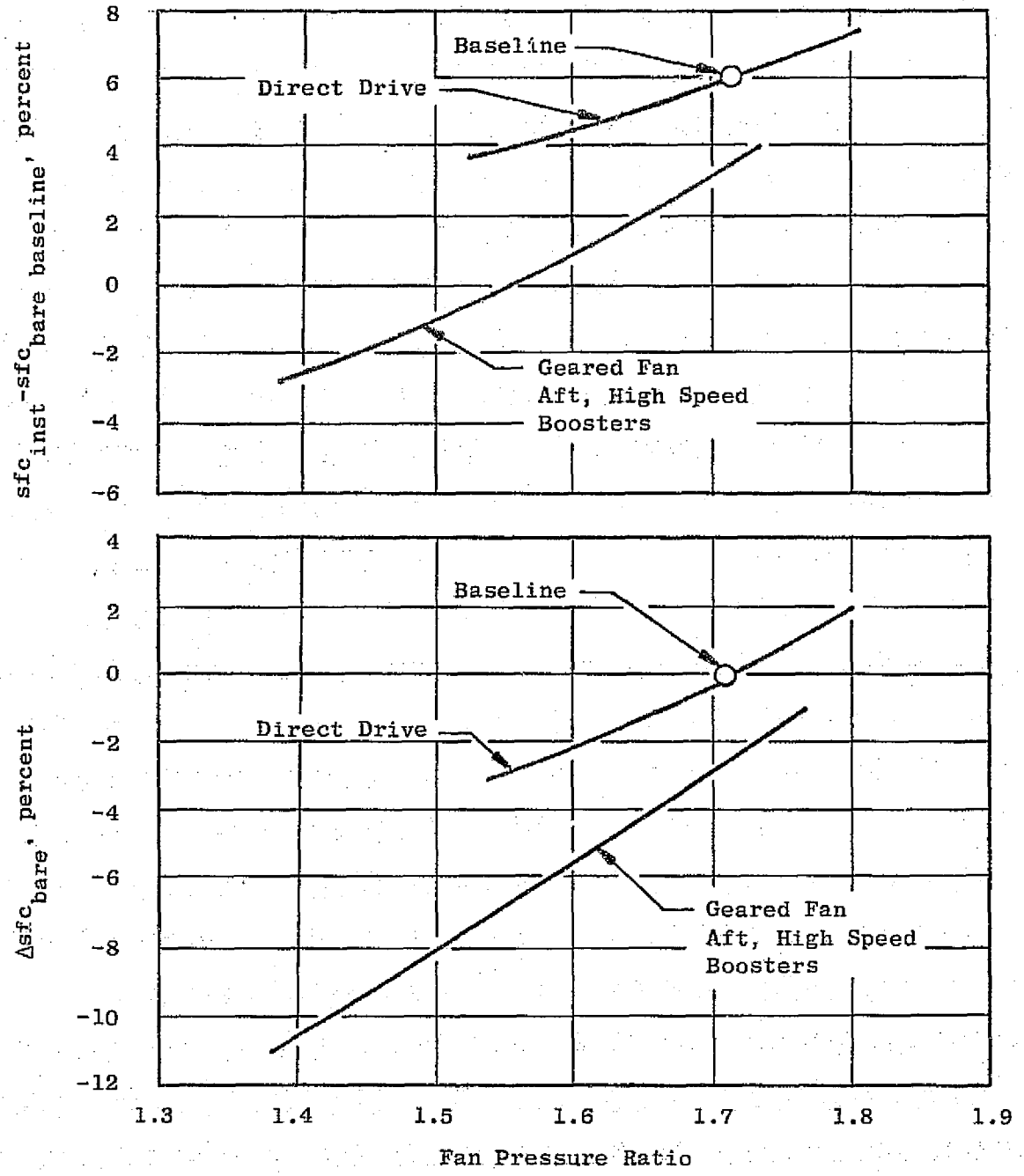

Figure 15. Geared Engines, Bare and Installed sfc Trends.

The installed weight (Figure 16) tends to increase at lower fan pressure ratios; as a result, minimum fuel is consumed at a fan pressure ratio of about 1.5 (as illustrated in Figure 17). The fan pressure ratio for minimum DOC is higher, approximately 1.6 (also illustrated in Figure 17). An analysis of the contributions to the mission fuel saved, and DOC reduction, of the 1.71 pressure ratio, front-booster, geared fan is presented in Table XV.

The use of high speed aft boosters was investigated in conjunction with the 1.71 pressure ratio fan. The results, shown in Table XVI, indicate that this engine has a fuel reduction approximately the same as the forward-boost, geared fan of the same pressure ratio. The sensitivity of the geared-fan DOC results, as related to the input used in the Task I Study, is discussed in Task II. It should be noted that the trends in DOC and W_f, as a function of fan pressure ratio, are primarily due to cycle (sfc) and engine weight effects. For that matter, the engine weight trend itself is related to the cycle since bypass ratio, and therefore LP spool and core weights, vary inversely with fan pressure ratio. It was assumed for the purpose of this study that the trends of Figure 17 would apply to various configurations of geared engines. Each configuration of interest was, therefore, evaluated and its relative merits compared at a selected fan pressure ratio.

3.5.2 Variable-Boost, Twin-Spool Turbofan

The use of variable boost was studied as a feature for the aft high speed booster engine with a 1.71 fan pressure ratio. The engine was sized at an overall cycle pressure ratio of 45:1 at the 10670 m (35,000 ft)/Mach 0.8 max. climb point. At sea level takeoff, the booster pressure ratio was reduced by the use of variable booster stators until the overall pressure was reduced to that of the baseline engine at takeoff. In this manner, the thermal efficiency advantage of higher pressure at altitude conditions resulted in an sfc improvement without the penalties associated with designing for higher compressor discharge pressures and temperatures and increased turbine cooling flow at sea level.

Table XVII indicates a 2% (4.6 to 2.6) bare sfc improvement for the variable-boost feature evaluated on a cruise sized basis. Note that in Task II, as a result of refined analysis, an improvement of 1.3% resulted for the variable-boost feature when sized at cruise. Takeoff sizing is discussed in Task II.

A unique, triple-spool turbofan (Figure 18) was designed with a single-stage LP turbine driving a high speed booster rotor located ahead of the fan. Either a variable-area, booster-drive turbine nozzle or a bypass bleed duct around the booster-drive turbine could be used to reduce power to the booster and reduce the booster pressure ratio for sea level operation. It should be mentioned that while the cruise-sized, triple-spool, variable-boost engine had a slight advantage over the twin-spool, forward-boost configuration, the loss in takeoff thrust due to the variable-boost feature kept the engine from meeting the takeoff field length of 3.2 km (10,500 ft). Characteristics of

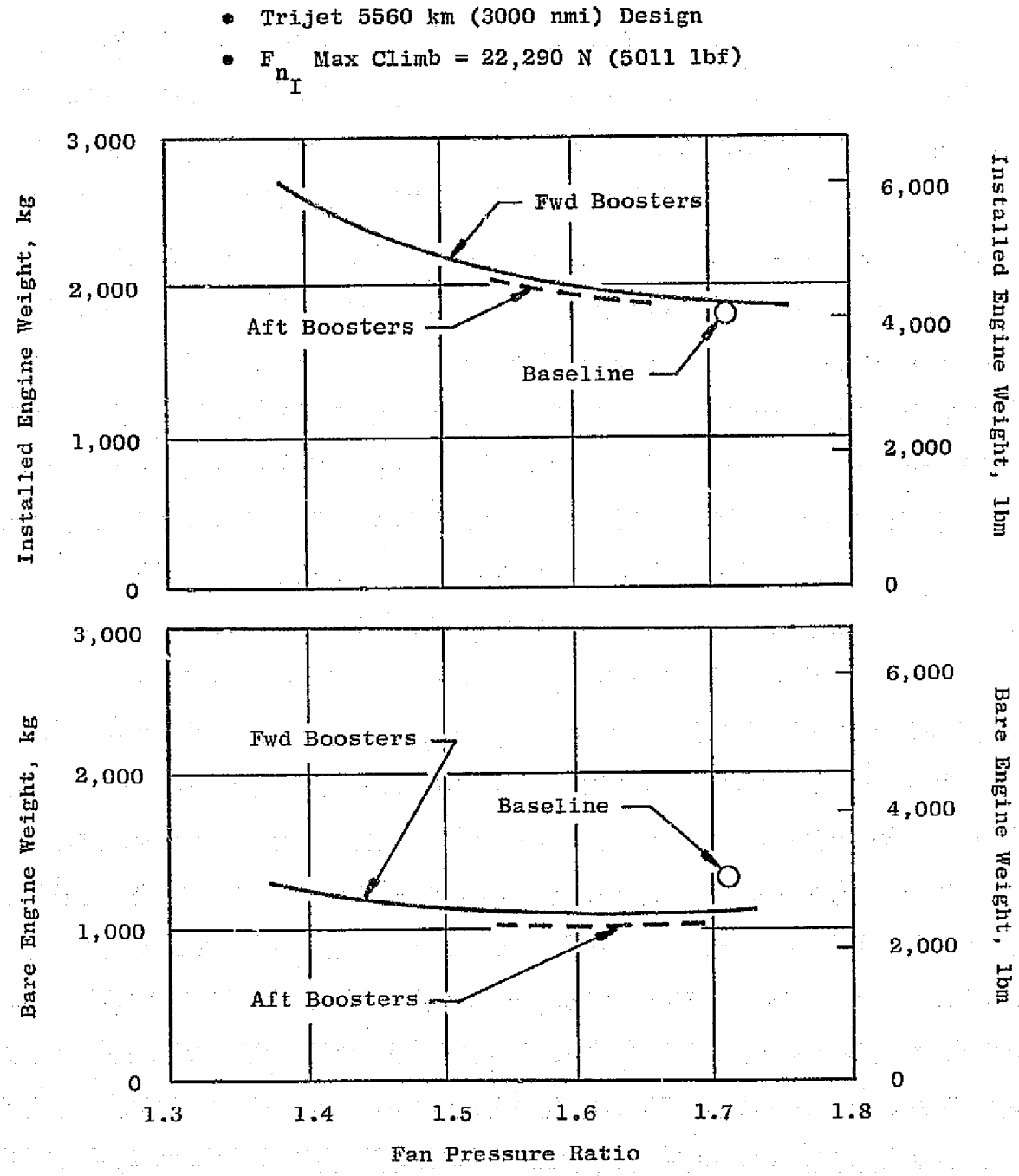

Figure 16. Geared Engines, Bare and Installed Engine Weight Trends.

- Trijet 5560 km (3000 nmi) Design
- Evaluation at 55% Load Factor, 1300 km (700 nmi) Mission
- 10,670 m (35,000 ft), Mach 0.8, +10° C (+18° F), 95% Max Cruise

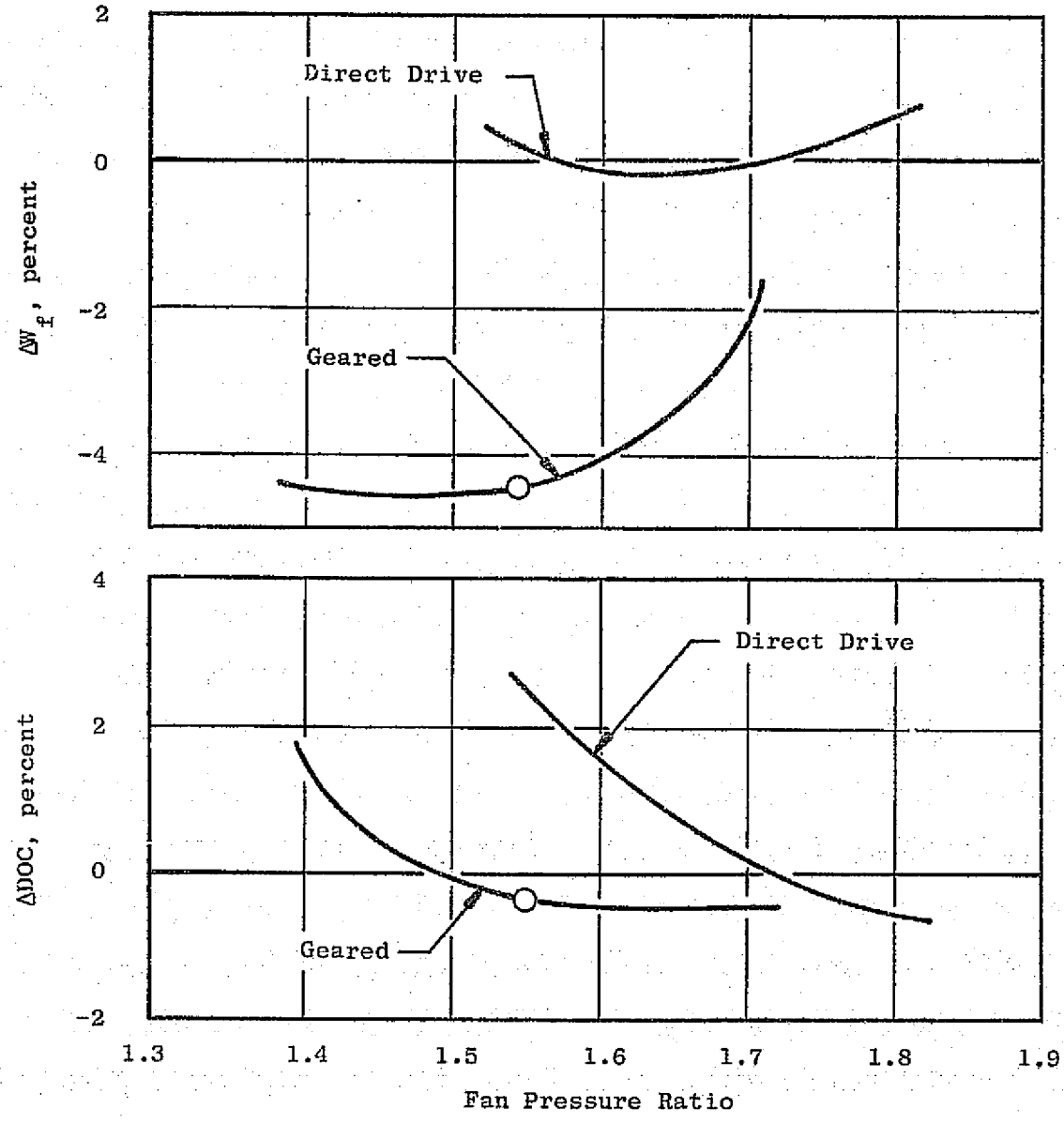

Figure 17. Geared Vs. Direct-Drive Fan, Forward Boosters.

Table XV. Forward-Boost, Geared-Fan Vs. Baseline Engine.

- Trijet, 5560 km (3000 nmi) Design
- Evaluation at 55% Load Factor, 1300 km (700 nmi) Mission, Cruise Sized.
- 10.670 m (35,000 ft)/Mach 0.8/ + 10° C (+18° F)/95% Max. Cruise.

Parameter	Baseline Engine Pressure Ratio 1.71	Forward-Boost, Geared-Fan Engine			
		Pressure Ratio 1.71	Δ's	ΔDOC	ΔW_f
Engine Weight kg (lbm)	1042 (2298)	1090 (2410)	50 (112)	0.19	0.29
Engine Initial Price, Δ%	Base	-	+5.2	+0.20	-
Engine Replacement, Δ%	Base	-	-5.2	-0.22	-
sfc, Bare	Base	-	-2.5	-0.98	-2.71
Subtotal (Engine Δ's)	-	-	-	-0.81	-2.42
Installed Weight, kg (lbm)	804 (1772)	839 (1850)	35 (78)	0.14	0.20
Installed Price, Δ%	Base	-	4.6	0.11	-
Drag, N (lbf)	1160 (260)	1200 (270)	40 (10)	0.10	0.28
Subtotal (Installed Δ's)	-	-	-	+0.35	+0.48
Totals	-	-	-	-0.46	-1.94

Table XVI. Aft, High Speed Boost Vs. Baseline Engine.

- Trijet, 5560 km (3000 nmi) Design
- Evaluation at 55% Load Factor, 1300 km (700 nmi) Mission, Cruise Sized.
- 10,670 in. (35,000 ft)/Mach 0.8/+10° C (+18° F)/95% Max. Cruise.

Parameter	Baseline Engine Pressure Ratio 1.71	Aft-Boost, Geared-Fan Engine			
		Pressure Ratio 1.71	Δ's	ΔDOC	ΔW_f
Engine Weight kg (lbm)	1042 (2298)	1059 (2334)	17 (36)	0.05	0.09
Engine Initial Price, Δ%	Base	-	+0.9	+0.04	-
Engine Replacement Price, Δ%	Base	-	-9.1	-0.39	-
sfc, Bare	Base	-	-2.6	-1.00	-2.82
Subtotal (Engine Δ's)	-	-	-	-1.30	-2.73
Installed Weight, kg (lbm)	804 (1772)	843 (1858)	39 (86)	0.14	0.19
Installed Price, Δ%	Base	-	4.9	0.11	-
Drag, N (lbf)	1160 (260)	1200 (270)	40 (10)	0.08	0.27
Subtotal (Installed Δs)	-	-	-	+0.35	+0.46
Totals	-	-	-	-0.95	-2.27

Table XVII. Geared Fan, Aft High Speed Boosters.

- Trijet, 5560 km (3000 nmi) Design
- Evaluation at 55% Load Factor, 1300 km (700 nmi) Mission, Cruise Sized
- 10,670 m (35,000 ft), Mach 0.8, +10° C (+18° F), 95% Max. Cruise

	Baseline Pressure Ratio 1.71	Nonvariable Boost				Variable Boost			
		Pressure Ratio 1.71	Δ's	ΔDOC	ΔW_f	Pressure Ratio 1.71	Δ's	ΔDOC	ΔW_f
Engine Weight kg (lbm)	1042 (2298)	1059 (2334)	17 (36)	0.05	0.09	978 (2157)	-64 (-141)	-0.24	-0.26
Engine Initial Price, Δ%	Base	-	0.9	0.04	-	-	-1.3	-0.06	-
Engine Replacement Price, Δ%	Base	-	-9.1	-0.39	-	-	-11.3	-0.48	-
sfc, Bare	Base	-	-2.6	-1.00	-2.82	-	-4.6	-1.79	-4.97
Subtotal (Engine Δ's)	-	-	-	-1.30	-2.73	-	-	-2.57	-5.33
Installed Weight, kg (lbm)	804 (1772)	843 (1858)	39 (86)	0.14	0.19	840 (1851)	39 (79)	0.13	0.20
Installed Price, Δ%	Base	-	4.9	0.11	-	-	2.8	0.07	-
Drag, N (lbm)	1160 (260)	1200 (270)	40 (10)	0.08	0 27	1168 (262)	8 (2)	0.02	0.05
Subtotal (Installed Δ's)	-	-	-	+0.35	+0.46	-	-	+0.22	+0.25
Totals	-	-	-	-0.95	-2.27	-	-	-2.35	-5.08

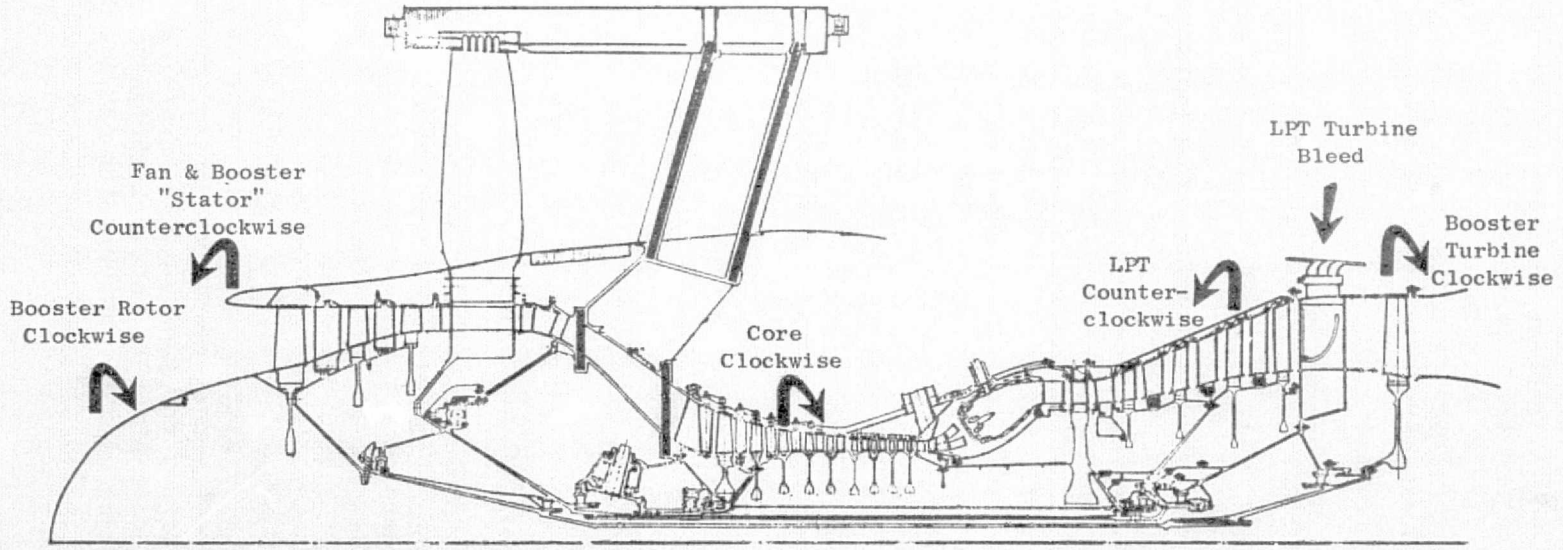

Figure 18. Triple-Rotor Turbofan.

this triple-spool engine, both cruise sized and takeoff sized, are tabulated in Table XVIII.

The variable-boost feature tends to reduce the altitude thrust lapse; hence, the benefits of the variable-boost feature are less for takeoff-sized engines because the engine for this condition has to increase from a 1.53 m (60.2 in.) fan to a 1.62 m (63.6 in.) fan diameter. As a result, the installed weight increases and tends to offset much of the sfc improvement. A summary of the variable-boost characteristics is presented in Table XIX.

3.5.3 Variable-Pitch, Geared-Fan Engine

For the very high bypass ratio turbofan engines (fan pressure ratio = 1.4), the thrust reverser weight and price trends tend to offset the sfc benefits and contribute to an economic penalty (DOC) relative to the higher fan pressure ratio (lower bypass) engines. Use of a variable-pitch fan for thrust reversal eliminates the penalties associated with the large reverser; this led to the study of a geared, variable-pitch, 1.4 pressure ratio fan engine to determine its merits relative to the geared, fixed-pitch, 1.4 pressure ratio fan. The variable-pitch, geared-fan cycle data are summarized in Table XIV and the engine cross section is shown in Figure 19; the fan was scaled from the NASA QCSEE demonstrator engine (Reference 5).

Evaluation results for the variable-pitch fan are shown in Table XX; comparable results for the 1.4 fan pressure ratio, fixed-pitch fan are also shown in Table XX. Although there is some reduction in installed weight for the variable-pitch fan, it is small compared to the sfc penalty. The sfc penalty is due primarily to the restriction of the variable-pitch fan engine to a separate-flow configuration, the fixed-pitch engine being based on mixed exhaust. It should be noted that a mixed-flow, variable-pitch fan is not feasible because of inevitable reingestion of hot core gases during reverse-thrust operation. In either case, the 1.4 fan pressure ratio is inferior to a fixed-pitch, geared turbofan of a higher fan pressure ratio.

3.6 EVALUATION PROCEDURE: TURBOPROPS

The study of turboprops was included because of the potential sfc improvement over the turbofan. This potential improvement is associated with the high propulsive efficiency of a propeller relative to a fan. Projected improvements in propeller technology have made a Mach 0.8 turboprop transport plausible.

The comparison of turboprops to turbofans inevitably involves the aircraft as well as the propulsion system design. In order to make this comparison in the most consistent manner possible, equivalent turbofan and turboprop aircraft were designed for the transcontinental and intercontinental missions. A four-engine, transcontinental, turbofan-powered aircraft was chosen (rather than the trijet used in the turbofan studies) to eliminate

Table XVIII. Triple-Spool Engine Vs. Baseline Engine.

- Trijet, 5560 km (3000 nmi) Design
- Evaluation at 55% Load Factor, 1300 km (700 nmi) Mission, Cruise Sized
- 10,670 m (35,000 ft), Mach 0.8, +10° C (+18° F), 95% Max. Cruise

	Baseline Pressure Ratio 1.71	3 Spool, Takeoff Sized				3 Spool, Cruise Sized			
		Pressure Ratio 1.71	Δ's	ΔDOC	ΔW_f	Pressure Ratio 1.71	Δ's	ΔDOC	ΔW_f
Engine Weight kg (lbm)	1042 (2298)	1170 (2580)	128 (282)	0.47	0.72	1022 (2254)	-20 (-44)	-0.07	-0.11
Engine Initial Price, Δ%	Base	-	5.6	0.25	-	-	-0.5	-0.02	-
Engine Replacement Price, Δ%	Base	-	1.8	0.08	-	-	-4.6	-0.20	-
sfc, Bare	Base	-	-2.0	-0.77	-2.13	-	-2.0	-0.77	-2.13
Subtotal (Engine Δ's)	-	-	-	+0.03	-1.41	-	-	-1.06	-2.24
Installed Weight, kg (lbm)	804 (1772)	894 (1970)	90 (198)	0.33	0.50	794 (1750)	-10 (-22)	-0.04	-0.06
Installed Price, Δ%	Base	-	11.2	0.28	-	-	2.1	0.05	-
Drag, N (lbf)	1160 (260)	1310 (294)	150 (34)	0.08	0.21	1170 (264)	10 (4)	0.08	0.21
Subtotal (Installed Δ's)	-	-	-	+0.69	+0.71	-	-	+0.09	+0.15
Totals	-	-	-	+0.72	-0.70	-	-	-0.97	-2.09

Table XIX. Thrust Lapse Comparison of Variable-Boost Engines.

- Trijet 5560 km (3000 nmi) Design Range
- Evaluation at 55% Load Factor, 1300 km (700 nmi) Mission

	Baseline	Aft Boost Geared Fan	Twin Spool Variable Boost		Triple Spool Variable Boost	
			Cruise Speed	Takeoff Speed	Cruise Speed	Takeoff Speed
Fan Tip Diameter, m (in.)	1.55 (61.2)	1.57 (61.8)	1.45 (56.9)	1.53 (60.1)	1.53 (60.2)	1.62 (63.6)
F_n at SLS +15° C Takeoff, N (+27° F) (lbf)	88,960 (20,000)	89,850 (20,200)	79,760 (17,930)	88,960 (20,000)	80,070 (18,000)	88,960 (20,000)
Bare F_n at 10,670 m +10° C/Mach 0.8 Max. Climb, N (35,000 ft +18° F) (lbf)	23,440 (5270)	23,490 (5280)	23,460 (5274)	26,169 (5882)	23,490 (5280)	26,160 (5880)
Installed F_n at 10,670 m +10° C/Mach 0.8 Max. Climb, N (35,000 ft +18° F) (lbf)	22,290 (5010)	22,290 (5010)	22,290 (5010)	24,860 (5589)	22,290 (5010)	24,820 (5580)
(F_n at Max. Climb)/(F_n at SLS Takeoff)	0.264	0.261	0.294	0.294	0.294	0.294

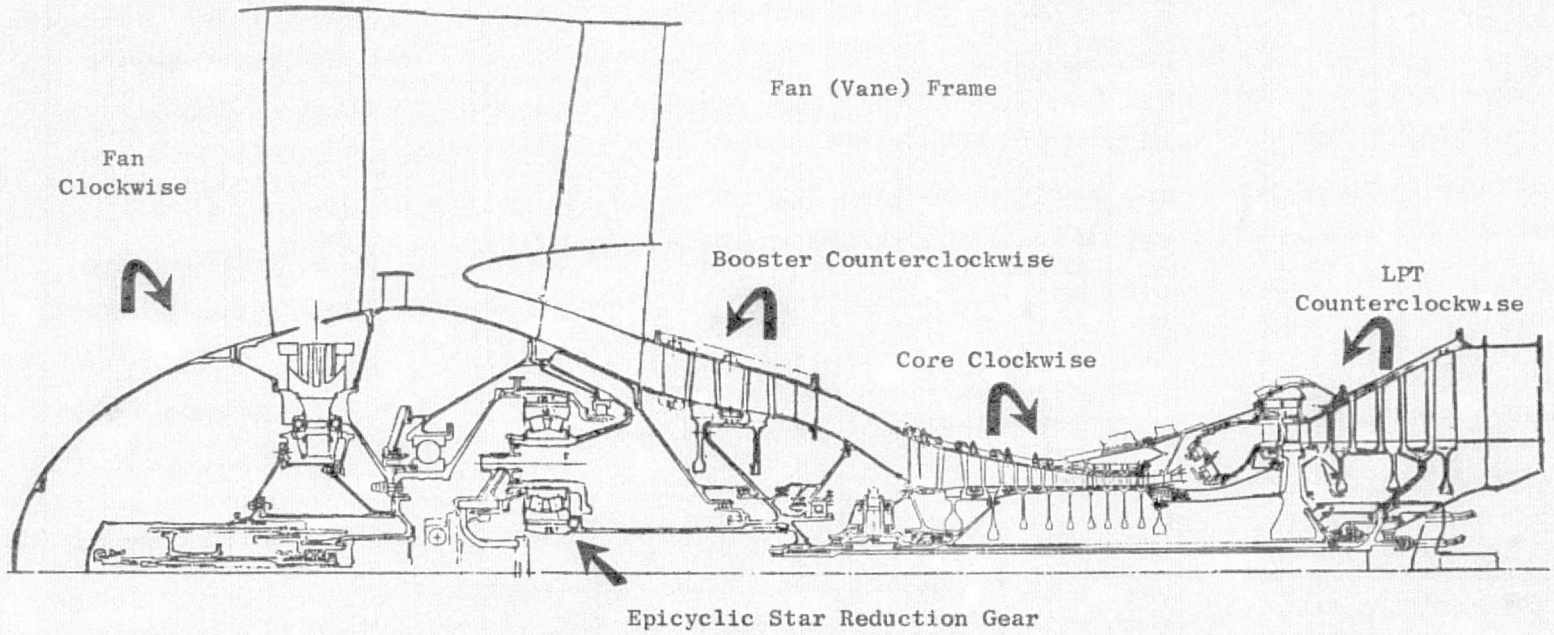

Figure 19. Variable-Pitch Fan.

Table XX. Separate-Flow, 1.4 Pressure Ratio, Geared Fans Vs. Baseline Engine.

- Trijet, 5560 km (3000 nmi) Design
- Evaluation at 55% Load Factor, 1300 km (700 nmi) Mission, Cruise Sized
- 10,670 m (35,000 ft), Mach 0.8, +10° C (+18° F), 95% Max. Cruise

	Baseline Pressure Ratio 1.71	Variable-Pitch, Reversible				Fixed-Pitch			
		Pressure Ratio 1.4	Δ's	ΔDOC	ΔW_f	Pressure Ratio 1.4	Δ's	ΔDOC	ΔW_f
Engine Weight kg (lbm)	1042 (2298)	1670 (3685)	630 (1387)	2.32	3.55	1250 (2764)	120 (465)	0.78	1.19
Engine Initial Price, Δ%	Base	-	22.1	0.97	-	-	10.6	0.46	-
Engine Replacement Price, Δ%	Base	-	-1.3	-0.05	-	-	-4.8	-0.21	-
sfc, Bare	Base	-	-6.3	-2.46	-6.83	-	-10.6	-4.17	-11.6
Subtotal (Engine (Δ's)	-	-	-	+0.78	-3.28	-	-	-3.14	-10.4
Installed Weight, kg (lbm)	804 (1772)	833 (1836)	29 (64)	0.11	0.16	1365 (2988)	552 (1216)	2.03	3.06
Installed Price, Δ%	Base	-	7.6	0.18	-	-	67.6	1.63	-
Drag, N (lbf)	1160 (260)	1820 (410)	660 (150)	1.20	3.32	1770 (397)	610 (137)	1.06	2.96
Subtotal (Installed Δ's)	-	-	-	+1.49	+3.48	-	-	+4.72	+6.02
Totals	-	-	-	+2.27	+0.20	-	-	+1.58	-4.38

three- versus four-engine aircraft differences. Table XXI outlines the evaluation procedure, which is quite similar to that used for turbofans. A comparison of the four baseline aircraft is presented in Table XXII with baseline propulsion system data included. The single-rotation propeller, base-technology level, was used as described in the following section.

Aircraft aerodynamic and structural assumptions were the same for the turboprop and turbofan aircraft with the exception of a cabin noise suppression weight penalty estimate of 363 kg (800 lb) and a 3 and 5% increase in horizontal and vertical tail areas which was reflected in the aircraft drag and weight.

The mission trade factors derived from the baseline-aircraft design data and economic analysis are given in Tables XXIII and XXIV for incremental propulsion system changes.

3.7 TURBOPROP STUDIES

The turboprop studies utilized a high pressure spool, with technology equal to the turbofan engine, and a low pressure compressor (booster) driven by a four-stage, low pressure turbine. The propeller and gearset data were supplied under subcontract by Hamilton Standard, Division of United Technology; a summary of that data is given in Table XXV. Three levels of technology were evaluated: single rotation with current-technology weights, single rotation with advanced-technology weights, and a counterrotating propeller with advanced-technology weights. A tip speed of 244 m/sec (800 ft/sec), eight blades, and a disc loading of 289,000 W/m^2 (36 hp/ft^2) were recommended by Hamilton Standard. A major objective was to provide a small diameter propeller to minimize the impact upon the aircraft design. Preliminary studies showed that the high tip speed was advantageous at Mach 0.8/10,670 m (35,000 ft) for the high disc-loading design. The disc-loading selection also represented a weight/efficiency trade as illustrated in Figure 20. Weight increased rapidly when disc loading was decreased below 289,000 W/m^2 (36 hp/ft^2); on the other hand, the performance gain was small.

A summary of the turboprop engine cycle features is given in Table XXVI. The baseline core engine design, scaled as necessary, was employed for the turboprops. On the basis of preliminary studies, the core thrust was chosen at approximately 10% of total thrust to minimize sfc. The installed engine and inlet (kidney shaped behind the propeller) features are illustrated in Figure 21. The maximum nacelle diameter is 35% of the propeller diameter at the top and even larger at the bottom where the engine envelope is limiting.

The turboprop engine, Figure 22, has three booster and four low pressure turbine stages. The performance is compared to the turbofan engine in Table XXVII at the max. climb sizing point. The sfc comparison is made at 95% max. cruise power which is representative of the average thrust for the design mission. The installed power curves are shown in Figure 23 for the two engines. The propeller is held at 244 m/sec (800 ft/sec) tip speed, and

Table XXI. Turboprop Evaluation Procedure.

- Baseline turboprop-aircraft designs for identical mission/payload as turbofans.
- Baseline aircraft 5560 km (3000 nmi)/200 PAX transcontinental: four engines.
  10,190 km (5500 nmi)/200 PAX intercontinental: four engines.
- Mission trade factors for engine changes determined.
- Baseline turboprop: single rotation advanced technology with advanced-technology engine.
- Effects of changes in installed engine characteristics determined for each turboprop engine variation studied.
- Weight, cost and drag effects include the pylon to the wing. They did not include structural effects of the propeller on the aircraft wing design.
- Effects of engine price related to production cost, 1974 $.
- Turboprop maintenance costs derived by summing engine, prop, and gearbox and then compared to turbofan.
- Engines scaled to thrust required by baseline aircraft:

  Engine scaling exponents; weight, 1.25; price, 0.55

  Propeller scaling exponents; weight, 1.24; price, 0.50

  Gear scaling exponents; weight, 1.50; price, 0.50

  Installation scaling exponents; weight, 1.1; price, 0.80

Table XXII. Turboprop Vs. Turbofan Baseline-Aircraft Comparison.

Mission Range, km (nmi) PAX	Transcontinental 5560 (3000) 200		Intercontinental 10,190 (5,500) 200	
Four Engines	Turbofan	Turboprop*	Turbofan	Turboprop*
TOGW, kg (lbm)	98,470 (217,100)	97,880 (215,800)	144,000 (317,400)	139,000 (306,600)
Wing Loading kg/m^2 (lb/ft^2)	684 (140)	684 (140)	732 (150)	732 (150)
Wing AR	12	12	12	12
Wing Sweep, 1/4 Chord, degrees	25	25	25	25
TOBFL, m (ft)	2320 (7600)	1920 (6300)	2650 (8700)	2190 (7200)
Rate of Climb m/min (ft/min)	91 (300)	91 (300)	91 (300)	91 (300)
Takeoff C_L	2.75	2.75	2.75	2.75
Average Cruise L/d	16.9	16.6	18.4	18.0
Takeoff (Static) F_n/W, N/kg (lbf/lbm)	2.55 (0.260)	3.17 (0.323)	2.38 (0.243)	2.98 (0.304)

*Base Technology

Table XXIII. Turboprop Mission Trade Factors, Average Mission.

	Transcontinental		Intercontinental	
Range, km (nmi)	1300 (700)		3700 (2000)	
Load Factor, %	55		55	
Fuel Cost, $\$/m^3$ (¢/gal)	79.2 (30)		118.9 (45)	
Change (Per Engine)	ΔDOC, %	ΔW_f, %	ΔDOC, %	ΔW_f, %
1% sfc	0.41	1.15	0.72	1.49
45.4 kg (100 lb) Engine or Installation	0.21	0.33	0.21	0.31
$10,000 Initial Engine Price	0.11	-	0.064	-
$10,000 Spare Parts Engine Price	0.11	-	0.074	-
$10,000 Installation Price	0.11	-	0.064	-
$1.0 Maintenance Cost/Flight-hr	0.37	-	0.27	-
$0.1 Maintenance Man-hr/Flight-hr	0.81	-	0.59	-

Table XXIV. Turbofan Mission Trade Factors, Average Mission.

- Turbofans Designed for Direct Comparison to Turboprops

	Transcontinental Quadjet		Intercontinental Quadjet	
Range, km (nmi)	1300 (700)		3700 (2000)	
Load Factor, %	55		55	
Fuel Cost, $/m^3 (¢/gal)	79.2 (30)		118.9 (45)	
Change (Per Engine)	ΔDOC, %	ΔW_f, %	ΔDOC, %	ΔW_f, %
1% sfc	0.45	1.15	0.97	1.51
45.4 kg (100 lb) Engine or Installation	0.23	0.35	0.23	0.34
$10,000 Engine Initial Price	0.11	-	0.062	-
$10,000 Engine Parts Price	0.10	-	0.067	-
$1.0 Maintenance Cost/Flight-hr	0.33	-	0.24	-
$0.1 Man-hr/Flight-hr	0.73	-	0.53	-

Table XXV. Turboprop Design Data Supplied by Hamilton Standard Division.

- Constant Propeller Thrust
- Propeller, Gearset, and Envelope Information Supplied

	Single Rotation Basic Weight	Single Rotation Advanced Weight	Counterrotation Advanced Weight
N_B	8	8	4/4
U_T, m/sec (ft/sec)	244 (800)	244 (800)	244 (800)
D_T, m (ft)	4.9 (16)	4.9 (16)	4.7 (15.5)
Disc Loading, W/m^2 (hp/ft^2)	289,000 (36)	289,000 (36)	289,000 (36)
η^*_{Prop}	0.797	0.797	0.846
$D_{Nacelle}$, m (in.)	1.71 (67.2)	1.71 (67.2)	1.71 (65.1)
Prop Weight, kg (lb)	857 (1890)	767 (1690)	748 (1650)
Gear Weight, kg (lb)	658 (1450)	617 (1360)	689 (1520)
Propeller and Gear Cost**, 1000 $	212	226	254
Maintenance Man-hr/1000 Flight-hr, $	53	53	89
Maintenence Material Cost**/1000 Flight-hr, $	850	890	1530
Oil Tank + Heat-Exchanger Weight, kg (lb)	30 (66)	12 (27)	14 (30)

*10,670 m (35,000 ft), Mach 0.8, +10° C (+18° F), Max. Climb

**1974$, Production Quantity: 3200 Units

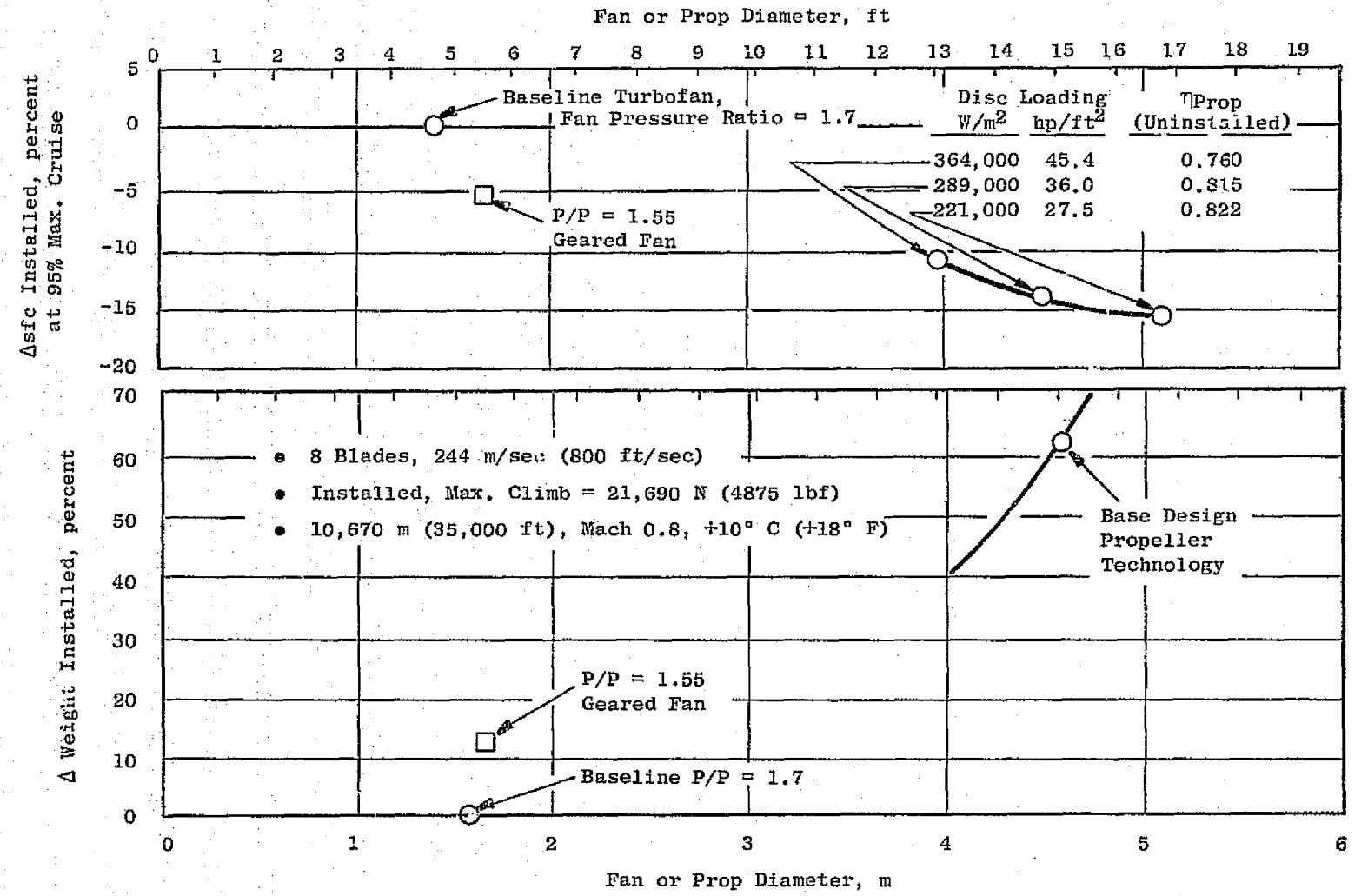

Figure 20. Effect of Propeller Size.

Table XXVI. Turboprop Cycle and Key Features.

	Baseline Turbofan Mixed Flow	Turboprops*	
		Single-Rotation Prop	Counterrotating Prop
Gear Type	Direct Drive	Double Branch Offset	Double Branch Offset
		GR = 9.2	GR = 9.2
Prop/Fan N_B	28	8	8
$U_T/\sqrt{\theta}$, m/sec (ft/sec)	494 (1620)	-	-
U_T, m/sec (ft/sec)	466 (1530)	244 (800)	244 (800)
P/P	1.71	1.05	1.05
P/P at Max. Climb**	38	38	38
T_{41} at Max. Climb, ° C (° F)	1370 (2500)	1370 (2500)	1370 (2500)
Takeoff T_{41} ° C (° F)	1430 (2600)	1430 (2600)	1430 (2600)
Core Extraction Fn_{Core}/Fn_{Total} %	29	10	10
Core Compressor P/P	14	14	14
Supercharge P/P (Fan Hub + Booster)	2.75	2.75	2.75
LP Component Efficiency	Advanced Technology →		

*Prop and Gear Data Supplied by Hamilton Standard Division Under Subcontract

**10,670 m (35,000 ft), Mach 0.8, Max. Climb.

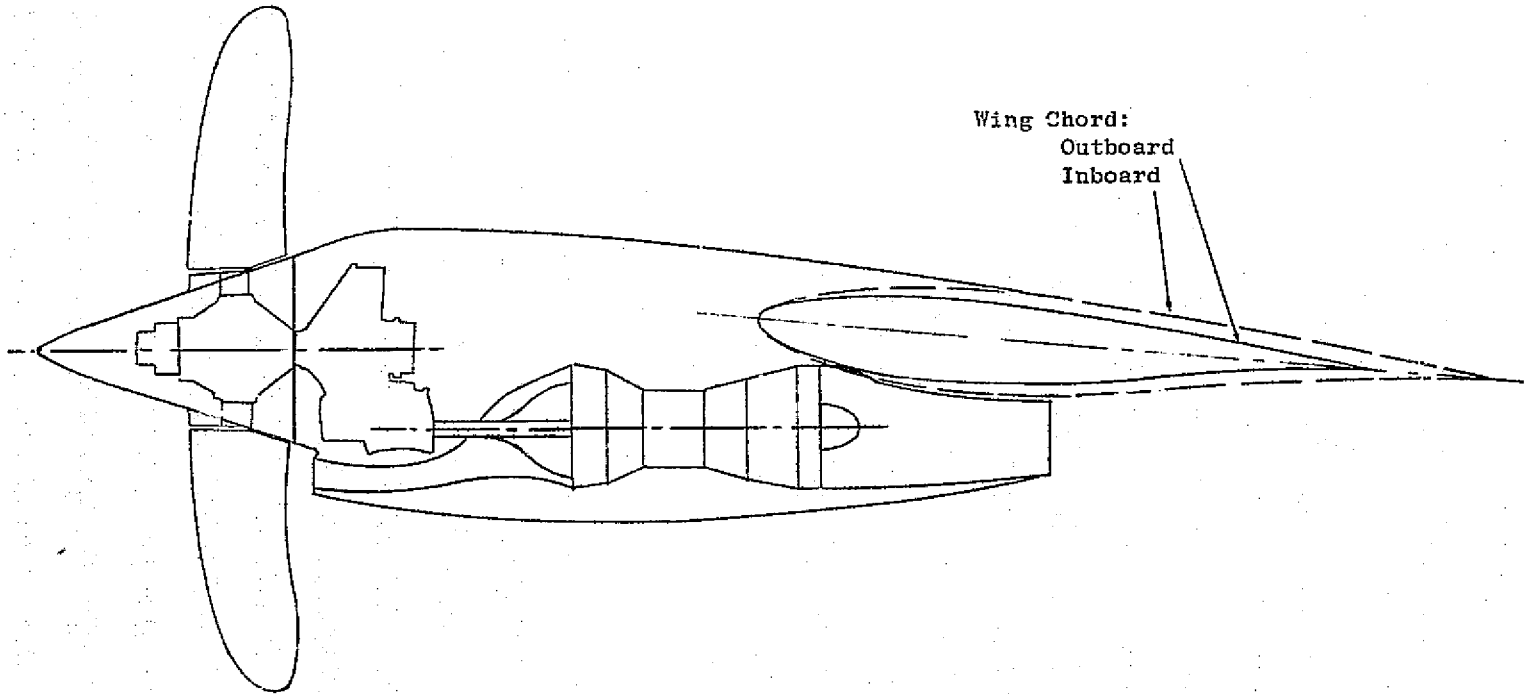

Figure 21. Turboprop Installation.

- 10,670 m (35,000 ft), Mach 0.8, +10° C (+18° F), Max. Climb

Cycle Pressure Ratio = 38
Turbine Inlet Temperature = 1370° C (2500° F)
At Takeoff Power = 1430° C (2600° F)

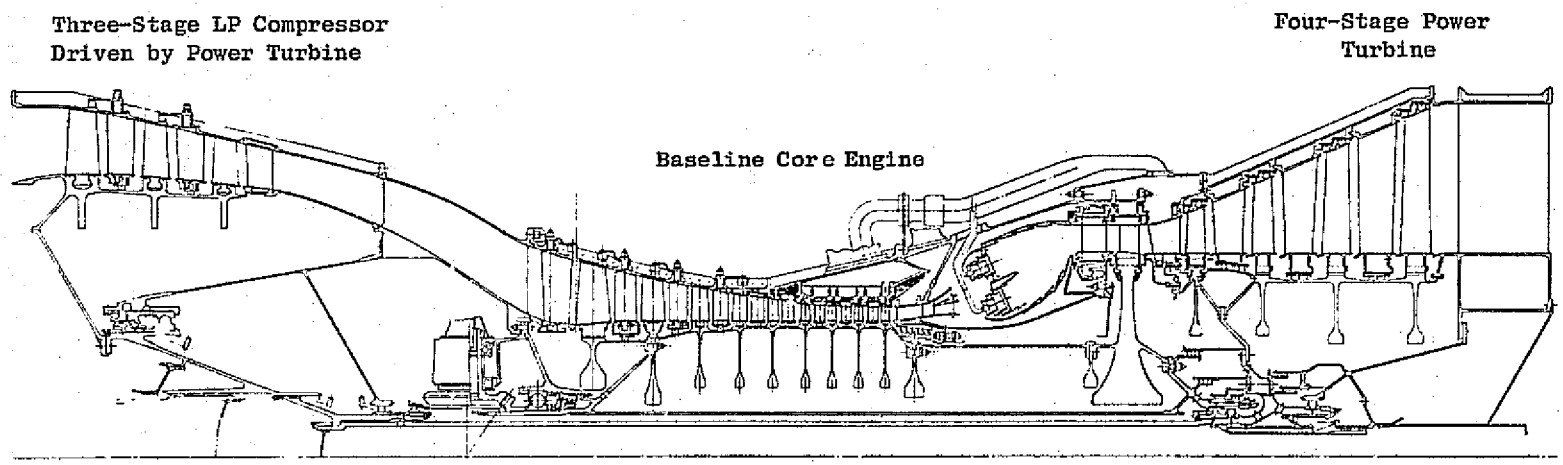

Figure 22. Turboprop Engine.

Table XXVII. Turboprop Vs. Turbofan Engines Cycle and Performance Comparison.

- 10,670 m (35,000 ft), Mach 0.8, +10° C (+18° F)

	Baseline Turbofan		Base Technology Prop	
Flight Condition	Max. Climb	95% Max. Cruise	Max. Climb	95% Max. Cruise
η_{Gear}	-		0.99	
Propeller Power, kW (hp)			4678 (6273)	
U_T, m/sec (ft/sec)	467 (1533)		244 (800)	
η_{Prop}	-		0.797	
F_{Prop}, N (lbf)	-		15,360 (3453)	
F_{Core}, N (lbf)	-		1860 (418)	
F_{Bare}, N (lbf)	16,530 (3715)		17,210 (3870)	
sfc_{Bare}, Δ%	Base		-15.4	
Disc Loading, W/m^2 (hp/ft^2)	-		289,000 (36)	
$D_{Prop/Fan}$, m (ft)	1.3 (4.3)		4.0 (13.2)	
Installed F_n, N (lbf)	15,700 (3530)	13,580 (3052)	16,150 (3630)	13,970 (3140)
Installed sfc, Δ%		Base		-14.9
Corrected Fan Flow, kg/sec (lbm/sec)	241 (532)			
Core Corrected Airflow, kg/sec (lbm/sec)	13.2 (29.1)		11.4 (25.2)	
Nacelle Friction/F_n, %	3.3		3.7	
Nacelle Pressure/F_n, %	1.6		2.0	
Wing Scrubbing/F_n, %	-		0.5	
Total Drag/F_n, %	4.9		6.2	

- 10,670 m (35,000 ft), Mach 0.8, Standard Day
- Base Turbofan sfc at 95% Max. Cruise

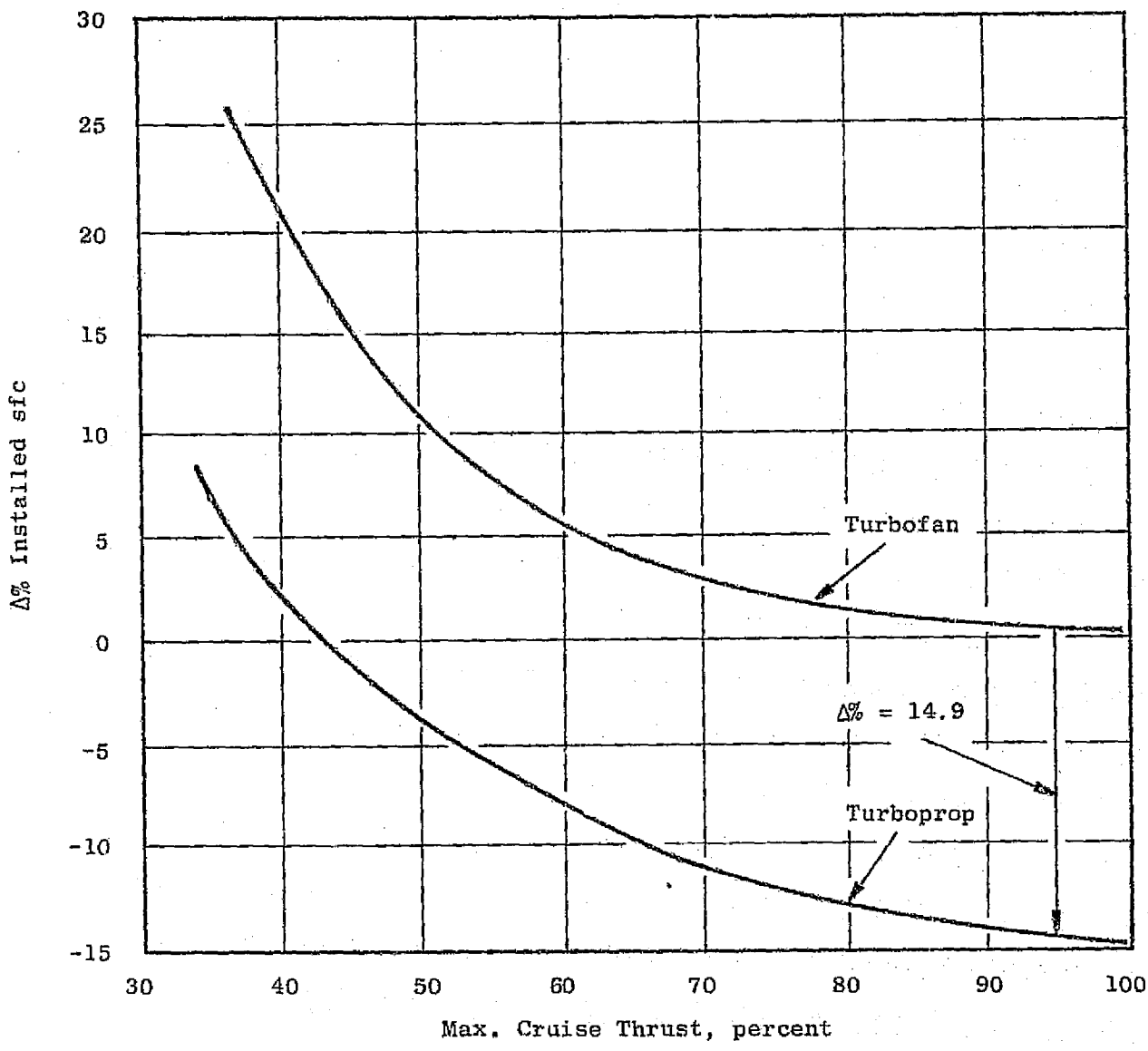

Figure 23. Part-Power sfc Trend, Turboprop Vs. Turbofan.

the booster stator vanes are closed to provide flow matching as power is reduced. This is done to keep propeller efficiency high at lower thrusts.

Engine weight, cost, and maintenance estimates were made and added to the gearset and propeller information supplied by Hamilton Standard Division. Similar estimates were made for the nacelle, including the pylon, to arrive at overall installed weights and costs. The results, when scaled into the proper installed mission thrust, are shown in Tables XXVIII, XXIX, and XXX for the three technology levels in the transcontinental mission.

Because of the more refined evaluation, some of the Task II results for the turboprop differ in some degree from the Task I parametric analysis presented in this section. For the base-technology case, for example, an installed sfc reduction of 14.9% is offset partly by a weight increase of 680 kg (1500 lb). The net result, however, is still a substantial fuel saving of 14.8%. There is also an engine price increase of 7.7% which, together with the other factors (including a small maintenance reduction), results in a 3.4% lower DOC. Similar results are obtained for the other cases, with the largest gains seen for the counterrotating propeller.

3.7.1 Shrouded Propeller

A brief study of a shrouded propeller was undertaken. The shrouded propeller represents a hybrid between a conventional propeller and a very high bypass turbofan.

The shrouded propeller has two possible advantages over the conventional propeller: first, the use of outlet guide vanes will recover the swirl energy usually lost in the single-rotation propeller; second, due to the higher pressure ratio, the diameter can be reduced from that of a conventional propeller of equal thrust. The disadvantages of the shrouded propeller are the weight and drag associated with the cowl. The design conditions chosen for this study are listed in Table XXXI. The very large, variable-pitch fan, or propeller, installation is shown schematically in Figure 24.

An engine evaluation, using a fan efficiency of 90% and a short, minimum-weight inlet and cowl, is presented in Table XXXII. Only a very small improvement in bare engine sfc was obtained. The installed sfc is 5.2% higher than the turboprop because of the fan cowl drag which is 12.9% of the thrust. When combined with a 907 kg (2000 lb) weight increase, the net effect is a large fuel increase relative to the turboprop.

If the cowl pressure drag is arbitrarily taken at 50% of the friction drag, the sensitivity curves of Figure 25 show that the mission fuel would still be 6% higher than the turboprop. No further study of the shrouded propeller was undertaken because of the undesirable fuel usage, relative to the conventional propeller, that was indicated.

Table XXVIII. Base-Technology, Single-Rotation Turboprop Vs. Baseline Turbofan.

Common Features:

- Constant Cycle P/P and T_{41}
- Advanced Core Components
- Four-Engine, 5560 km (3000 nmi), Transcontinental, 200 PAX Aircraft
- \$79.2/m^3 (30¢/gal) Fuel
- Evaluation at 55% Average Mission Load Factor, 1300 km (700 nmi) Mission
- 95% Max. Cruise, 10,670 m (35,000 ft), Mach 0.8

	Advanced Turbofan	Base Technology Turboprop	Δ
F_n Bare, N	14,390	15,070	
(lbf)	(3235)	(3388)	
sfc, Δ%	Base		-16.1
Drag/F_n Bare, %	5.7	6.9	
F_n Installed, N	13,580	13,970	
(lbf)	(3052)	(3140)	
sfc Installed, Δ%	Base		-14.9
Engine Weight, kg	673	457	-215
(lbm)	(1483)	(1008)	(-475)
Prop and Gear Weight kg	-	903	903
(lbm)	-	(1990)	(1990)
Nacelle Weight (including Pylon), kg	547	540	-7.3
(lbm)	(1206)	(1190)	(-16)
Total Installed Weight, kg	1220	1900	680
(lbm)	(2689)	(4189)	(1500)
Initial Installed Price, Δ%	Base	107.7	7.7
Maintenance L&M, Δ%	Base	96.5	-3.5
TOGW, Δ%	Base		-0.67
Block Fuel, Δ%	Base		-14.8
DOC, Δ%	Base		-3.4
ΔROI, Points	Base		-0.03

Table XXIX. Base-Technology, Single-Rotation Turboprop Vs. Baseline Turbofan.

Common Features:

- Constant Cycle P/P and T_{41}
- Advanced Core Components
- Four-Engine, 5560 km (3000 nmi), Transcontinental, 200 PAX Aircraft
- \$79.2/m^3 (30¢/gal) Fuel
- Evaluation at 55% Average Mission Load Factor, 1300 km (700 nmi) Mission
- 95% Max. Cruise, 10,670 m (35,000 ft), Mach 0.8

	Advanced Turbofan	Base Technology Turboprop	Δ
F_n Bare, N	14,390	15,070	
(lbf)	(3235)	(3388)	
sfc, Δ%	Base		
Drag/F_n Bare, %	5.7	6.9	-16.1
F_n Installed, N	13,580	13,970	
(lbf)	(3052)	(3140)	-14.9
sfc Installed, Δ%	Base		-215
Engine Weight, kg	673	457	(-475)
(lbm)	(1483)	(1008)	
Prop and Gear Weight kg	-	823	
(lbm)	-	(1815)	
Nacelle Weight (including Pylon), kg	547	540	-7.2
(lbm)	(1206)	(1190)	(-16)
Total Installed Weight, kg	1220	1820	601
(lbm)	(2689)	(4013)	(1324)
Initial Installed Price, Δ%	Base	100	0
Maintenance L&M, Δ%	Base	96.0	-4.0
TOGW, Δ%	Base		-1.4
Block Fuel, Δ%	Base		-15.3
DOC, Δ%	Base		-3.5
ΔROI, Points	Base		-0.02

Table XXX. Counterrotating Turboprop Vs. Baseline.

Common Features:

- Constant Cycle P/P and T_{41}
- Advanced Core Components
- Four-Engine, 5560 km (3000 nmi), Transcontinental, 200 PAX Aircraft
- \$79.2/m^3 (30¢/gal) Fuel
- Evaluation at 55% Average Mission Load Factor, 1300 km (700 nmi) Mission
- 95% Max. Cruise, 10,670 m (35,000 ft), Mach 0.8

	Advanced Turbofan	Base Technology Turboprop	Δ
F_n Bare, N	14,390	14,230	
(lbf)	(3235)	(3200)	
sfc, Δ%	Base		-20.7
Drag/F_n Bare, %	5.7	6.9	
F_n Installed, N	13,580	13,190	
(lbf)	(3052)	(2966)	
sfc Installed, Δ%	Base		-19.5
Engine Weight, kg	673	425	-247
(lbm)	(1483)	(938)	(-545)
Prop and Gear Weight kg	-	900	
(lbm)	-	(1984)	
Nacelle Weight (including Pylon), kg	547	507	-40
(lbm)	(1206)	(1118)	(-88)
Total Installed Weight, kg	1220	1833	613
(lbm)	(2689)	(4040)	(1351)
Initial Installed Price, Δ%	Base	103.7	3.7
Maintenance L&M, Δ%	Base	97.0	-3.0
TOGW, Δ%	Base		-4.0
Block Fuel, Δ%	Base		-20.8
DOC, Δ%	Base		-5.2
ΔROI, Points	Base		+0.12

Table XXXI. Shrouded Turboprop Vs. Baseline Turbofan.

- Prop and Gear Data Supplied by Hamilton Standard Div. Under Subcontract

	Baseline Turbofan Mixed Flow	Shrouded Prop* Separate Flow
Gear Type	Direct Drive	Epicyclic 2-Stage Reduction GR = 9.0
Prop/Fan N_B	28	6
$U_T/\sqrt{\theta}$, m/sec (ft/sec)	494 (1620)	229 (750)
U_T, m/sec (ft/sec)	466 (1530)	216 (710)
P/P	1.71	1.08
Overall P/P Max. Climb*	38	38
Max. Climb* T_{41}, ° C ° F	1370 (2500)	1370 (2500)
Takeoff T_{41}, ° C ° F	1430 (2600)	1430 (2600)
Core Extraction $F_{n\ Core}/F_{n\ Total}$, %	29	10
Inlet Ram Recovery	1.0	1.0
Fan Nozzle Velocity Coefficient	-	0.999
Core Nozzle Velocity Coefficient	0.997	0.997
Core Compressor P/P	14	14
Supercharge P/P	2.75	2.75
LP Component Efficiency	Advanced Technology	

*10,670 m (35,000 ft), Mach 0.8, Max. Climb.

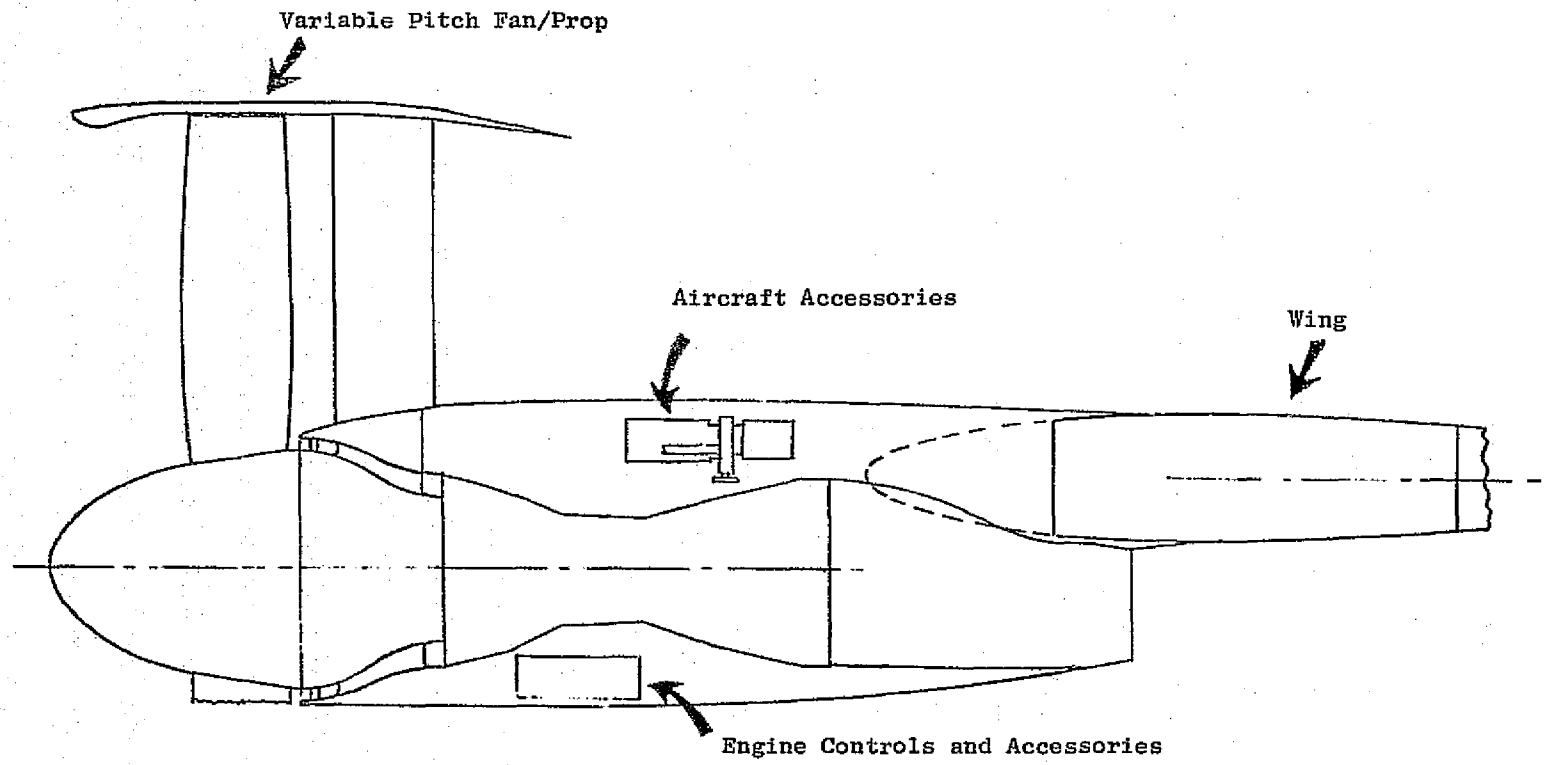

Figure 24. Shrouded-Propeller Installation.

Table XXXII. Shrouded-Propeller Engine Evaluation.

- Constant Cycle Pressure Ratio, Advanced Core Components
- Installed in a Four-Engine, 5560 km (3000 nmi) Transcontinental Aircraft, 200 PAX
- Evaluation at 55% Load Factor, 1300 km (700 nmi) Mission, 79.2 $/m^3 (30 ¢/gal) Fuel

	Turbofan	Single-Rotation Turboprop	Shrouded Prop
Fan/Prop Diameter, m (ft)	1.3 (4.3)	4.0 (13.2)	3.36 (11.00)
Bare F_n (1), N (lbf)	14,390 (3,235)	15,070 (3,388)	16,010 (3,600)
sfc (1), Δ%	Base	-16.1	-16.5
Drag/F_n	5.7	6.9	12.9
Installed F_n, N (lbf)	1,384 (3,052)	1,424 (3,140)	1,424 (3,140)
Installed sfc, Δ%	Base	-14.9	-10.5
$W_{2C}\sqrt{\theta}/\delta$, kg/sec (lbm/sec)	13.3 (25.0)	18.1 (33.9)	17.8 (33.4)
Engine Weight, kg (lbm)	673 (1,483)	457 (1,008)	880 (1,940)
Prop and Gear Weight, kg (lbm)	- -	903 (1,990)	1,061 (2) (2,340)
Nacelle Weight, kg (lbm)	547 (1,206)	540 (1,190)	653 (1,440)
Total Installed Weight, kg (lbm)	1,220 (2,687)	1,900 (4,189)	2,594 (5,720)
Δ Weight, kg (lbm)	Base Base	+680 (+1,500)	+1,374 (+3,030)
DOC, Δ%	Base	-3.4	+2.4 (3)
W_f, Δ%	Base	-14.8	-5.4

(1) 10,670 m (35,000 ft), Mach 0.8, 95% Max. Cruise
(2) Includes fan rotor assembly and gear
(3) Includes no propulsion system price difference between turboprop and shrouded prop

- No Cost Effects Included
- Transcontinental 5560 km (3000 nmi) Design
- Evaluation at 55% Load Factor, 1300 km (700 nmi) Mission

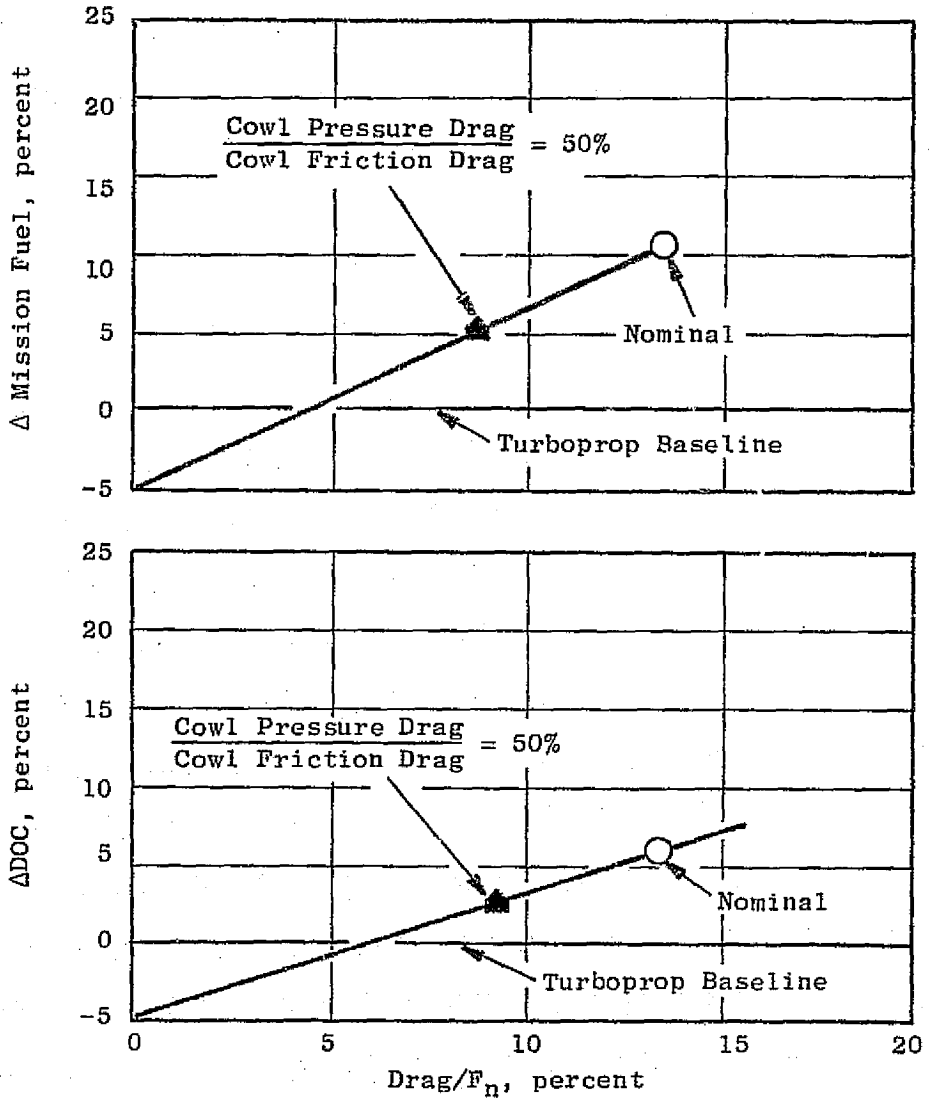

Figure 25. Shrouded-Propeller Sensitivity to Shroud-Drag Estimate.

3.8 RECOMMENDATIONS FOR TASK II

Preliminary evaluation results from the Task I parametric analysis are summarized in Figure 26. These results formed the basis for selecting the engines recommended for refined analysis in Task II. The selected engines were:

Geared 1.55 Pressure Ratio Fan - With the assumption that the forward-booster evaluation trends of fan pressure ratio apply to the aft-booster arrangement, this engine had a potential 4 to 5% fuel savings and a potential 1% DOC reduction over the advanced, baseline, direct-drive turbofan. The aft-booster version showed both a fuel-used and DOC advantage relative to the more unconventional forward-boost arrangement. A fan pressure ratio of 1.55 was selected as representing a good balance between fuel savings and DOC reduction.

Geared 1.55 Pressure Ratio Fan, Variable Aft Boosters - The variable-boost feature showed a potential for further fuel savings and DOC reduction for the cruise-sized configuration.

Turboprop with Single Rotation - The single-rotation turboprop showed approximately 14% fuel savings in the transcontinental mission. The counter-rotating propeller was not chosen; it was considered too great a development risk relative to the current propeller-technology base.

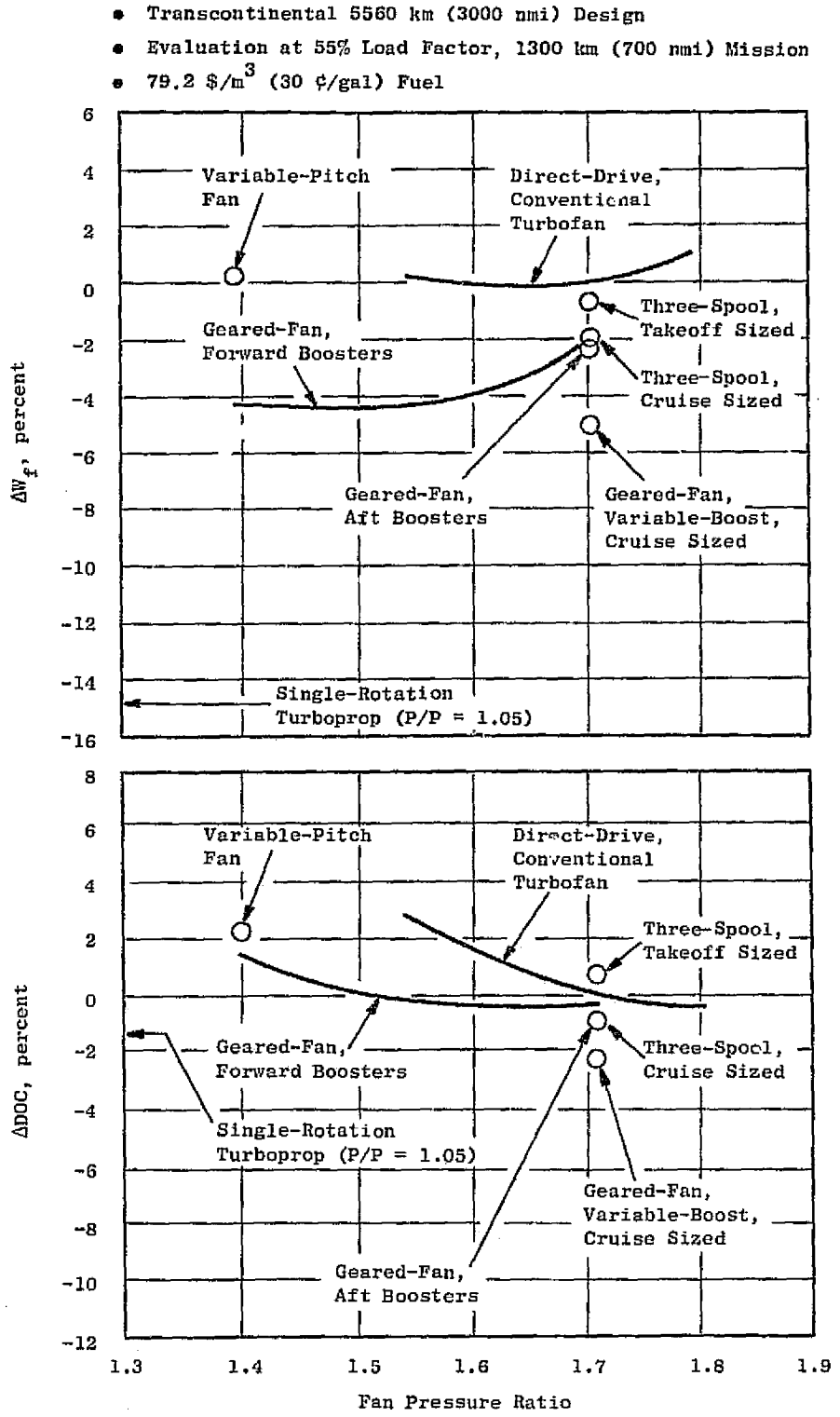

Figure 26. Summary of Task I Parametric Study Results.

SECTION 4.0

SUMMARY OF TASK I RESULTS

The results of the cycle investigations involving heat exchangers are summarized in Table XXXIII. There was a potential bare-engine advantage of 5 to 10%, relative to a high pressure ratio conventional cycle, for the regenerative cycles with a moderate pressure drop and regenerators located at the turbine exit; however, the physical size of the regenerator was such that there was a loss in installed sfc when nacelle drag was taken into account. The only system that showed a potential for an improvement in installed sfc involved an advanced rotory regenerator in an interturbine location. Although Task I studies did not show any appreciable advantage in fuel usage for this cycle, because of the high weight estimated, the interturbine regenerator cycle and design data were reviewed and updated in the Task II studies to confirm the results obtained in Task I.

Results of the novel engine-arrangements investigations are summarized in Table XXXIV. The geared fan showed sufficient potential for improved fuel consumption to be recommended for Task II. Of the various geared-fan arrangements evaluated, the more conventional aft-booster arrangement was selected. A parametric study, summarized in Figure 27, was conducted in which the 1.55 fan pressure ratio cycle was selected for the geared-fan engine.

The geared variable-boost concept indicated a potential for improvement in fuel usage due to the higher cruise cycle pressure ratio possible with the cruise-sized engines. This concept was applied to both the geared turbofan and the turboprop in Task II.

The results of the Task I investigation of turboprops for Mach 0.8 transports are summarized in Table XXXV. A large potential for improved fuel usage was indicated for the 80% level of propeller efficiency estimated for the Hamilton Standard high disc-loading design. Although the counter-rotating propeller concept showed a greater improvement in fuel usage, the joint recommendation of General Electric and Hamilton Standard was to focus on the single-row/rotation propeller for Task II.

Table XXXIII. Summary of Heat-Exchanger Cycles.

- Regeneration: Potential Advantage of 5 to 10% in Bare Engine sfc.
- Intercooling and Reheat Concepts: No Payoff
- Most Promising Regenerative Engine:
  - Interturbine Rotary Regenerator with Advanced Ceramic Elements - 1.55 Fan Pressure Ratio
  - 6.5% Improvement in Installed sfc Versus Baseline
  - 60% Installed Weight Penalty
  - Small Net Effect on Fuel Usage, Large Increase in DOC
- Similar Results Would Be Obtained For Turboprop

Table XXXIV. Summary of Novel Engine Arrangements.

- Geared Fans
  - Aft Booster Arrangement: Slightly Better than Front Boost
  - Fan Pressure Ratio = 1.55, Bypass 9.5
  - 4.5% Improvement in Fuel Usage, Small Potential Improvement in DOC.
- Very High Bypass Fans
  - Neither Fixed- or Variable-Pitch Versions Showed any Advantage
- Variable-Boost Concept
  - Showed +2% Fuel-Usage Improvement: Benefit in DOC only if Cruise Sized
  - Could also be applied to Engines with Variable Aft Boosters
- Recommended for Task II Refined Analysis
  - Geared Fan with 1.55 Fan Pressure Ratio, Aft Boosters, Baseline Core
  - Normal and Variable-Boost Versions of Above.

- Transcontinental 5560 km (3000 nmi) Design
- Evaluation at 55% Load Factor, 1300 km (700 nmi) Mission
- 10,670 m (35,000 ft), Mach 0.8, +10° C (+18° F), 95% Max. Cruise

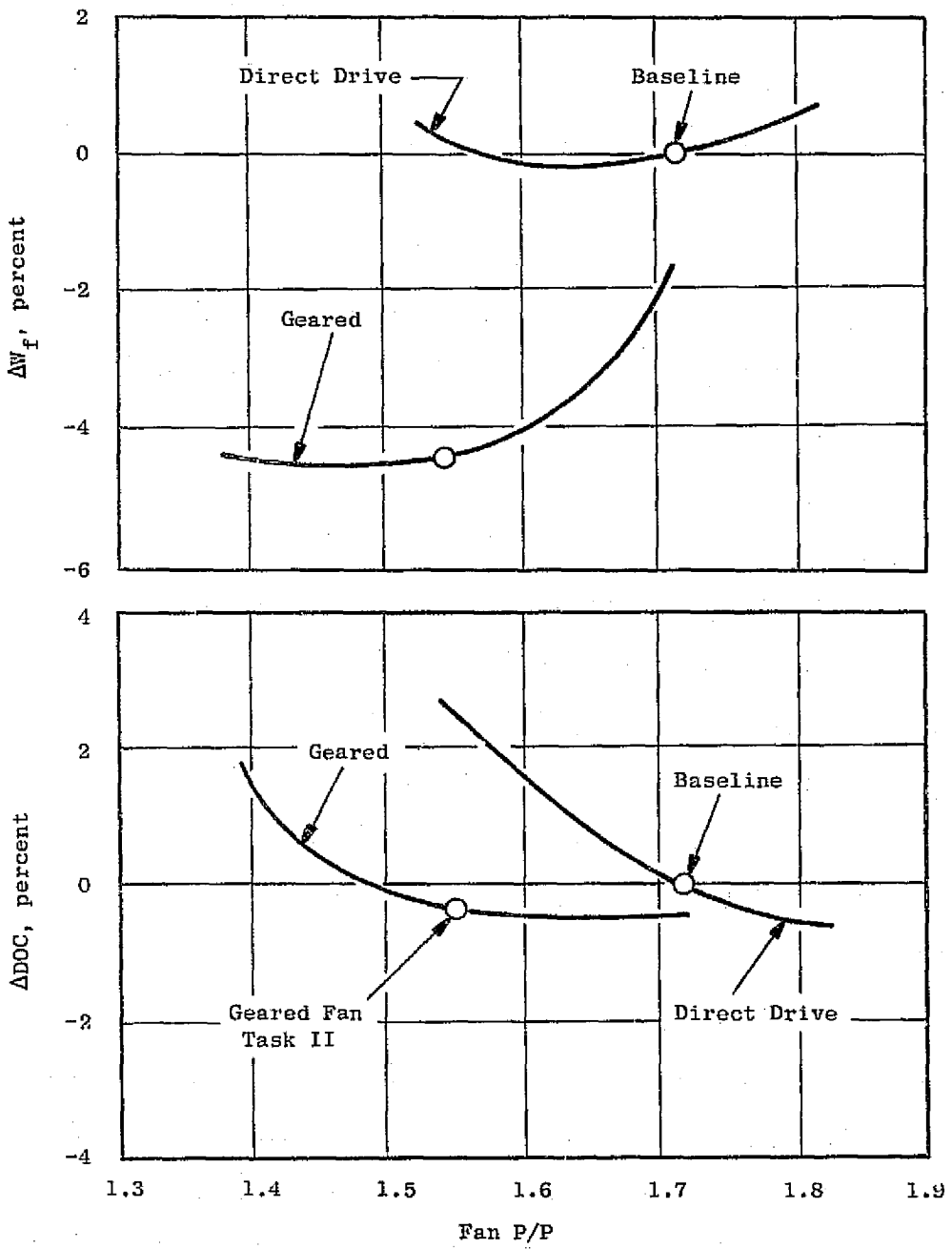

Figure 27. Engine Evaluation: Geared Vs. Direct-Drive Fan.

Table XXXV. Summary of Turboprops.

- Installed sfc Improvement of 15% Estimated using Hamilton Standard Propeller Data.
- Installed Weight Penalty: 60% for Same Installed Cruise Thrust
- Impact Upon Aircraft (Four-Engine Turboprop versus Four-Engine Turbofan Transcontinental):
  - 14% Improvement in Fuel Usage
  - About the Same TOGW
  - Impact upon DOC Uncertain Because of Related Assumptions
- Advanced Counterrotating Propeller Increased sfc Advantage 4.5%
- Shrouded Propeller: Weight and Drag of Shroud Negated any Performance Advantage
- Recommended for Task II Refined Analysis:
  - High Disc-Loading, Single-Row Propeller with Offset Gearset, Hamilton Standard Data
  - Turboprop Engine, LP Compressor on Same Spool as Propeller, Baseline Core Engine
  - Under-Wing Installation

SECTION 5.0

TASK II REFINED EVALUATION

5.1 BASELINE ENGINE AND INSTALLATION

Presented in Figure 28 is a cross-section view of the installed baseline engine used for comparative purposes in this study and in Figure 29 a cross section of the baseline engine itself.

As can be noted in Table XXXVI, many advanced design features, that were derived and evaluated during the NASA-sponsored STEDLEC contract (NAS3-19201) studies (References 1 and 2), have been incorporated into the engine.

5.1.1 Basic Engine Design Features

Extensive use of composite materials was made both in rotating and in stationary parts. To improve the overall LP system efficiency, an advanced high tip speed fan aerodynamic design was utilized to lower the loading as much as possible on the direct-drive LPT.

Clearance control was used in both passive (in the HPC) and active (in the HPT) forms.

A double-annular design combustor with a primary (low power) and secondary (high power) combustor zone was used to provide low emissions. The primary combustors were used to maintain a rich, low power, combustion process to reduce HC and CO emissions at low power settings; on the other hand, the secondary combustor was fueled at higher power settings for a leaner, low NO_x, combustion process.

The high pressure turbine utilized advanced, directionally solidified, blade materials with impingement and film cooling. Ceramics were incorporated into the inner and outer HPT vane bands and over the HPT blade as an abradable shroud.

The low pressure turbine utilized cooling on the first-stage blades and the first- and second-stage vanes.

Advanced, directionally solidified (DS) blades were used in stage 1 and 2 of the LPT. High aerodynamic loading was employed to reduce the number of stages to four with a deswirl vane-frame used for the exhaust frame. High aspect-ratio blading was used in the last two stages to raise the pure-tone frequencies out of the most bothersome range of perceived noise.

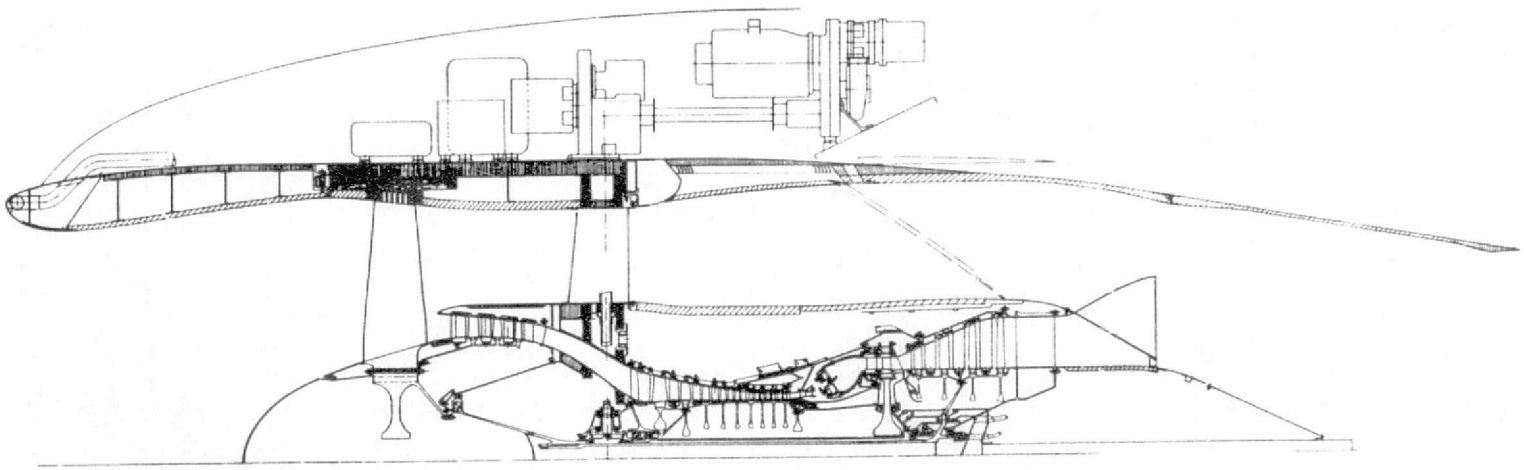

Figure 28. Baseline Installation.

- 10,670 m (35,000 ft), Mach 0.8, +10° C (+18° F), Max. Climb

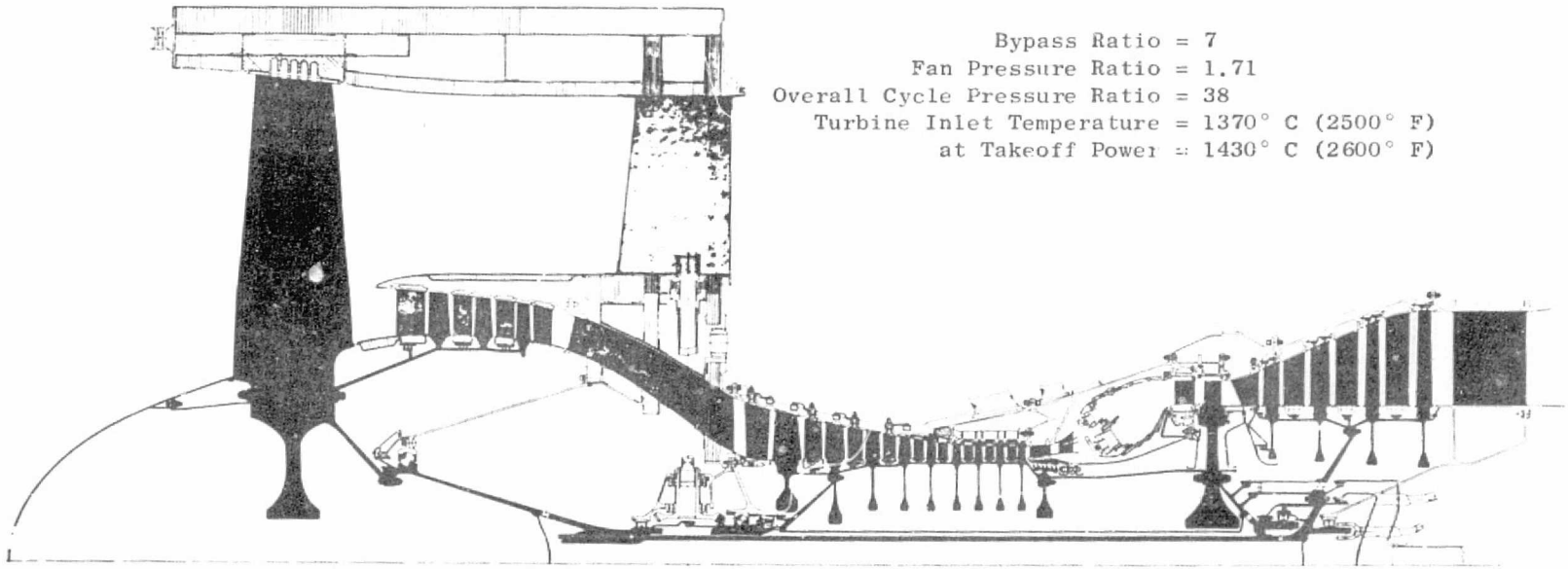

Figure 29. Baseline Engine.

Table XXXVI. Baseline-Turbofan, Advanced-Design Features.

Fan	Composite Blades
	High Tip Speed [494 m/sec (1620 ft/sec)], 1.7 P/P
	Composite Vane/Frame, Fan Case and Containment
Core Compressor	High $U_T/\sqrt{\theta}$ [523 m/sec (1750 ft/sec)], 14:1 P/P in 9 Stages
	Clearance Control Casing
Combustor	Double Dome for Low Emissions
High Pressure Turbine	
	Single Stage with 4:1 P/P
	Active Clearance-Control Features
	Advanced Ni-Base DS Blades with Film/Impingement Cooling
	Ceramic Shrouds and Nozzle Bands
Low Pressure Turbine	
	High Aerodynamic Loading
	Advanced Ni-Base DS Blades, Stage 1 Cooled
	High Aspect Ratio and Increased Spacing on Rear Stages, Turbine-Noise Reduction

5.1.2 Installation Design Features

The baseline-installation layout for the turbofan engine is shown in Figure 28. The general installation features are listed in Table XXXVII. All cold parts are advanced composite materials. The portion of the nacelle over the fan is integrated with the fan casing and frame. The design is axisymmetric except for the accessories and pylon.

Table XXXVII. General Turbofan Installation Design Features.

- Short, Thin Inlets
- Long Duct, Mixed Flow: 75% Effectivity
- FAR 36 minus 10 Goal
- Inlet Bulk Absorber; Fan Duct: Phased M.D.O.F
- Exhaust: High Frequency LPT and S.D.O.F
- Integrated Fan Casing/Cowl/Frame
- Nonbifurcated, Cascade-Type, Fan Reverser
- No Core Reverser, Core Spoiling
- Engine Accessories Under Pylon Cowl
- Aircraft Accessories in Pylon Strut
- Advanced Composites

The inlet is thin, relative to current practice, since it is based on a high ratio of highlight diameter to maximum diameter, consistent with cruise at Mach 0.8. The honeycomb-reinforced outer wall is joined to the acoustic structure of the inner wall by circumferential webs; inlet acoustic treatment is bulk absorber material packed into cells of composite material. The forward lip is anti-iced; the aft end of the inlet is supported by the fan cas casing.

The fan reverser, duct, and nozzle transmit all axial loads into the fan casing. The reverser cascades are covered by internal blocker doors and outer translating cowls. The mixed-flow exhaust system is designed for a mixing effectiveness of 75% and ends in a converging-diverging nozzle.

The engine-accessories gearbox is mounted on the fan casing and is covered by an extension of the pylon shroud. A horizontal power-takeoff shaft connects to the aircraft-accessory gearbox mounted on the pylon strut. The shaft is disconnected to remove the engine, leaving the aircraft accessories undisturbed.

The acoustic treatment in the fan casing, the blocker doors of the reverser, the fan duct, and the core cowl are integrated into a phased, multiple-degree-of-freedom system. The low pressure turbine is designed for high acoustic frequency and the tail cone contains single-degree-of-freedom (S.D.O.F.) treatment. All of this acoustic treatment is structurally integrated with the components to increase strength and stiffness.

5.2 REGENERATIVE ENGINE

5.2.1 Regenerative Engine Cycle

As a result of the preliminary screening of heat-exchanger cycles, the interturbine-regenerator engine was chosen for further investigation. The basic concept of this cycle involves extraction of heat between the high and low pressure turbines and returning it to the combustor inlet.

A parametric study, the results of which are presented in Figure 8, led to selection of a cycle for Task II. The cycle was chosen to have an overall design-point pressure ratio of 32 which yielded a minimum sfc. A maximum turbine takeoff inlet temperature of 1540° C (2800° F) was selected since a higher value would have required cooling the regenerator hot-side ducting. The design fan pressure ratio was set at 1.55 since this yielded better installed sfc than the 1.71 fan pressure of the baseline engine. The selected cycle is defined and compared with two conventional cycles in Table XXXVIII and XXXIX. The booster, core, and turbine-stage parameters are compared at the aerodynamic design point for the regenerative engine and two turbofan engines in Table XL.

One significant item to be noted for the interturbine regenerative engine is the bypass ratio level. The bypass ratio of the regenerator-engine is 7.0; however, the geared engine at the same fan pressure ratio is 9.9. The point to be made is that, for a given level of thrust, the regenerative cycle requires a larger core engine; this is due to the low temperature of the flow entering the LPT which reduces the energy available per kg/sec (lb/sec) of core flow.

A separate-flow configuration was chosen for two reasons: first, the temperature in the core stream exhaust is low, therefore relatively little thermal efficiency improvement can be achieved from mixing; second, a separate-flow system integrates well with the overall engine configuration.

The heat exchanger chosen for this study was a rotating ceramic drum wrapped around the core engine as shown in Figure 30. This configuration was chosen because it had the minimum impact on engine length or diameter.

Table XXXVIII. Regenerative Engine Vs. Baseline Direct-Drive Engine (Pressure Ratio 1.71).

- Trijet, 5560 kg (3000 nmi) Design
- Evaluation at 55% Load Factor, 1300 km (700 nmi) Mission

	Sea Level Static, +15° C (27° F), Takeoff		10,670 m (35,000 ft), Mach 0.8, -10° C (18° F), Max. Climb Aerodynamic Design Point	
	Baseline	Regenerative, Direct Drive	Baseline	Regenerative, Direct Drive
F_n, N (lbf)	88,960 (20,000)	85,080 (19,127)	23,440 (5270)	24,050 (5407)
Drag/F_n, %			4.9	7.3
Installed F_n, N (lbf)	88,960 (20,000)	85,080 (19,127)	22,290 (5010)	22,290 (5010)
sfc, Δ%			Base	-4.8
Installed sfc, Δ%			Base	-3.0
Bypass Ratio	7.5	7.3	6.9	7.0
Overall P/P	30	24	38	32
T_{41}, ° C (° F)	1430 (2600)	1540 (2800)	1370 (2500)	1480 (2700)
Fan D_T, m (in.)			1.55 (61.2)	1.89 (74.4)
Fan $W\sqrt{\theta}/\delta$, kg/sec (lbm/sec)			342 (755)	507 (1117)
Fan-Tip Pressure Ratio			1.71	1.55
Fan $W\sqrt{\theta}/\delta$ AA, kg/sec-m^2 (lbm/sec-ft^2)			211 (43.2)	211 (43.2)
Fan R_H/R_T			0.38	0.38
Fan Hub Pressure Ratio			1.61	1.48
Fan $U_T/\sqrt{\theta}$, m/sec (ft/sec)			494 (1620)	415 (1360)

Table XXXIX. Regenerative Engine Vs. Geared Fan (pressure Ratio 1.55).

- Trijet, 5560 kg (3000 nmi) Design
- Evaluation at 55% Load Factor, 1300 km (700 nmi) Mission

	Sea Level Static, +15° C (27° F), Takeoff		10,670 m (35,000 ft), Mach 0.8, +10° C (18° F), Max. Climb Aerodynamic Design Point	
	Geared	Regenerative, Direct Drive	Geared	Regenerative, Direct Drive
F_n, N (lbf)	96,700 (21,740)	85,080 (19,127)	23,710 (5330)	24,050 (5407)
Drag/F_n, %			6.0	7.3
Installed F_n, N (lbf)	96,700 (21,740)	85,080 (19,127)	22,290 (5010)	22,290 (5010)
sfc, Δ%			Base	-4.8
Installed sfc, Δ%			Base	-3.0
Bypass Ratio	10.5	7.3	9.9	7.0
Overall P/P	29.2	24	38	32
T_{41}, ° C (° F)	1430 (2600)	1540 (2800)	1370 (2500)	1480 (2700)
Fan D_T, m (in.)			1.72 (67.9)	1.89 (74.4)
Fan $W\sqrt{\theta}/\delta$, kg/sec (lbm/sec)			433 (954)	507 (1117)
Fan-Tip Pressure Ratio			1.55	1.55
Fan $W\sqrt{\theta}/\delta$ AA, kg/sec-m^2 (lbm/sec-ft^2)			211 (43.2)	211 (43.2)
Fan R_H/R_T			0.35	0.38
Fan Hub Pressure Ratio			1.3	1.48
Fan $U_T/\sqrt{\theta}$, m/sec (ft/sec)			396 (1300)	415 (1360)

Table XL. Cycle Conditions.

- 10,670 m (35,000 ft), Mach 0.8, +10° C (18° F), Maximum Climb

Component	Engine	Base	Geared	Regenerator
	P/P	1.71	1.55	1.55
	No. of Stages	3	2	3
Booster	$U_T/\sqrt{\theta}$, m/sec	249	405	232
	(ft/sec)	(816)	(1330)	(760)
	Boost Pressure Ratio	1.71	2.11	1.57
	Boost and Fan Pressure Ratio	2.75	2.75	2.32
Core	$W_{2C}\sqrt{\theta}/\delta$, kg/sec	18.7	17	32
	(lbm/sec)	(41.3)	(38)	(70)
	Pressure Ratio	14	14	14
HPT	No. of Stages	1	1	2
	Pressure Ratio	3.8	3.8	3.46
	ΔH, kJ/kg	488	481	504
	(Btu/lbm)	(210)	(207)	(217)
	$\bar{\psi}_P$	0.87	0.87	0.7
LPT	No. of Stages	4-1/2	3	3
	ΔH, kJ/kg	456	488	351
	(Btu/lbm)	(196)	(210)	(151)
	$\bar{\psi}_P$	1.63	0.77	0.79
	Gear Ratio	Direct	2.6	Direct
Regenerator	ε	---	---	0.90
	Leakage, %	---	---	1.0
	Carryover, %	---	---	2.0
	Core $\Delta P/P$, %	---	---	5.5
	ε Duct $\Delta P/P$, %	---	---	7.5
	Mixing Effectiveness	0.75	0.75	Separated

- 10,670 m (35,000 ft), Mach 0.8, +10° C (+18° F), Max. Climb

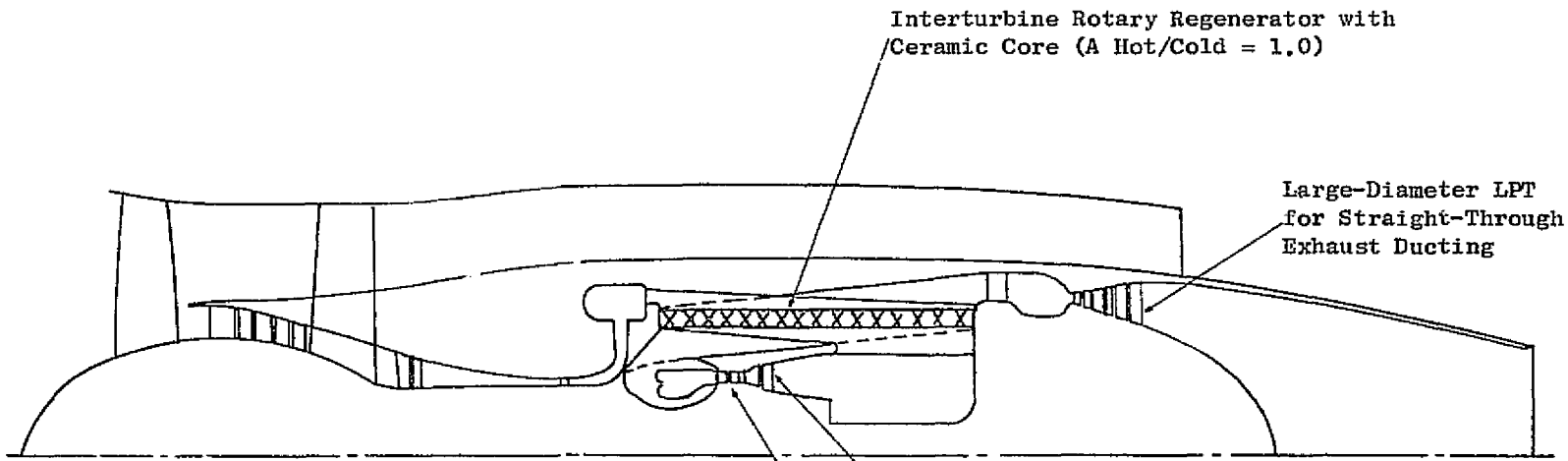

Bypass Ratio = 7
Fan Pressure Ratio = 1.55
Cycle Pressure Ratio = 32
Regenerator Efficiency = 0.9
Total Regenerator Pressure Loss = 8.4%
Turbine Inlet Temperature = 1480° C (2700° F)
At Takeoff Power = 1540° C (2800° F)

Figure 30. Regenerative Turbofan.

The ceramic design was assumed to be an advanced-technology, porous structure of the type described in Table XLI. The regenerator had an effectiveness of 0.9 and, with the regenerator plus ducting, a pressure loss of 12.75%.

The regenerator cycle had a 4.8% bare sfc advantage over the geared engine; the installed sfc advantage was reduced to 3% as a result of the increased drag associated with the installation.

5.2.2 Regenerator Engine Design

The selected engine incorporates a single-stage fan and three booster stages directly driven by an uncooled three-stage low pressure turbine. The nine-stage high pressure compressor is driven by a two-stage turbine. A double-dome, annular combustor was chosen for low emissions.

A two-stage HP turbine design was utilized to reduce the core engine diameter and thereby facilitate installation of the ceramic drum heat exchanger around the core engine.

A large pitch-diameter LP turbine was used to permit the flow leaving the regenerator to enter the LP turbine with a short transition duct and with a minimum of turning. Use of a large pitch diameter allowed the three-stage turbine to direct-drive the 1.55 pressure ratio fan without excessive aerodynamic loading.

There are three main components to the heat-exchanger system. The first component is the ceramic heat-exchanger drum which permits radial flow through tiny, 362/cm^2 (2100/in^2), radial holes in the ceramic. As the drum rotates, hot and cold gas flow in alternate directions through the holes. Hot gas from the HPT exhaust flows radially outward through the drum, heating the ceramic. As the drum rotates it passes into the cold HPC discharge where cold gases flow radially inward to be heated by the ceramic heat exchanger. The alternative gas-flow direction is provided by rotating the drum under the hot and cold discharge ducting. The gas direction reversal should provide a self-cleaning action for the ceramic exchanger.

The second major component of the system is the cold and hot HPC ducting. The cold ducting takes HPC discharge air and passes it radially inward where an opposing duct collects the hot HPC air and transfers it to the combustor.

A third major component of the system is the hot and cold HPT discharge ducting. Cooled nickel-alloy ducting collects the HPT discharge air and passes it outward through the ceramic exchanger. An opposing collector duct on the outside of the drum takes the cooled HPT exhaust and conducts it to a 360° plenum chamber and into the first-stage low pressure turbine vanes.

A high temperature-capability, cast-nickel-alloy duct was used to distribute the high temperature HPT exhaust flow to the ceramic drum. However, to reduce the overall weight of the header and distributor/collector ducts, a Ti-Al alloy was applied. This lightweight alloy was utilized on the HPC

Table XLI. Rotary-Regenerator Design Summary.

W_{2C} Corrected kg/sec (lb/sec)	31.0 (68.4)
Type	Rotary Drum
Material	"Corning 9455" Type
Porosity/Holes cm^2 ($in.^2$)	0.64/372 (2400)
Total Drum Surface Area m^2 (ft^2)	2.71 (29.1)
Diameter, m (ft)	1.0 (3.3)
Thickness, m (ft)	0.4 (0.14)
Length, m (ft)	0.85 (2.8)
A_{Hot}/A_{Cold}	1.0
Weight, kg (lb)	78.9 (174)
Effectiveness	0.90
Angular Velocity, rpm	83
% Carryover	1.7
% Leakage	1.0
$\Delta P/P$ Core, %	5.25
$\Delta P/P$ Ducting, %	7.5

cold side and the LPT cold-side ducting. Use of the advanced alloy, instead of more conventional nickel alloys, reduced the overall weight of metal regenerator structure by 97 kg (210 lb) in the design size.

Figure 31 is a schematic illustrating the regenerator system as related to the core engine. Figure 32 illustrates the flow directions within the regenerator structure itself. The flow circuits were divided in half so an overall pressure-force balance on the regenerator would be achieved, but local pressure unbalances created large forces on the regenerator restraint system.

The unbalanced pressure loads were resisted by two continuous circular beams on each end of the rotary regenerator. All headers, distributors, collector seals, and ceramic-drum bearings and drives were secured to these two beams. Axial restraint was achieved by tying in the aft beam to the aft turbine frame.

5.2.3 Installation Design

The long-duct, separate-flow arrangement was chosen for the regenerative engine based on a trade study of installed sfc. Figure 33 shows the installed regenerator engine compared to the conventional, baseline-turbofan engine. It is apparent that the regenerator engine is considerably longer than its conventional counterpart; this results primarily from the larger core engine and additional length between the turbines. The result is increased weight and cost, relative to the baseline-turbofan installation, even with extensive use of composites in the cooler part of the nacelle and fan duct.

5.2.4 Engine Evaluation

Table XLII presents a comparison of the baseline engine with 1.7 fan pressure ratio, the geared engine with 1.55 fan pressure ratio, and the regenerator engine.

On the basis of fuel burned, the regenerative engine lies between the baseline engine and the geared fan. When compared to an engine of the same fan pressure ratio, the extra weight of the regenerator engine offset the thermal efficiency benefit.

The regenerative engine evaluation indicated a poorer DOC when compared with the conventional cycles. This results from the fact that the regenerator engine required a larger core engine for any given level of thrust; consequently, a heavier and more expensive engine resulted. In addition, the regenerator and associated ducting contributed to the weight and cost penalties of the engine.

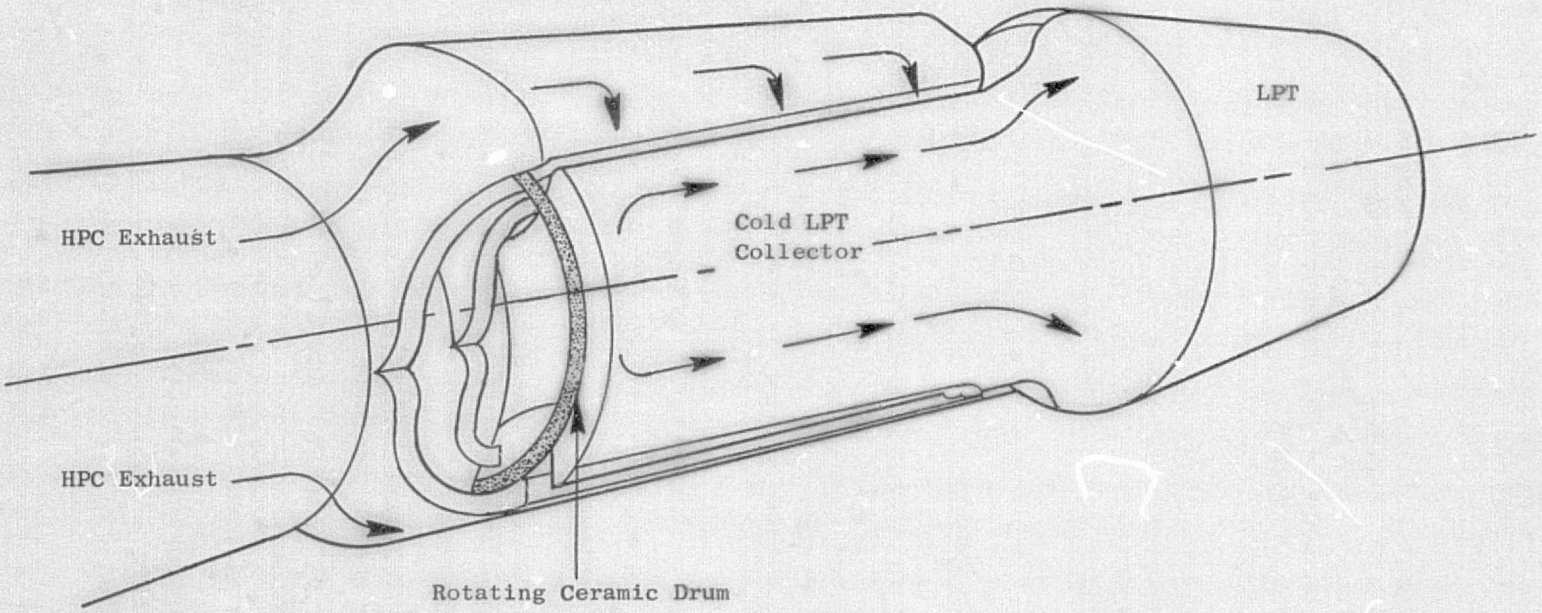

Figure 31. Interturbine Regenerator Exterior Schematic View and Flowpaths.

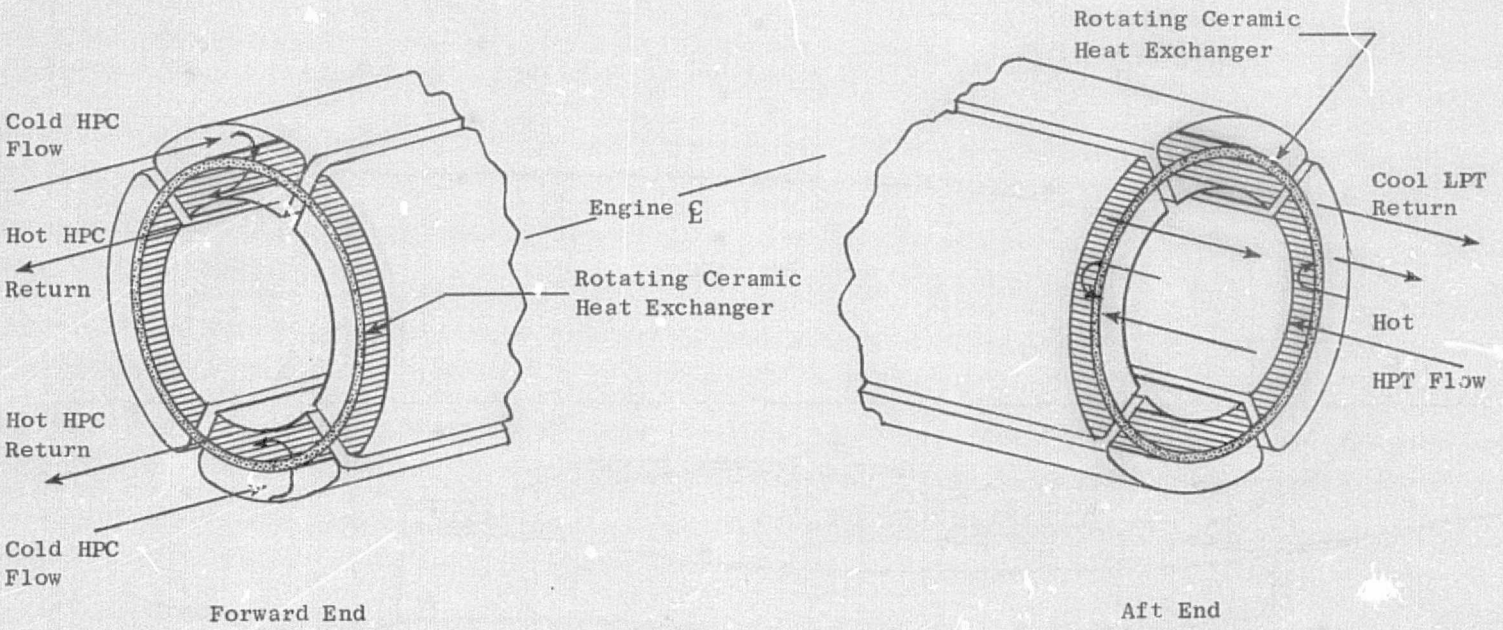

Figure 32. Interturbine Regenerator Flow Schematic.

- Scaled to Same F_n

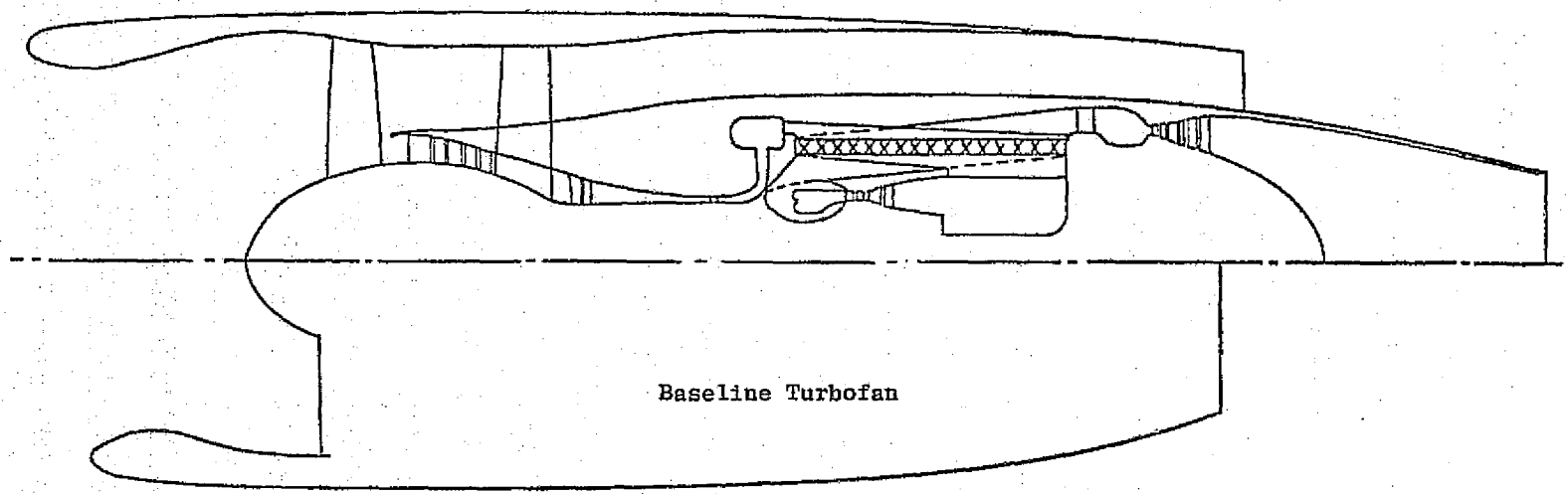

Figure 33. Installed Regenerator Engine Vs. Baseline Turbofan.

Table XLII. Comparison of Regenerative Engine to Baseline and Geared Engines.

- Trijet 5560 km (3000 nmi) Design
- Evaluation at 55% Load Factor, 1300 km (700 nmi) Mission
- $79.2/m^3$ (30¢/gal) Fuel

	Baseline, Pressure Ratio 1.71 Turbofan	Regenerative Turbofan, P/P = 1.55			Geared Fan, Pressure Ratio 1.55	Regenerative Turbofan, P/P = 1.55		
		Δ's	ΔDOC%	ΔW_f%		Δ's	ΔDOC%	ΔW_f%
Engine Weight, kg (lb)	1070 (2360)	+1116 (+2460)	+4.1	+6.3	+1100 (2425)	+1084 (2390)	+4.0	+6.1
Engine Initial Price, Δ%	Base	+44.9	+2.0	0	Base	+37.9	+1.87	
Engine Maintenance, Δ%	Base	+37.9	+1.9		Base	+35.0	+1.83	
*sfc, Δ%	Base	-10.9	-4.3	-11.9	Base	-4.8	-0.9	-5.2
Subtotal			+3.7	-5.6			+5.8	+0.9
**Installed Weight, kg (lb)	803 (1770)	+367 (+810)	+1.36	+2.1	984 (2170)	+186 (+410)	+0.7	+1.05
**Installed Price, Δ%	Base	29.0	+0.7	---	Base	11.9	+0.33	---
**Drag/F_n, % (*)	4.9	+2.4	+1.14	+2.9	6.0	1.3	+0.77	-1.95
Subtotal (Installed Δ's)			+3.20	+5.0			+1.80	+3.0
Installed sfc, Δ%	Base	-8.2			Base	-3		
Totals			+6.9	-0.6			+7.6	+3.9

* 10,670 m (35,000 ft), Mach 0.8, +10° C (18° F), 95% Max. Cruise

** Includes Pylon

5.3 GEARED TURBOFANS

5.3.1 Geared-Fan Engine Cycle Definition

The cycle and performance features of the 1.55 pressure ratio geared fan are compared with those of the baseline engine in Table XLIII with both sized for the transcontinental mission. The indicated installed sfc improvement is 5.3% due to a combination of propulsive efficiency gain and better fan and fan turbine efficiencies.

The variable-boost feature was added and is compared to the nonvariable-boost, geared fan in Table XLIV. The installed sfc reduction was improved from 5.3 to 6.7% due to the cycle pressure ratio increase to 45:1 from 38:1 at the design point. The rolling takeoff thrust decreased from 72300 N (16260 lbf) to 64100 N (14410 lbf) for the variable-boost, geared fan, a factor to be considered when evaluating the application of such an engine.

For comparison, the sfc results are superposed on the previous Task I trends in Figure 34.

5.3.2 Geared-Fan Engine Design and Installation

Two 1.55 pressure ratio geared-fan engines were considered in Task II: one with fixed boost and the other employing a variable-boost feature.

The geared-fan engine, shown in Figure 35, utilizes a high speed, three-stage LPT that directly drives a two-stage, aft booster and is geared through a 2.63:1 gearset to drive the low tip-speed, composite-blade fan. This arrangement necessitated an intermediate frame (shown between the booster exit and the HPC inlet).

The gearbox was mounted forward of the fan rotor, in the spinner area, to shorten the overall engine length and to enhance gearbox maintenance. Removal of the spinner permits complete inspection and, if necessary, removal of the complete gearset. The fan rotor-suspension design permits on-wing gearset overhaul/replacement if so desired.

The gearset is a six-star epicyclic gear. A schematic of a star gear is shown in Figure 36. Advanced gear and bearing technology was used, coupled with conservative stress levels, to produce a long design-service life. Improved bearing materials were used to provide a smaller gearbox volume and a B10 system bearing life of 36,000 hours. Materials used for the design were capable of allowing full utilization of the lubricating oil temperature capacity. This permits lower cooling oil flow rates and decreased weight and size of the oil cooling and scavenging system.

The core engine was the same as that used for the baseline engine. The first-stage vane and blade of the three-stage LPT were air cooled. An advanced, directionally solidified, blade material was used for the first-

Table XLIII. Comparison of Geared and Baseline Engines.

• Trijet, 5560 km (3000 nmi) Design

		Cruise-Sized, Geared Fan				Baseline, Direct-Drive Turbofan			
Power Rating		Takeoff	Takeoff	Max. Climb	Max. Cruise	Takeoff	Takeoff	Max. Climb	Max. Cruise
Altitude, m (ft)		0 (0)	0 (0)	10,670 (35,000)	10,670 (35,000)	0 (0)	0 (0)	10,670 (35,000)	10,670 (35,000)
Mach No.		0	0.25	0.8	0.8	0	0.25	0.8	0.8
ΔT_{ISA}, °C (°F)		+15 (+27)	+15 (+27)	+10 (+18)	+10 (+18)	+15 (+27)	+15 (+27)	+10 (+18)	+10 (+18)
F_n, N (lbf)		96,700 (21,740)	72,300 (16,260)	23,700 (5330)	21,800 (4890)	68,960 (20,000)	68,500 (15,400)	23,400 (5270)	21,500 (4830)
Drag, N (lbf)				1420 (320)	1420 (320)			1160 (260)	1160 (260)
Installed F_n, N (lbf)				22,300 (5010)	20,300 (4570)			22,300 (5010)	20,300 (4570)
sfc, Δ%					-6.4				Base
Installed sfc, Δ%					-5.3				Base
Bypass Ratio				9.9	10.1			6.9	7.1
Overall Pressure Ratio				37.9	35.7	29.5		38.1	35.9
T_{41}, °C (°F)		1430 (2600)	1430 (2600)	1370 (2500)	1330 (2420)	1430 (2600)	1430 (2600)	1370 (2500)	1330 (2420)
Fan	D_T, m (in.)	1.72 (67.9)	1.72 (67.9)	1.72 (67.9)	1.72 (67.9)	1.55 (61.2)	1.55 (61.2)	1.55 (61.2)	1.55 (61.2)
	$W_2\sqrt{\theta}/\delta$, kg/sec (lbm/sec)			433 (954)				342 (755)	
	Bypass Pressure Ratio			1.55	1.51			1.71	1.65
	$W_2\sqrt{\theta}/\delta$ AA, kg/sec-m^2 (lbm/sec-ft^2)			211 (43.2)				211 (43.2)	
	$U_T/\sqrt{\theta}$, m/sec (ft/sec)			396 (1300)				494 (1620)	
	R_H/R_T			0.35				0.38	
	Hub Pressure Ratio			1.30				1.61	
Booster	No. of Stages	2	2	2	2	3	3	3	3
	$U_T/\sqrt{\theta}$, m/sec (ft/sec)			405 (1330)				249 (816)	
	Boost Pressure Ratio			2.11				1.71	
	Boost and Fan Pressure Ratio			2.75				2.75	
Core	$W_{2C}\sqrt{\theta}/\delta$, kg/sec (lbm/sec)			17.2 (38.0)				18.7 (41.3)	
Compressor Pressure Ratio				14				14	
HPT	No. of Stages	1	1	1	1	1	1	1	1
	Pressure Ratio			3.8				3.8	
	ΔH, kJ/kg (Btu/lbm)			481 (207)				488 (210)	
	$\bar{V}_P$			0.87				0.87	
LPT	No. of Stages	3	3	3	3	4-1/2	4-1/2	4-1/2	4-1/2
	Pressure Ratio			6.4				5.7	
	ΔH, kJ/kg (Btu/lbm)			488 (210)				456 (196)	
	$\bar{V}_P$			0.77				1.63	
	Gear Ratio	2.6	2.6	2.6	2.6	Direct	Direct	Direct	Direct
Mixing Effectiveness		75	75	75	75	75	75	75	75

Table XLIV. Geared Fan Vs. Geared Fan with Variable Booster.

- Trijet, 5560 km (3000 nmi) Design

		Cruise-Sized, Geared Fan				Baseline, Direct-Drive Turbofan			
Power Rating		Takeoff	Takeoff	Max. Climb	Max. Cruise	Takeoff	Takeoff	Max. Climb	Max. Cruise
Altitude, m (ft)		0 (0)	0 (0)	10,670 (35,000)	10,670 (35,000)	0 (0)	0 (0)	10,670 (35,000)	10,670 (35,000)
Mach No.		0	0.25	0.8	0.8	0	0.25	0.8	0.8
ΔT_{ISA}, °C (°F)		+15 (+27)	+15 (+27)	+10 (+18)	+10 (+18)	+15 (+27)	+15 (+27)	+10 (+18)	+10 (+18)
F_n, N (lbf)		96,700 (21,740)	72,300 (16,260)	23,700 (5330)	21,600 (4890)	85,700 (19,270)	64,100 (14,410)	23,700 (5320)	21,700 (4870)
Drag, N (lbf)				1420 (320)	1420 (320)			1380 (310)	1380 (310)
Installed F_n, N (lbf)				22,300 (5010)	20,300 (4570)			22,300 (5010)	20,300 (4560)
sfc, Δ%					-6.4				-7.6
Installed sfc, Δ%					-5.3				-6.7
Bypass Ratio				9.9	10.1			9.5	9.7
Overall Pressure Ratio				37.9	35.7			45.5	42.8
T_{41}, °C (°F)		1430 (2600)	1430 (2600)	1370 (2500)	1330 (2420)	1430 (2600)	1430 (2600)	1370 (2500)	1330 (2420)
Fan	D_T, m (in.)	1.72 (67.9)	1.72 (67.9)	1.72 (67.9)	1.72 (67.9)	1.73 (68.0)	1.73 (68.0)	1.73 (68.0)	1.73 (68.0)
	$W_2\sqrt{\theta}/\delta$, kg/sec (lbm/sec)			433 (954)				434 (956)	
	Bypass Pressure Ratio			1.55	1.51			1.55	1.51
	$W_2\sqrt{\theta}/\delta$ AA_1, kg/sec-m^2 (lbm/sec-ft^2)			211 (43.2)				211 (43.2)	
	$U_T/\sqrt{\theta}$, m/sec (ft/sec)			396 (1300)				396 (1300)	
	R_H/R_T			0.35				0.38	
	Hub Pressure Ratio			1.30				1.30	
Booster	No. of Stages	2	2	2	2	3	3	3	3
	$U_T/\sqrt{\theta}$, m/sec (ft/sec)			405 (1330)				405 (1330)	
	Boost Pressure Ratio			2.11				2.55	
	Boost and Fan Pressure Ratio			2.75				2.75	
Core	$W_{2C}\sqrt{\theta}/\delta$, kg/sec (lbm/sec)			17.2 (38.0)				15.3 (33.8)	
Compressor Pressure Ratio				14				14	
HPT	No. of Stages	1	1	1	1	1	1	1	1
	Pressure Ratio			3.8				4.1	
	ΔH, kJ/kg (Btu/lbm)			481 (207)				509 (219)	
	$\bar{\psi}_p$			0.87				0.89	
LPT	No. of Stages	3	3	3	3	3	3	3	3
	Pressure Ratio			6.4				7.0	
	ΔH, kJ/kg (Btu/lbm)			488 (210)				495 (213)	
	$\bar{\psi}_p$			0.77				0.87	
	Gear Ratio	2.6	2.6	2.6	2.6	2.6	2.6	2.6	2.6
Mixing Effectiveness		75	75	75	75	75	75	75	75

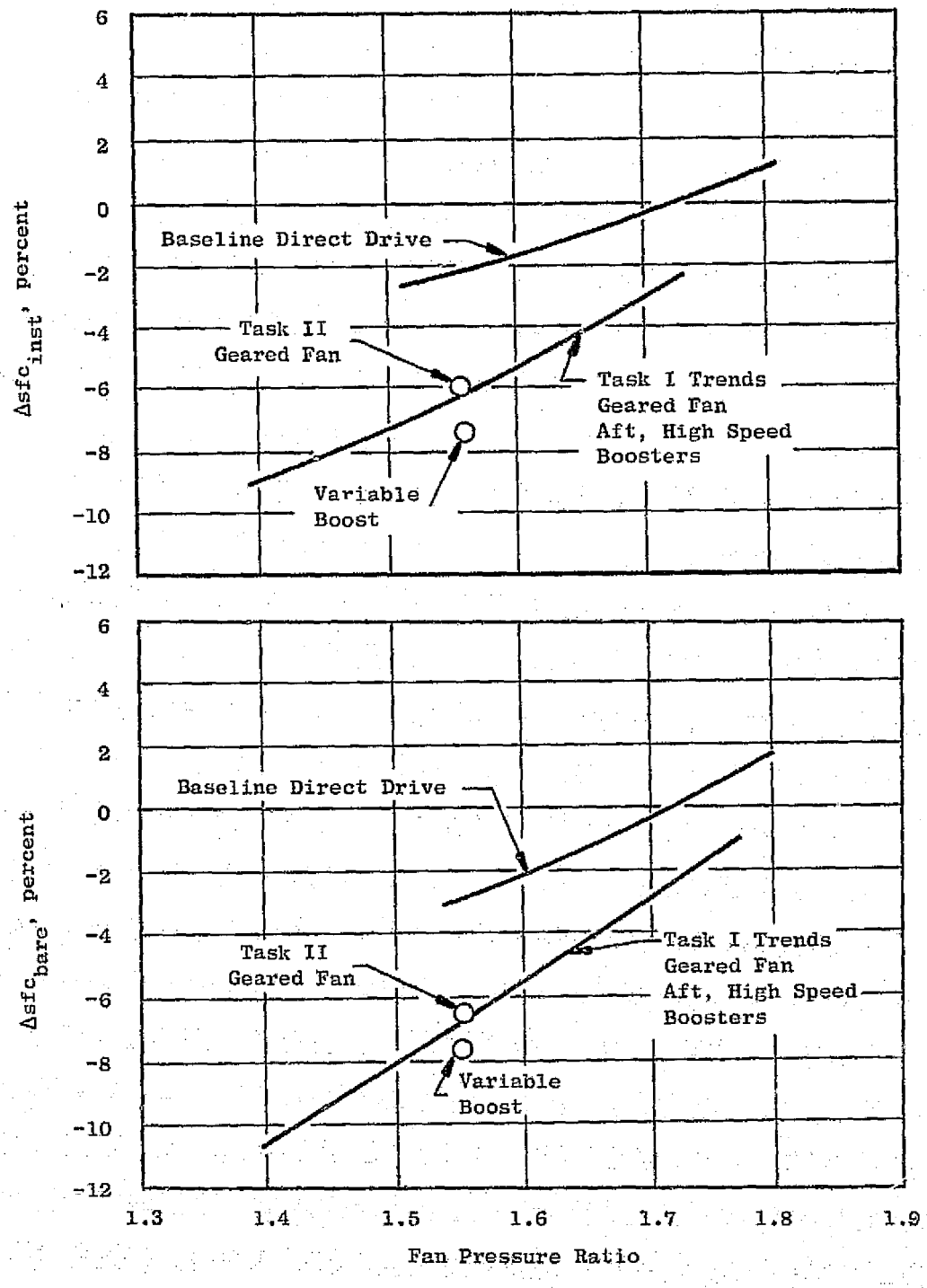

Figure 34. Geared Engines: Bare and Installed sfc Trends.

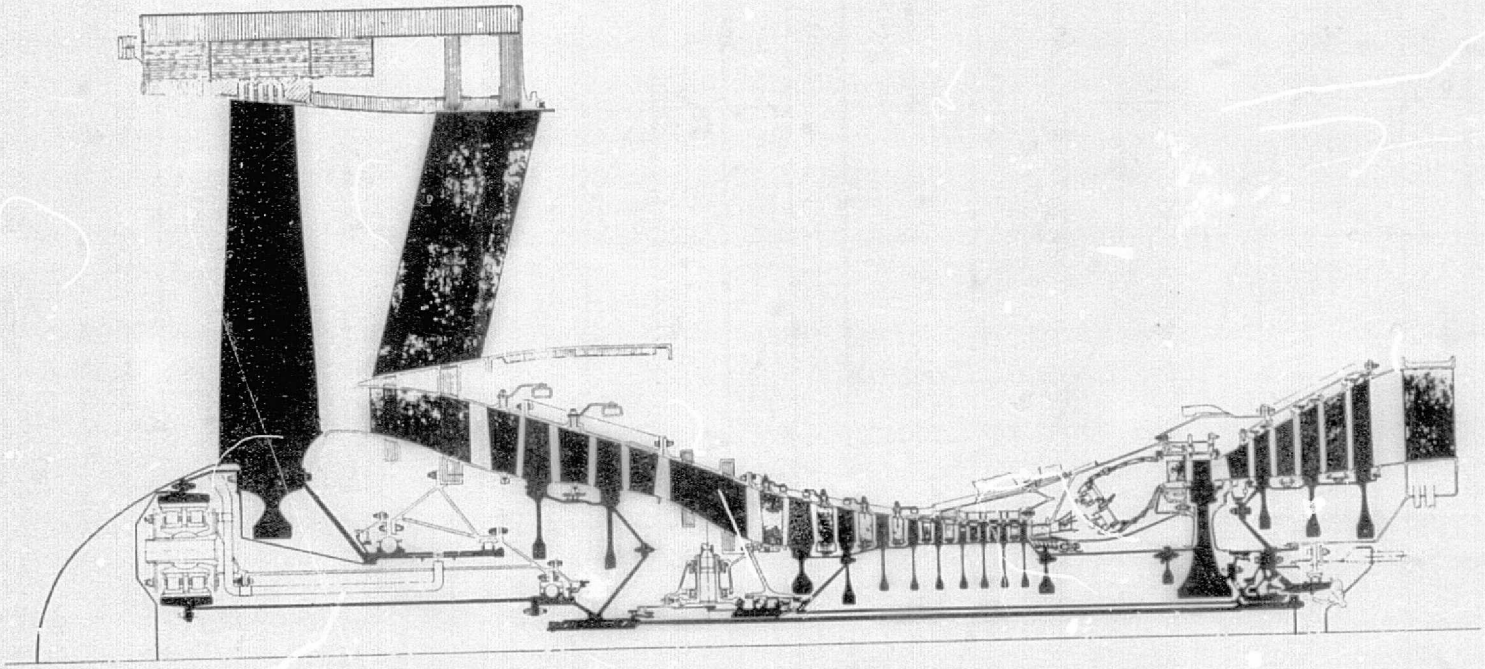

Figure 35. Geared Turbofan.

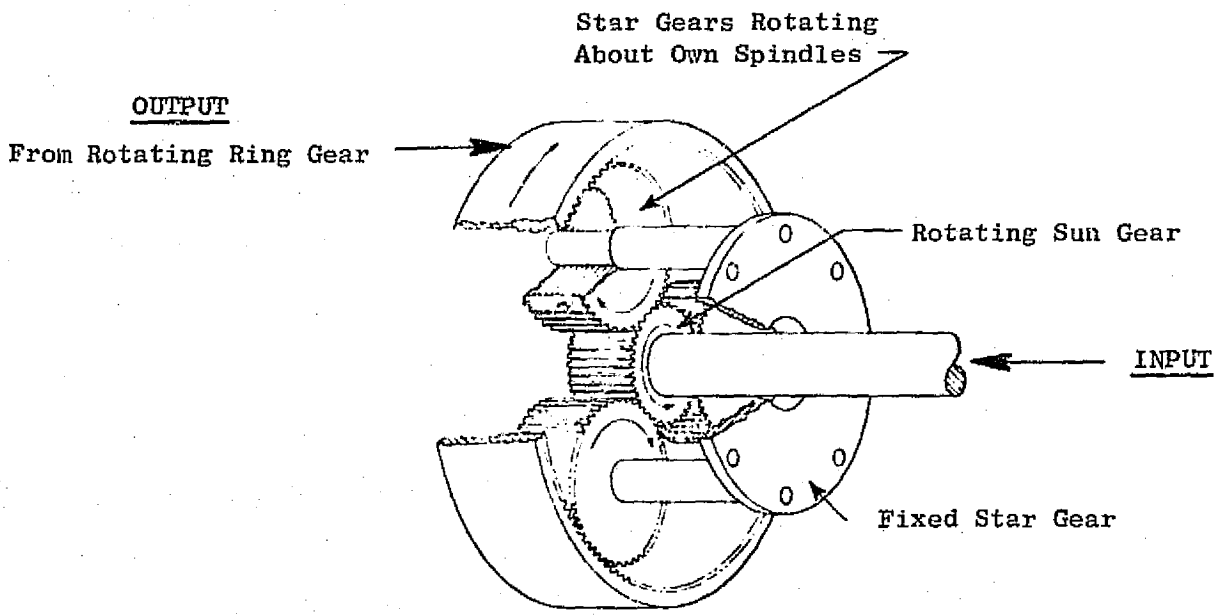

Figure 36. Star Geartrain Schematic.

stage blade. LPT loading was set to favor high efficiency. Due to the low LPT loading, the turbine exhaust frame did not require deswirl vanes.

Figure 37 is a cross section of the variable-boost, geared fan. The major difference from the standard geared fan was the use of one additional booster stage to achieve higher core supercharging, required by the cycle at cruise and climb, and a reduction in the core engine size relative to the fan.

The variable-boost feature was achieved through the variable-geometry vanes of the booster. A maximum overall pressure ratio of approximately 45:1 was obtained. At takeoff power, the booster was low-flowed to desupercharge the core such that the temperatures and pressures at the HPC exit were consistent with the baseline cycle. This avoided most of the mechanical design problems associated with the use of very high cycle pressure ratios.

The installation design of the geared-fan engines involved no basic differences from the baseline-turbofan design. The same aerodynamic, acoustic, and construction principles were applied; therefore, the description is the same as presented in Section 5.1.

Specific differences among the various designs were in dimensional values, especially the fan casing length, and the airflow values in the inlet and the fan duct. All weights and prices used in the study were scaled from the baseline installation.

5.3.3 Engine Economic Factors

Evaluation of the economic factors required two separate steps. The first was to estimate initial engine price differences (as related to manufacturing cost differences) and incorporate this information into the economic analysis of each of the engines studied. The second step was to define engine part-replacement factors over the life of the engine, taking experience on CF6 engines into account. From this, and the estimated engine-part prices, an estimate of the replacement-part cost per hour of engine service was developed. A constant factor for labor, proportional to the parts replacement costs, based upon experience with CF6 engines was then added, resulting in a total maintenance cost per hour of engine service. This maintenance cost estimate was then compared with a similar estimate for the baseline engine and the difference incorporated in the economic analysis of the engine.

5.3.4 Engine Evaluation

The geared fan was evaluated versus the baseline turbofan; a comparison is presented in Table XLV. The net fuel saved in the transcontinental mission was 4.6% with a 0.6% DOC reduction. It can be seen that the sfc reduction was the biggest factor involved, but was partially offset by installation weight and drag increases.

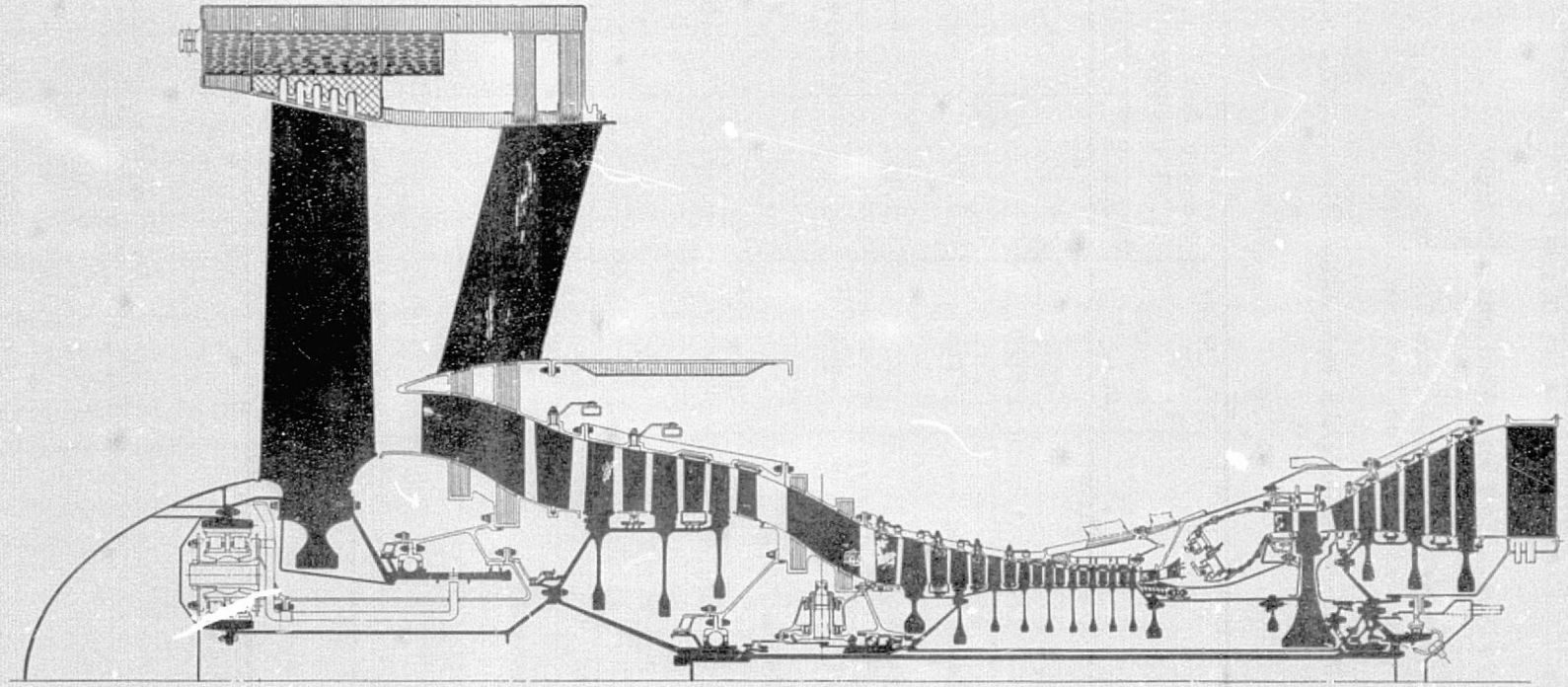

Figure 37. Geared Variable-Boost Fan.

Table XLV. Engine Evaluation: Geared Fan Vs. Baseline Direct Drive.

- Trijet, 5560 km (3000 nmi) Design
- Evaluation at 55% Load Factor, 1300 km (700 nmi) Mission, Cruise Sized
- 79.2$/$m^3$ (30¢/gal) Fuel Cost

Parameter	Aft Boost 1.55 Pressure Ratio Δ's	Geared Fan 1.55 Pressure Ratio	
		ΔDOC %	ΔW_f
Engine Weight, kg (lb)	+27 (+60)	0.10	0.16
Engine Initial Price, Δ%	+5.0	0.23	---
Engine Maintenance, Δ%	+2.7	0.12	---
Bare sfc, Δ%	-6.4	-2.52	-6.98
Subtotal (Engine Δ's)		-2.07	-6.82
*Installed Weight, kg (lb)	181	0.67	1.01
*Installed Price, Δ%	+15.2	0.37	---
*Drag/Thrust, %	+1.1	+0.43	+1.17
Subtotal (Installed Δ's)		+1.49	+2.23
Installed sfc, Δ%	-5.3		
Totals		-0.6	-4.6

*Including Pylon

The variable-boost engine, geared fan is compared to the geared fan in Table XLVI. On a cruise-sized basis there was a reduction of 1.7% in fuel used and 1% in DOC. However, on a takeoff-sized basis the improvement in fuel used was eliminated and there was a net penalty in DOC. It should also be noted, for the cruise-size case, a penalty in takeoff field length results.

Both the variable- and nonvariable-boost Task II cruise-sized, geared-engine characteristics are superposed on the Task I ΔDOC and ΔW_f trends, for comparison, in Figure 38.

The geared-fan engine DOC reduction depends on the gearset-maintenance assumptions (nominal) indicated in Figure 39. Estimated levels were used in the nominal results presented. In Figure 40 the effect of future fuel costs on the geared-fan engine payoff is shown; nominal value was assumed. The DOC advantage of the geared-fan engine would nearly double with a fuel price increase from 79.2\$/m^3 (30¢/gal) to 158.5\$/m^3 (60¢/gal).

5.4 TURBOPROPS

5.4.1 Propeller and Gear Design

The propellers chosen for this study were high disc-loading, variable-pitch propellers with 244 m/sec (800 ft/sec) design tip speed. Two cases were studied, both eight-bladed, single-rotation, but with basic- and advanced-technology levels of weight. The propeller data used in this study were supplied by Hamilton Standard Division of UTC; a summary is provided in Table XLVII.

The "basic" weights represent a level of technology which is expected to be available for commercial service in the mid-1980's, based on currently expected R&D funding. An "advanced" level of technology would offer further improvements in weight and performance which could be available in the same time period if additional R&D funding is applied. Column two of Table XLVII shows the estimated weight of the basic configuration utilizing advanced material and manufacturing technology.

Blades and Spinner - The "basic" blades consist of a hollow, high strength steel, structural member (spar); an external carbon epoxy hybrid shell shaped to the correct airfoil contour; aluminum-honeycomb fill between shell and spar; and a titanium leading-edge erosion sheath. The spinner is a fiberglass composite structure. Advanced technology would lead to development of a hollow, titanium spar with an attendant weight reduction.

Disc - The "basic" disc assembly consisted of the disc, blade-retention balls and integral races, clamps, and pitch-change trunnions. The steel disc was integral with the fan tailshaft which transferred propeller loads to the gearcase and mounts. Studies between titanium discs and steel discs with integral retention have shown little differences in weight, based on

Table XLVI. Engine Evaluation: Variable Boost Vs. Fixed Boost, 1.55 Pressure Ratio Geared Fan.

- Trijet 5560
- Evaluation at 55% Load Factor, 1300 km (700 nmi) Mission
- 79.2$/$m^3$ (30¢/gal) Fuel

Parameter	Fixed-Boost Geared Fan	Variable-Boost, Cruise-Sized			Variable-Boost, Takeoff-Sized		
		Δ's	ΔDOC %	ΔW_f %	Δ's	ΔDOC %	ΔW_f %
Engine Weight, kg (lb)	1100 (2425)	-18 (-40)	-0.07	-0.13	+154 (+340)	+0.57	+0.88
Engine Initial Price, Δ%	Base	-0.5	-0.03	---	+6.8	+0.29	---
Engine Maintenance, Δ%	Base	-4.9	-0.22	---	+3.6	+0.16	---
Bare sfc, Δ%	Base	-1.2	-0.46	-1.26		-0.46	-1.26
Subtotal (Engine Δ's)			-0.78	-1.39		-0.56	-0.38
*Installed Weight, kg (lb)	986 (2174)	-31 (-70)	-0.12	-0.17	+104 (+230)	+0.39	+0.58
*Installed Price, Δ%	Base	-3.0	-0.07		+8.8	+0.21	---
*Drag/Thrust, %	Base	-0.1	-0.04	-0.11	-0.1	-0.4	-0.11
Subtotal (Installed Δ's)	Base		-0.23	-0.28		+0.56	+0.47
Installed sfc, Δ%	Base	-1.3					
Totals			-1.0	-1.7		+1.1	+0.10

*Includes Pylon

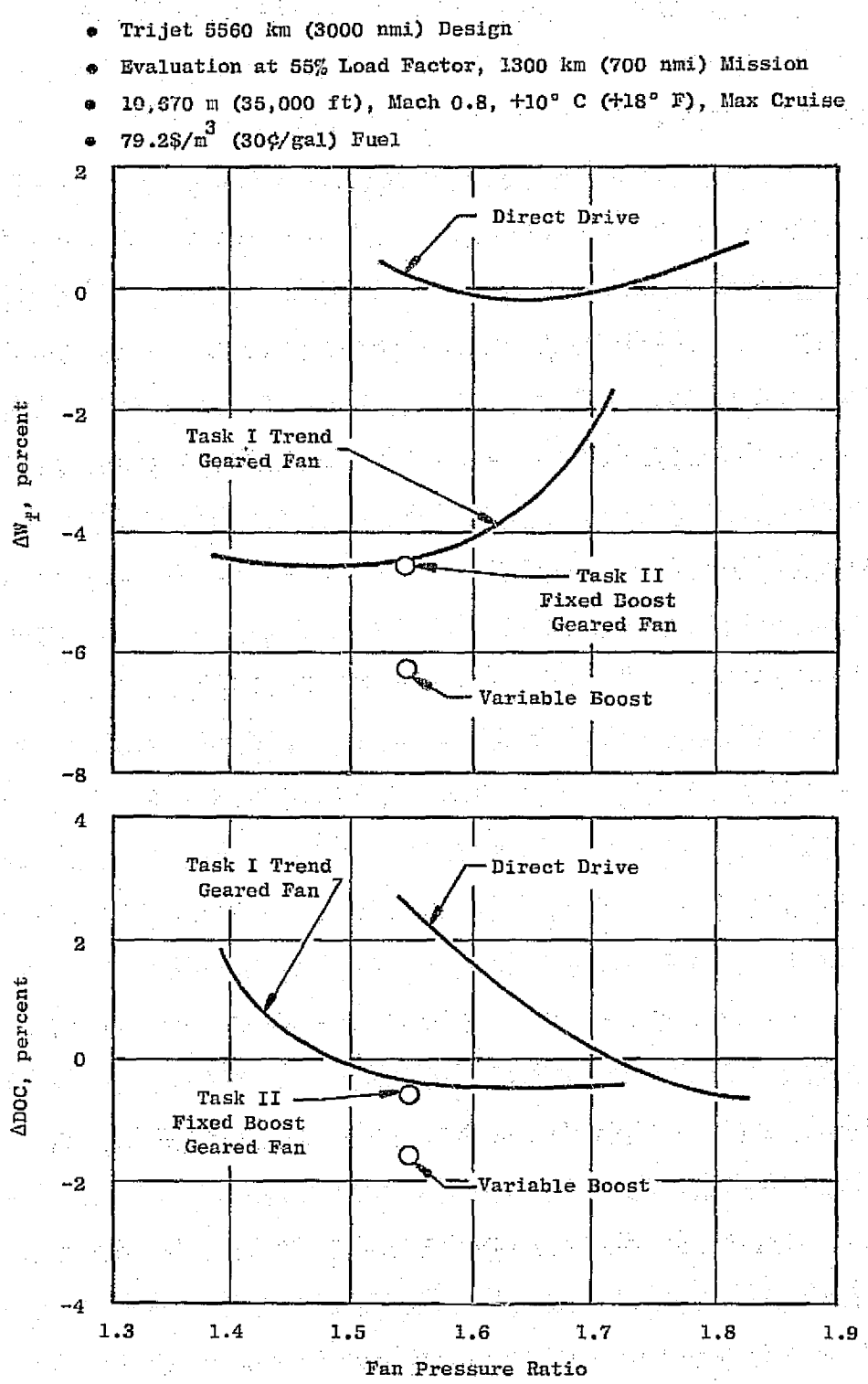

Figure 38. Engine Evaluation: Geared Vs. Direct-Drive Fan, Forward Boosters.

- Trijet 5560 km (3000 nmi) Design
- Evaluation at 55% Load Factor, 1300 km (700 nmi) Mission

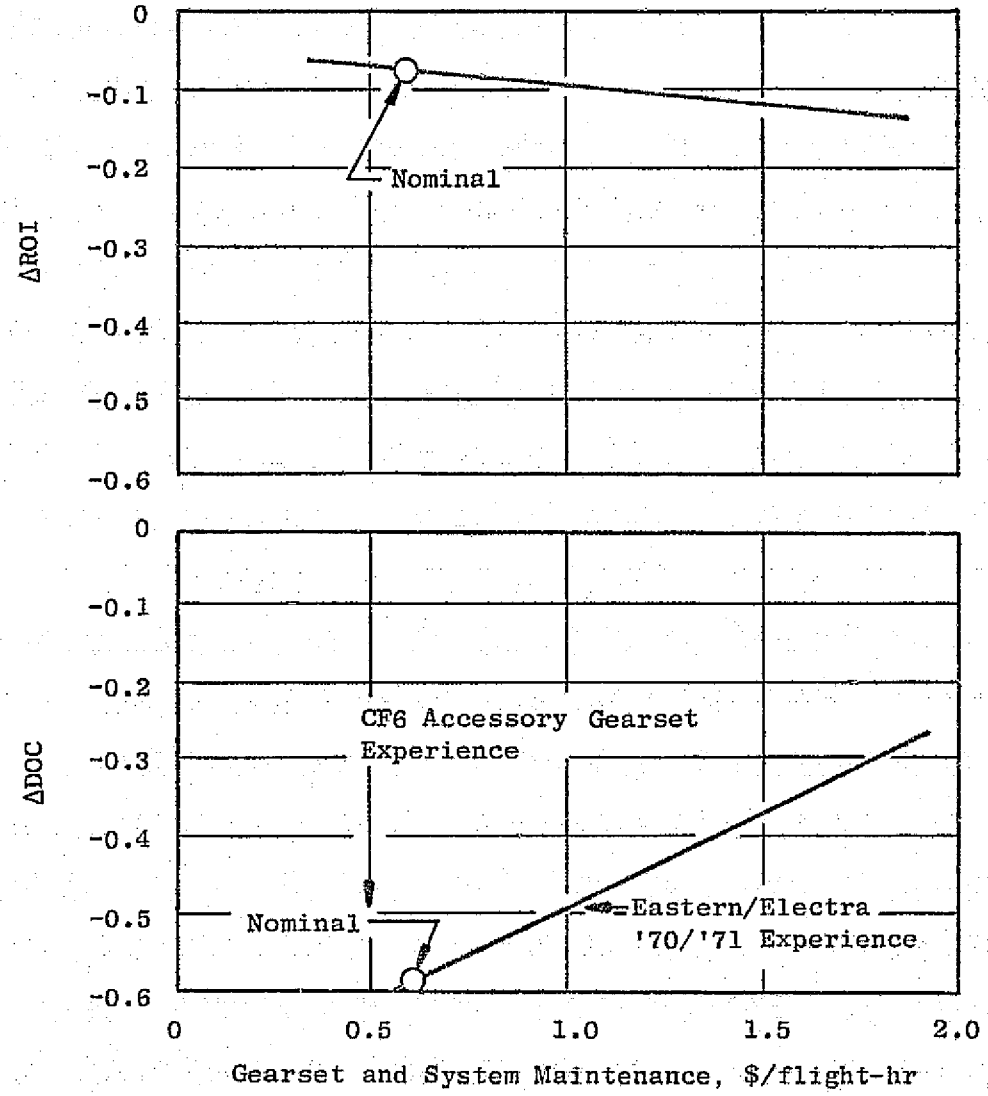

Figure 39. Sensitivity of Geared-Fan Engine Evaluation to Gearset and System Maintenence.

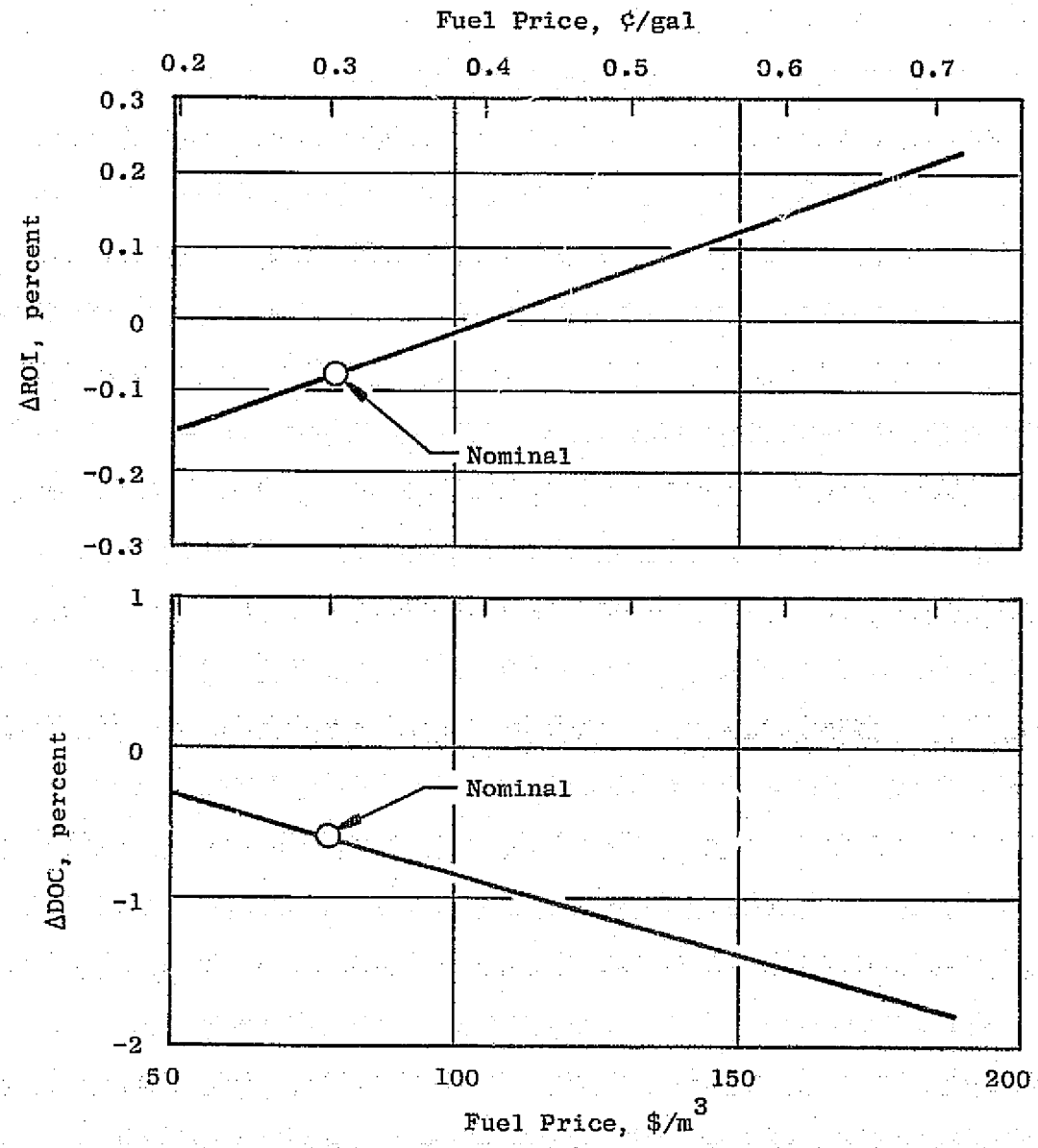

Figure 40. Effect of Fuel Price on Evaluation of Geared-Fan Engines.

Table XLVII. Turboprop Design Data Supplied by Hamilton Standard Division.

- Constant Propeller Thrust
- Propeller, Gearset, and Envelope Information

Parameter	Single Rotation Basic Weight	Single Rotation Advanced Weight
N_B	8	8
U_T, m/sec (ft/sec)	244 (800)	244 (800)
D_T, m (ft)	4.88 (16)	4.88 (16)
Disc Loading, W/m^2 (hp/ft^2)	289,000 (36)	289,000 (36)
*η_{Prop}	0.797	0.797
$D_{Nacelle}$, m (in.)	1.71 (67.2)	1.71 (67.2)
Propeller Weight, kg (lb)	857 (1890)	767 (1690)
Gear Weight, kg (lb)	658 (1450)	617 (1360)
**Propeller and Gear Cost, 1000 $	212	226
Maintenance Labor/1000 Flight-hr, $	440	440
**Maintenance Material Cost/1000 Flight-hr, $	680	7410
Oil Tank + Heat Exchanger Weight, kg (lb)	30 (65)	12 (27)

*10,670 m (35,000 ft), Mach 0.8, +10° C (+18° F), Max. Climb
**1974 $, Production Quantity 3200 Units

present day fracture mechanic allowables. With an advance in the state-of-the-art of fracture mechanics, titanium weight saving in the disc and tail-shaft can be envisioned.

Pitch-Change System - The "basic" weights were based on a mechanical pitch-change actuator, utilizing a harmonic drive, although other concepts, including hydraulic pistons and vane motors, should be considered before arriving at a final concept. The harmonic-drive concept is currently being developed for the NASA QCSEE program and has the advantages of high reliability, light weight, reasonable production cost, and good maintainability. The system features an in-place, blade-angle lock and a redundant, remote, blade-angle control. Advanced development of the harmonic drive and improved manufacturing technique should show a weight saving.

Reduction Gearing - The reduction gearing was sized for infinite life based on maximum engine torque with maximum allowable stresses consistent with today's state-of-the-art gearboxes. The weight was based on the use of a titanium welded housing, vacuum-melt AMS 6265 steel for gears, and Vimvar double-vacuum-melt M50 for bearings. The gearing system module has a calculated mean time between failures (MBTF) of approximately 40,000 hours. For advanced technology, improvements in gear and bearing geometry and materials are envisoned.

Cooling and Lubrication - Gearbox cooling was accomplished by the use of a separate heat exchanger. An overall gearbox efficiency of 99% was assumed by the use of proper oil management, baffling, and scavenging techniques. A centrifugal air/oil separator was used to minimize oil tankage weight. Advanced-technology weight saving would be based on the development of high temperature, 232° C (450° F), gearboxes and lubricants.

Accessories - Weight for accessory drives, such as aircraft hydraulics and electrical power, were not included in the gearbox weight. It is felt that powering the accessory drives from the propeller gearbox would increase these gearbox weights but would maximize overall engine cycle efficiency, simplify the engine accessory gearbox, and perhaps simplify accessory cooling.

Control - A study was conducted to establish a desirable propeller-speed schedule. The study indicated that constant propeller speed during cruise provided a favorable sfc trend. In the chosen design, propeller speed was held at 244 m/sec (800 ft/sec) down to approximately 85% maximum cruise, at which point the LP compressor required a speed reduction.

5.4.2 Turboprop Cycle and Performance

The baseline turboprop cycle used in the Task II study was the same as that used in Task I, i.e., an overall cycle pressure ratio of 38 at 10,670 m (35,000 ft), Mach 0.8, +10° C (18° F), maximum climb and a takeoff T_{41} of 1430° C (2600° F). In addition to the baseline cycle, a variable-boost cycle pressure ratio of 46 at 10,670 m (35,000 ft), Mach 0.8, +10° C (18° F),

maximum climb was investigated. In the turboprop cycles, the LPT extraction was chosen to give a core thrust approximately 10% of total bare-engine thrust, this being a level shown to yield minimum sfc. This increased extraction for the turboprop cycle resulted in lower LP turbine inlet temperatures and, therefore, lower LPT cooling flow requirements. Table XLVIII presents these cycles along with a comparison to the baseline turbofan. Table XLIX gives the internal turbomachinery characteristics at the aerodynamic design point. The baseline-turboprop engine is illustrated in Figure 41. The variable-boost case differs in that it has an additional LPC stage.

Since the LP compressor is coupled to the propeller, the effect of the propeller-speed schedule was investigated. The results indicated that an sfc benefit was realized by operating the propeller at constant speed to as low a power as possible. The LP compressor stators were varied to maintain stall-free operation at constant speed. The Task II turboprop at 10,670 m (35,000 ft), Mach 0.8, + 10° C (+18° F) was operated at U_T = 244 m/sec (800 ft/sec) down to approximately 85% maximum cruise, at which point the LPC dictated a speed reduction. The baseline turboprop described had a 14.2% sfc advantage over the baseline turbofan at the average cruise-power setting.

The variable-boost concept was an attempt to improve the thermal efficiency of the cycle. The concept approach was to operate at a high cycle pressure ratio (i.e., 46) at altitude while reducing the cycle pressure ratio at sea level, thereby maintaining reasonable P_3 and T_3. As seen in Table XLVIII, this concept provided an additional 1.4% beyond the 14.2% sfc improvement.

In an attempt to reduce the turboprop weight and cost, a three-stage LPT was investigated. This configuration resulted in a 1.4% decrease in LPT efficiency, due to higher loading, since the LPT blade velocity and, therefore, the rpm were set by stress considerations. As a result of the lower rpm, the booster efficiency was increased by 1.1%. The net result was a 1.5% increase in installed sfc relative to the four-stage LPT design. Table L presents the details of this study.

Another study associated with the baseline cycle involved sizing of the engine with aircraft bleed and power extraction included. The purpose of the study was to determine whether or not sizing for these requirements altered the comparison between turbofan and turboprop. Both the baseline-turbofan and the turboprop core engines were resized to operate at 100% aerodynamic speed at 10,670 m (35,000 ft), Mach 0.8, +10° C (+18° F), maximum climb with aircraft bleed and power extraction. Table LI presents the details of this study; the net result was a reduction in the installed sfc advantage of the turboprop, from 14.2% to approximately 12.9%, over the turbofan.

Table XLVIII. Turboprop Variable-Boost Aerodynamic Design.

- Single-Rotation/Advanced-Technology Weight
- Transcontinental 5560 km (3000 nmi) Design

		Baseline Turbofan			Baseline Turboprop			Variable-Booster Turboprop		
Power Rating		Takeoff	Maximum Climb	Maximum Cruise	Takeoff	Maximum Climb	Maximum Cruise	Takeoff	Maximum Climb	Maximum Cruise
Altitude, m		0	10,670	10,670	0	10,670	10,670	0	10,670	10,670
(ft)		0	35,000	35,000	0	35,000	35,000	0	35,000	35,000
Mach No.		0	0.8	0.8	0	0.8	0.8	0	0.8	0.8
ΔT_0, ° C		+15	+10	+10	+15	+10	+10	+15	+10	+10
(° F)		+27	+18	+18	+27	+18	+18	+27	+18	+18
F_n, N		62,680	15,700		67,390	16,150			16,150	
(lbf)		(14,090)	(3530)		(15,150)	(3630)			(3630)	
Drag, % F_n			4.9			5.9			5.7	
Bare sfc, Δ %				Base			-15.1			-16.5
Installed sfc, Δ %				Base			-14.2			-15.6
Bypass Ratio			6.9							
Overall Pressure Ratio		29	38		29	38		29	46	
T_{41}, ° C		1430	1370		1430	1370		1430	1370	
(° F)		(2600)	(2500)		(2600)	(2500)		(2600)	(2500)	
Fan Prop	D_T, m	1.30	1.30	1.30	4.02	4.02	4.02	4.02	4.02	4.02
	(ft)	(4.28)	(4.28)	(4.28)	(13.2)	(13.2)	(13.2)	(13.2)	(13.2)	(13.2)
	$W_2\sqrt{\theta}/\delta$, kg/sec		241							
	(lbm/sec)		(532)							
	Fan Pressure Ratio		1.71			1.05			1.05	
	$W_2\sqrt{\theta}/\delta$ AA, kg/sec-m^2		1.82							
	(lbm/sec-ft^2)		(43.2)							
	$U_T/\sqrt{\theta}$, m/sec		494							
	(ft/sec)		(1620)							
	U_T, m/sec					244	243.8		244	244
	(ft/sec)					(800)	(800)		(800)	(800)
	R_H/R_T		0.38			0.23			0.23	
	Hub Pressure Ratio		1.61			1.023			1.023	

Table XLIX. Turboprop Aerodynamic Design.

● 10,670 m (35,000 ft), Mach 0.8, Max. Climb

Component	Parameter	Baseline Turbofan	Baseline Turboprop	Variable-Boost Turboprop
Booster	No. Stages	3	3	4
	$U_T/\sqrt{\theta}$, m/sec (ft/sec)	249 (816)	384 (1260)	367 (1205)
	Boost Pressure Ratio	1.71	2.75	3.43
	Boost and Fan Pressure Ratio	2.75	-	-
Core	$W_{2C}\sqrt{\theta}/\delta$, kg/sec (lbm/sec)	13.2 (29.1)	11.4 (25.2)	9.8* (21.6)*
	Pressure Ratio	14	14	13.6**
HPT	No. Stages	1	1	1
	Pressure Ratio	3.8	3.8	4.11
	ΔH, kJ/kg (Btu/lb)	488 (210)	488 (210)	511 (220)
	$\bar{\psi}_P$	0.87	0.87	0.86
LPT	No. Stages	4-1/2	4	4
	Pressure Ratio	5.7	9.53	10.6
	ΔH, kJ/kg (Btu/lb)	456 (196)	567 (244)	581 (250)
	$\bar{\psi}_P$	1.63	0.92	0.97
Cooling Air	Chargeable HPT, %	4.9	4.9	4.9
	Chargeable LPT, %	3.7	2.6	2.0
	Mixing Effectiveness	0.75	-	-

*For 100% Aerodynamic Speed: 9.98 kg/sec (22 lbm/sec)

**For 100% Aerodynamic Speed: 14

- 10,670 m (35,000 ft), Mach 0.8, +10° C (+18° F), Max. Climb

Cycle Pressure Ratio = 38
Turbine Inlet Temperature = 1370° C (2500° F)
At Takeoff Power = 1430° C (2600° F)

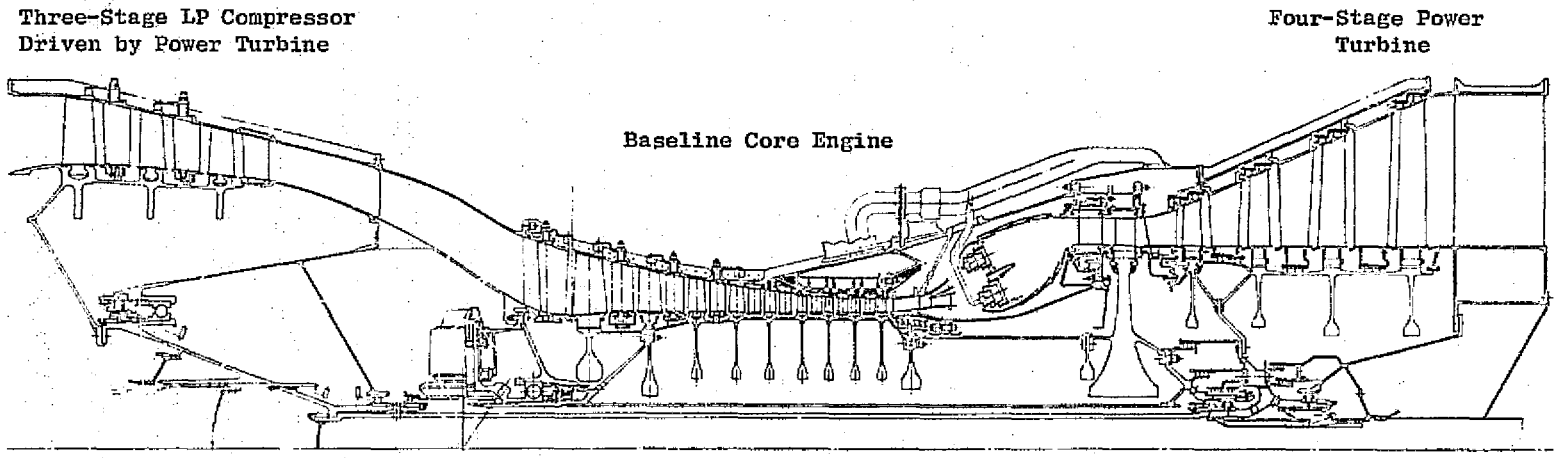

Figure 41. Turboprop Engine.

Table L. Turboprop LPT Staging Study.

- Single-Rotation/Advanced-Technology Weight
- Transcontinental 5560 km (3000 nmi) Design
- Evaluation at 55% Load Factor, 1300 km (700 nmi) Mission
- 10,670 m (35,000 ft), Mach 0.8, +10° C (+18° F), Max. Cruise

Parameter		Four-Stage LPT	Three-Stage LPT	ΔW_f, %	Δ DOC, %
Installed F_n, N (lbf)		16,150 (3630)	16,150 (3630)		
Propeller Diameter, m (ft)		4.0 (13.2)	4.0 (13.2)		
sfc, Δ %		Base	+1.5		
Upper Nacelle Diameter, m (in.)		0.70 (27.7)	0.70 (27.7)		
Lower Nacelle Diameter, m (in.)		0.98 (38.4)	0.97 (38.3)		
Installed sfc, Δ %		Base	+1.5	+1.7*	+0.7*
LPT	$\overline{\psi}_P$	1.07	1.20		
	$\Delta\eta_{TT}$	Base	-1.4		
	$\Delta W/W_{2C}$, %	Base	0		
Booster	No. Stages	3	3		
	$U_T/\sqrt{\theta}$, m/sec (ft/sec)	384 (1260)	363 (1190)		
	$\Delta\eta$	Base	+1.1		

*Negligible Weight and Price Effects; Four-Stage LPT chosen due to Performance Advantage

Table LI. Effect on Engine Evaluation of Designing for Aircraft Bleed and Power Extraction.

- Single-Rotation/Advanced Technology Weight
- Transcontinental 5560 km (3000 nmi) Design
- Evaluation at 55% Load Factor, 1300 km (700 nmi) Mission
- 10,670 m (35,000 ft), Mach 0.8, +10° C (18° F), Max. Cruise

Parameter	Without Bleed and Power Extraction		With Bleed and Power Extraction	
	Turbofan	Turboprop	Turbofan	Turboprop
D_{Tip}, m (ft)	1.30 (4.28)	4.02 (13.20)	1.30 (4.25)	4.02 (13.20)
$W_{2C}\sqrt{\theta}/\delta$, kg/sec (lbm/sec)	13.15 (29.0)	11.43 (25.2)	14.56 (32.1)	12.70 (28.0)
F_n Installed, N (lbf)	15,700 (3530)	16,060 (3610)	15,700 (3530)	16,060 (3610)
W_{BI}, kg/sec (lbm/sec)	0 0	0 0	0.58 (1.28)	0.58 (1.28)
Power Extraction, W (hp)	0 0	0 0	119,312 (160)	119,312 (160)
Installed sfc,* Δ %	Base	-14.2	Base	-12.9
Price, Δ %	Base	+57.7	Base	+53.2
Δ Installed Weight, kg (lbm)	Base Base	+544 (+1200)	Base Base	+526 (+1160)
Block W_f, Δ %	Base	-15	Base	-13.5
DOC, Δ %	Base	-4	Base	-3.8

*At average cruise power setting.

5.4.3 Turboprop Engine Design

The engine arrangement was the same for the fixed-boost engine as for the Task I engine. The Task II baseline-engine cross section is shown in Figure 41. No engine cross section was prepared for the variable-boost engine since it differs only in the addition of one LPC stage.

The low pressure compressor (LPC) was a threestage design based on current design practice. Variable stators were employed to match the desired propeller-speed schedule. Rotor speed was sufficiently low that a rolled-ring titanium drum with shallow discs could be used to reduce the cost. Tangential dovetails were used to attach titanium blades.

The booster stator was conventional titanium with split casing. The general arrangement was directed at modular maintenance so that the stator and rotor could be easily removed by unbolting one casing flange and one rotor flange.

The forward sump and shaft had two LP shaft bearings: thrust and radial. In addition, the shaft assembly included a fully loaded, lubricated, flexible spline to drive the quill shaft to the propeller gear box. The arrangement assumed that the engine would lubricate the aft spline of the quill shaft and that the propeller reduction-gear system would lubricate the forward end.

The intermediate frame (1) connected booster to compressor; (2) supported the PTO, booster rotor, compressor rotor and the accessory gear box; and (3) would serve as the forward engine mount. The frame construction was welded and brazed steel. Because of the relatively small diameter of the frame compared to the full fan frame of a turbofan engine, there was no significant weight or cost advantage for aluminum or composite.

The four-stage LPT operated at slightly higher speed and had a larger exit annulus area than the three-stage, geared-turbofan LPT. The higher speed, larger area, and additional stage all increased weight and cost.

Only the first-stage blade and the first- and second-stage vanes were cooled. Rotor cooling air was extracted externally from the compressor and conducted through the first-stage vanes to a rim-entry diffuser which supplied cooling air to the first-stage LPT rotor blades. Second-stage vane cooling came directly through casing passages to the vane tip; this air was also used to block the second-stage vane seal.

The LPT rotor had a separate firststage disc, because it had cooled blades, and was slightly different in construction and buildup from the last three stages. The last three stage discs were a welded assembly; the blades were cast with tip shrouds. First-stage blades were Ni76XB, the second stage R125, and the last two stages R80. The LPT stator had a split casing because of the welded rotor assembly; in addition, the split casing offered advantages for maintenance and inspection. The LPT could be removed as a module for maintenance.

The turbine frame was a welded IN 718 assembly similar to that used in the geared fans. The annulus area was larger because of the high turbine-work extraction of the turboprop. There were no outlet guide vanes required in the frame because of the low turbine-loading coefficient. The rear sump and bearings were comparable to the other study engines.

The core designs for the turboprops were based on the same core used in the baseline turbofan. The variable-boost core ran slightly faster, because of the higher boost pressure ratio, and was therefore slightly heavier.

5.4.4 Installation Configuration

The turboprop nacelle arrangement shown in Figure 42 is one of several potential concepts for installation on a Mach 0.8 aircraft. These concepts include over-the-wing and under-the-wing engines, inline gearbox and engine, offset gearbox and engine, and several turboprop locations with respect to the wing.

Figure 42 depicts an under-the-wing engine with an offset gearbox; this configuration was selected for further study in Task II for several reasons. For example, the under-the-wing location of the engine allowed easy access to the engine and engine accessories for normal inspection and maintenance; also, the offset gearbox arrangement allowed an inlet which provided good flow conditions to the engine.

The illustrated nacelle-downtilt angle and the distance between the rotor plane and wing quarter-chord were selected to minimize the one/per rev excitation factor, due to wing wash and steady aeroelastic effects, while maintaining whirl-flutter stability. The nacelle and spinner shapes were selected to provide the best possible installed prop-fan performance; however, with the nacelle frontal area dictated by aerodynamic requirements, wide latitude was available in gearbox and engine installation arrangement.

5.4.5 Engine Evaluation

The turboprop engine studied in Task II was evaluated in the two aircraft described in Table LII. The single-rotation propeller was chosen for the Task II study, and the summary results are presented for the advanced-technology weight version.

Tables LIII and LIV present a comparison of the turbofan and the selected single-rotation system in both the transcontinental and intercontinental aircraft. Figures 43 and 44 present a comparison of the installed price and weight differences between the turboprop and turbofan in the transcontinental aircraft.

The installed price for the turboprop system increased 8% relative to the turbofans because the price reduction due to the smaller engine is

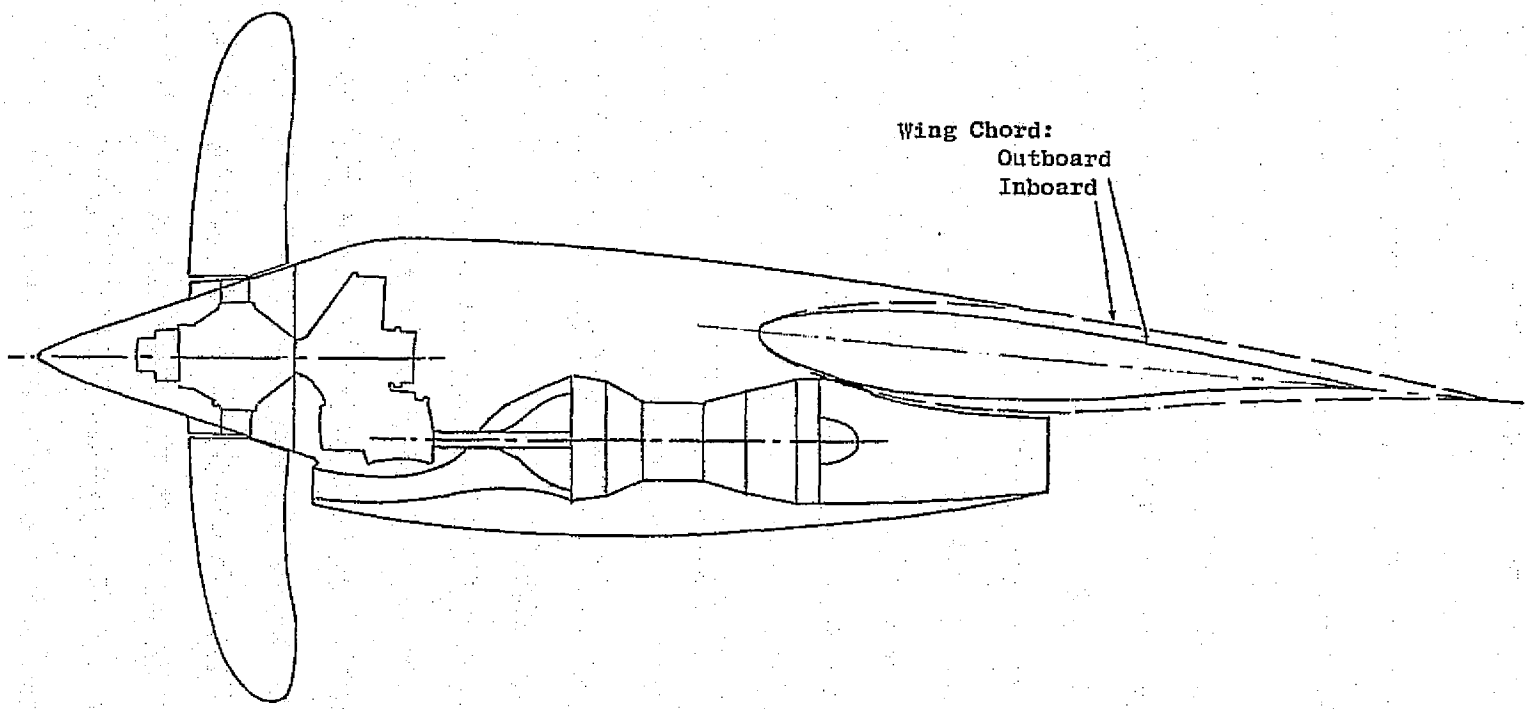

Figure 42. Turboprop Installation.

Table LII. Turboprop Versus Turbofan Baseline Aircraft.

Mission	Transcontinental		Intercontinental	
Range, km (nmi)	5560 (3000)		10,190 (5500)	
PAX	200		200	
Engine Type	Turbofan	Turboprop*	Turbofan	Turboprop*
No. Engines	4	4	4	4
TOGW, kg (lbm)	98,660 (217,500)	97,560 (214,900)	144,300 (318,200)	138,800 (306,000)
Structure Weight, kg (lbm)	49,420 (108,940)	49,670 (109,510)	62,570 (137,930)	61,710 (136,040)
Powerplant Weight, kg (lbm)	4,880 (10,760)	7,080 (15,600)	7,290 (16,080)	10,230 (22,560)
Payload, kg (lbm)	18,600 (41,000)	18,600 (41,000)	19,500 (43,000)	19,500 (43,000)
Fuel (Block + Reserve), kg (lbm)	25,770 (56,800)	22,130 (48,790)	54,970 (121,190)	47,360 (104,400)
Wing Loading, kg/m^2 (lbm/ft^2)	684 (140)	684 (140)	732 (150)	732 (150)
Wing AR	12	12	12	12
Wing Sweep, 1/4-Chord, degrees	25	25	25	25
TOBFL, m (ft)	2320 (7600)	1920 (6300)	2650 (8700)	2195 (7200)
Rate of Climb, m/min (ft/min)	91.4 (300)	91.4 (300)	91.4 (300)	91.4 (300)
Takeoff C_L	2.75	2.75	2.75	2.75
Average Cruise L/D	16.9	16.6	18.4	18.0
Takeoff F_n/W (static), N/kg (lbf/lbm)	2.55 (0.260)	3.17 (0.323)	2.38 (0.243)	2.92 (0.304)
Corrected Core Flow, kg/sec (lbm/sec)	13.2 (29.1)	11.4 (25.2)	18.1 (39.9)	15.4 (33.9)
Block Fuel, Δ % (55% Load Factor, Part Range)	Base	-15.0	Base	-13.7

*Single-Rotation/Advanced-Technology Weight

Table LIII. Turboprop Versus Turbofan Engine Evaluation, Transcontinental 5560 km (3000 nmi) Aircraft.

- Evaluation at 55% Load Factor, 1300 km (700 nmi) Mission
- 79.2 $/m^3 (30¢/gal) Fuel

Parameter	Advanced Turbofan	Advanced-Weight Turboprop
Bare F_n*, N	12,120	12,540
(lbf)	(2724)	(2820)
sfc, Δ %	Base	-14.2
Drag/F_n (Bare), %	6.8	8.0
F_{nI}, N	11,300	11,520
(lbf)	(2540)	(2590)
sfc_I, Δ %	Base	-13
Propeller Diameter, m	-	4.0
(ft)	-	(13.2)
Disc Loading, W/m^2	-	289,000
(hp/ft^2)	-	(36.0)
η_{Prop}**	-	0.816/0.760
Engine Weight, kg	671	463
(lbm)	(1480)	(1020)
Propeller Weight, kg	-	485
(lbm)	-	(1070)
Gear and System, kg	-	318
(lbm)	-	(700)
Nacelle Weight,*** kg	549	494
(lbm)	(1210)	(1090)
Total Installed Weight, kg	1220	1770
(lbm)	(2690)	(3900)
Installed Price, Δ %	Base	+8.3
Maintenance, Δ %	Base	-3.7
TOGW, kg	98,660	96,800
(lbm)	(217,500)	(213,400)
Block Fuel, Δ %	Base	-15
DOC, Δ %	Base	-4.0
Δ ROI, Points	Base	+0.6

*Average Cruise, 10,670 m (35,000 ft), Mach 0.8
**Bare/installed, at 95% Max. Cruise
***Including Pylon

Table LIV. Turboprop Versus Turbofan Engine Evaluation, Intercontinental 10,190 km (5500 nmi) Aircraft.

- Evaluation at 55% Load Factor, 3700 km (200 nmi) Mission
- 118.9 $/m^3 (45¢/gal) Fuel

Parameter	Advanced Turbofan	Advanced-Weight Turboprop
Bare F_n*, N	16,610	16,980
(lbf)	(3730)	(3790)
sfc, Δ %	Base	-14.6
Drag/F_n (Bare), %	6.8	8.0
F_{nI}, N	15,480	15,480
(lbf)	(3480)	(3480)
sfc_I, Δ %	Base	-13
Propeller Diameter, m	-	4.66
(ft)	-	(15.3)
Disc Loading, W/m^2	-	289,000
(hp/ft^2)	-	(36.0)
η_{Prop}**	-	0.816/0.760
Engine Weight, kg	1030	667
(lbm)	(2270)	(1470)
Propeller Weight, kg	-	703
(lbm)	-	(1550)
Gear and System, kg	-	503
(lbm)	-	(1110)
Nacelle Weight,*** kg	794	685
(lbm)	(1750)	(1510)
Total Installed Weight, kg	1820	2560
(lbm)	(4020)	(5640)
Installed Price, Δ %	Base	+10.4
Maintenance, Δ %	Base	-4.0
TOGW, kg	144,300	137,500
(lbm)	(318,200)	(303,200)
Block Fuel, Δ %	Base	-13.7
DOC, Δ %	Base	-5.2
Δ ROI, Points	Base	+1.2

*Average Cruise 10,670 m (35,000 ft), Mach 0.8
**Bare/installed, at 95% Max. Cruise
***Including Pylon

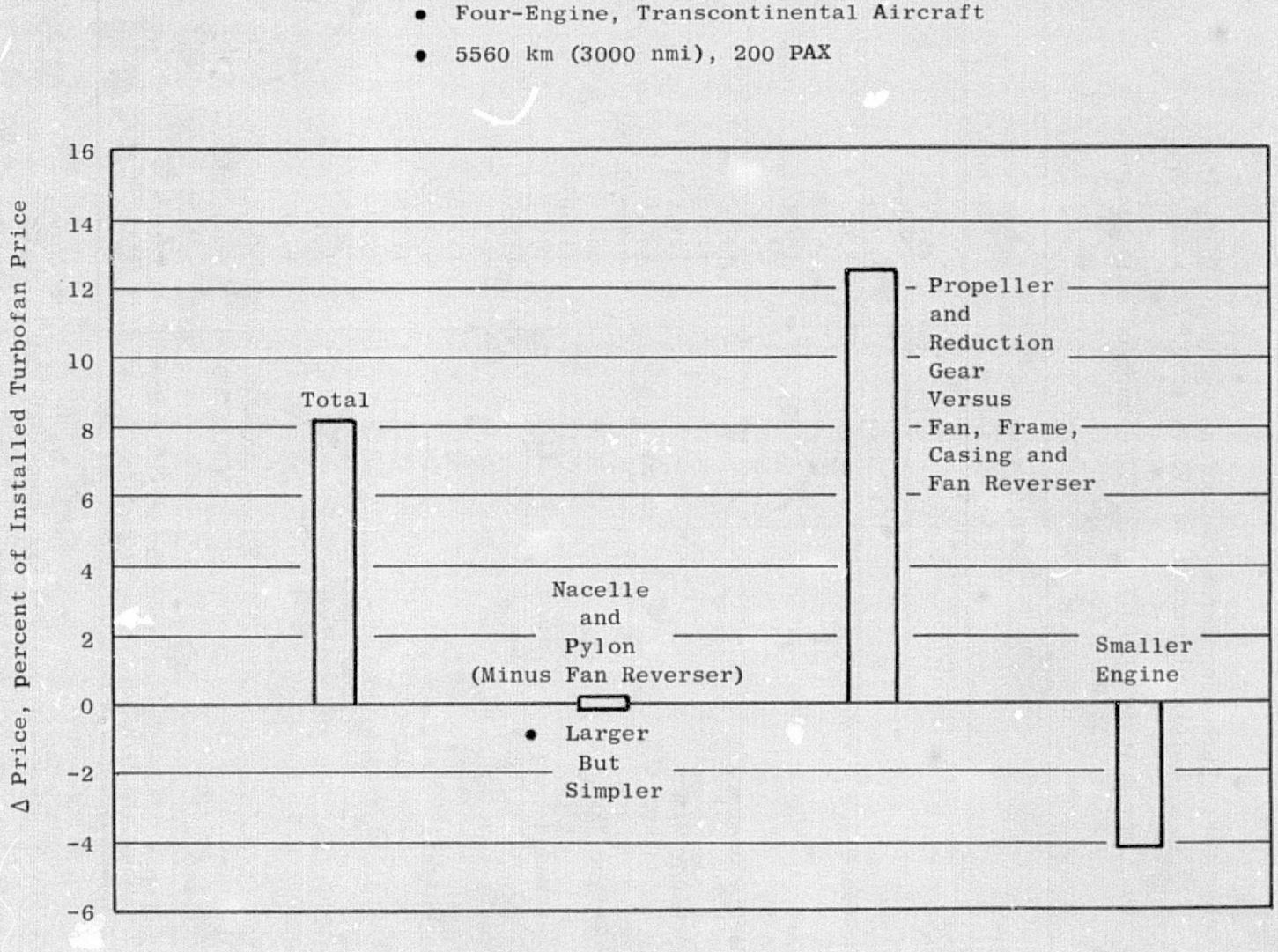

Figure 43. Installation Price Estimates: Baseline Turboprop Vs. Baseline Turbofan.

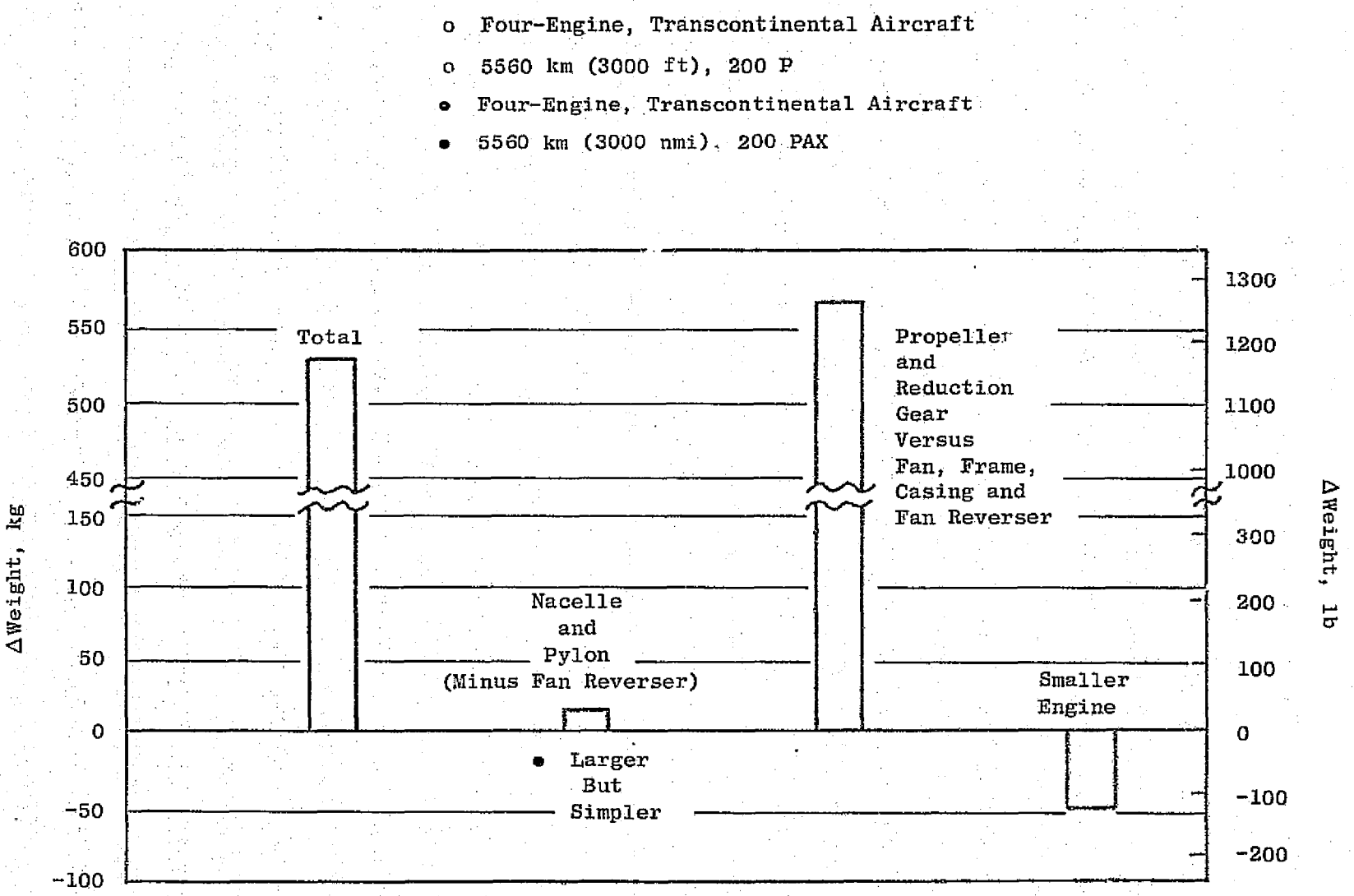

Figure 44. Installation Weight Estimates: Baseline Turboprop Vs. Baseline Turbofan.

overwhelmed by relatively higher costs of the propeller versus the fan. The effect of the price increase on DOC is small, about 0.1% in the transcontinental turboprop. The installed weight for the turboprop is approximately 540 kg (1,190 lb) heavier than the turbofan; again, the propeller system weight increases exceeded the core weight reduction. The effect on block fuel was about a 3.6% increase in the transcontinental turboprop aircraft; the block fuel reduction, cited in Table LIV, of 15% occurred because the sfc reduction overcame the effect of this weight increase. Similarly, the price effect was overcome by the fuel saving and resulted in a net DOC reduction of 4%. In both the intercontinental and transcontinental aircraft, the turboprop was a heavier and more costly engine, but the 14.2% bare sfc advantage at cruise offset these liabilities in terms of block fuel, DOC, and ROI.

In the transcontinental 1300 km (700 nmi) mission, approximately 30% of the fuel was consumed during climb; on the other hand, only 10% was consumed on the intercontinental 3700 km (2000 nmi) mission. During climb, the difference between the turboprop and turbofan sfc was approximately 22%. The combination of these two facts resulted in a larger fuel saving for the transcontinental aircraft (-15%) versus the intercontinental aircraft (-13.7%).

In the intercontinental 10190 km (2000 nmi) mission, the fuel burned amounted to 30% of DOC; however, it was 24% of DOC in the transcontinental aircraft. This fuel difference resulted in a greater DOC improvement for the intercontinental aircraft than for the transcontinental aircraft.

Table LV presents a comparison of the variable-boost turboprop and the basic turboprop. In addition to the basic 1.4% sfc advantage due to cycle pressure ratio, the engine was lighter for the same installed cruise thrust. The variable-boost engine had a lower takeoff thrust when sized for a given cruise thrust.

In the evaluation of the turboprop versus the turbofan, the main items of uncertainty were the levels of propeller and gearbox performance, maintenance, and price. In order to assess the impact of a deviation of any of these quantities, sensitivity studies were conducted. Figures 45 and 46 present the effect of propeller efficiency on fuel-burned and DOC respectively. A reduction in propeller efficiency (η_p) of 12.6 and 9% from the 81.6% level used in the study eliminates any fuel savings over the direct-drive and geared turbofan, respectively (Figure 47). A reduction of approximately 5% eliminates any DOC advantage over either turbofan engine.

Figure 47 presents the effect of propeller, plus gearbox maintenance, on the economics of the turboprop; the nominal values assumed in this study are indicated. It is apparent that a significant improvement beyond current maintenance levels must be made for the advanced turboprop to realize an economic advantage over the advanced turbofan. Figure 48 presents the effects of propeller and gear prices on turboprop economics. Figure 49 presents the impact of fuel price on DOC. The higher the fuel price, the greater the potential payoff of a higher priced but more fuel-conservative turboprop powerplant.

Table LV. Turboprop Evaluation, Variable Boost Vs. Nonvariable Boost.

- Single-Rotation/Advanced-Technology Weight
- Transcontinental 5560 km (3000 nmi) Design
- Evaluation at 55% Load, 1300 km (700 nmi)
- 79.2 $/m^3 (30¢/gal) Fuel

Parameter	Basic Turboprop	Variable-Boost Turboprop		
		Δ	Δ DOC	Δ W_f
Bare sfc, Δ %	Basic	-1.4	-0.58	-1.65
Engine Weight*, kg (lbm)	1270 (2810)	-73 (-160)	-0.33	-0.52
Initial Price*, Δ %		+1.0	+0.05	
Maintenance*, Δ %		-5.5	-0.31	
Subtotal Engine Δ's			-1.17	-2.17
Installation Weight, kg (lbm)	494 (1090)	-18 (-40)	-0.09	-0.15
Price, Δ %		-3.1	-0.07	
Drag/Thrust, %	6.0	0	0	0
Subtotal			-0.16	-0.15
Installed sfc, Δ %	Base	-1.4		
Total, %			-1.3	-2.3

*Includes propeller and gear

- Turboprop Versus Turbofan
- Single-Rotation/Advanced Technology Weight
- Transcontinental 5560 km (3000 nmi) Design
- Evaluation at 55% Load Factor, 1300 km (700 nmi) Mission
- 79.2$/$m^3$ (30¢/gal) Fuel
- TOGW = 96,780 kg (213,400 lbm)
- 10,670 m (35,000 ft), Mach 0.8, 95% Max. Cruise

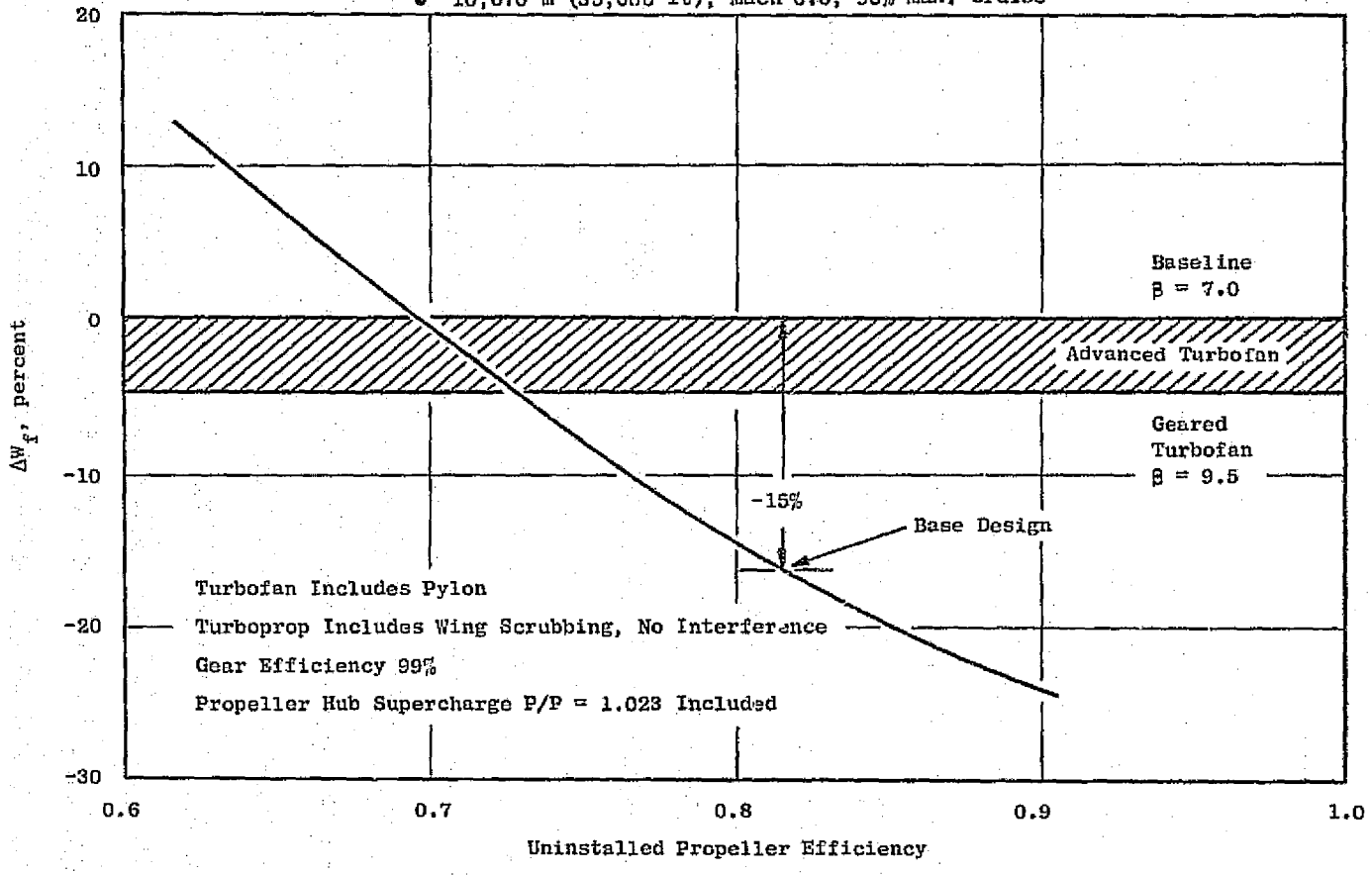

Figure 45. Sensitivity of Turboprop Fuel Saved to Prop Efficiency (η_p).

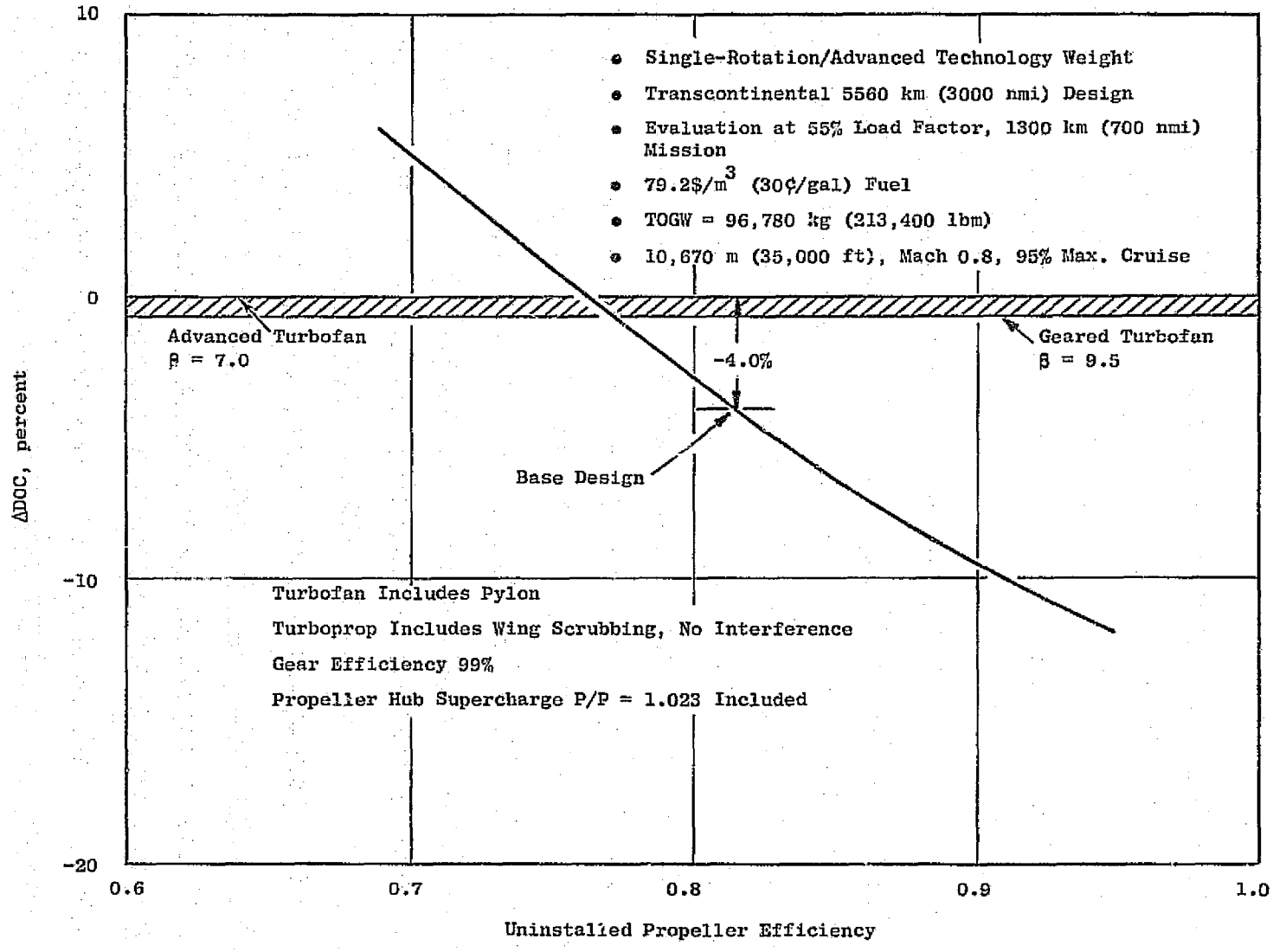

Figure 46. Sensitivity of Turboprop Economics to Propeller Efficiency.

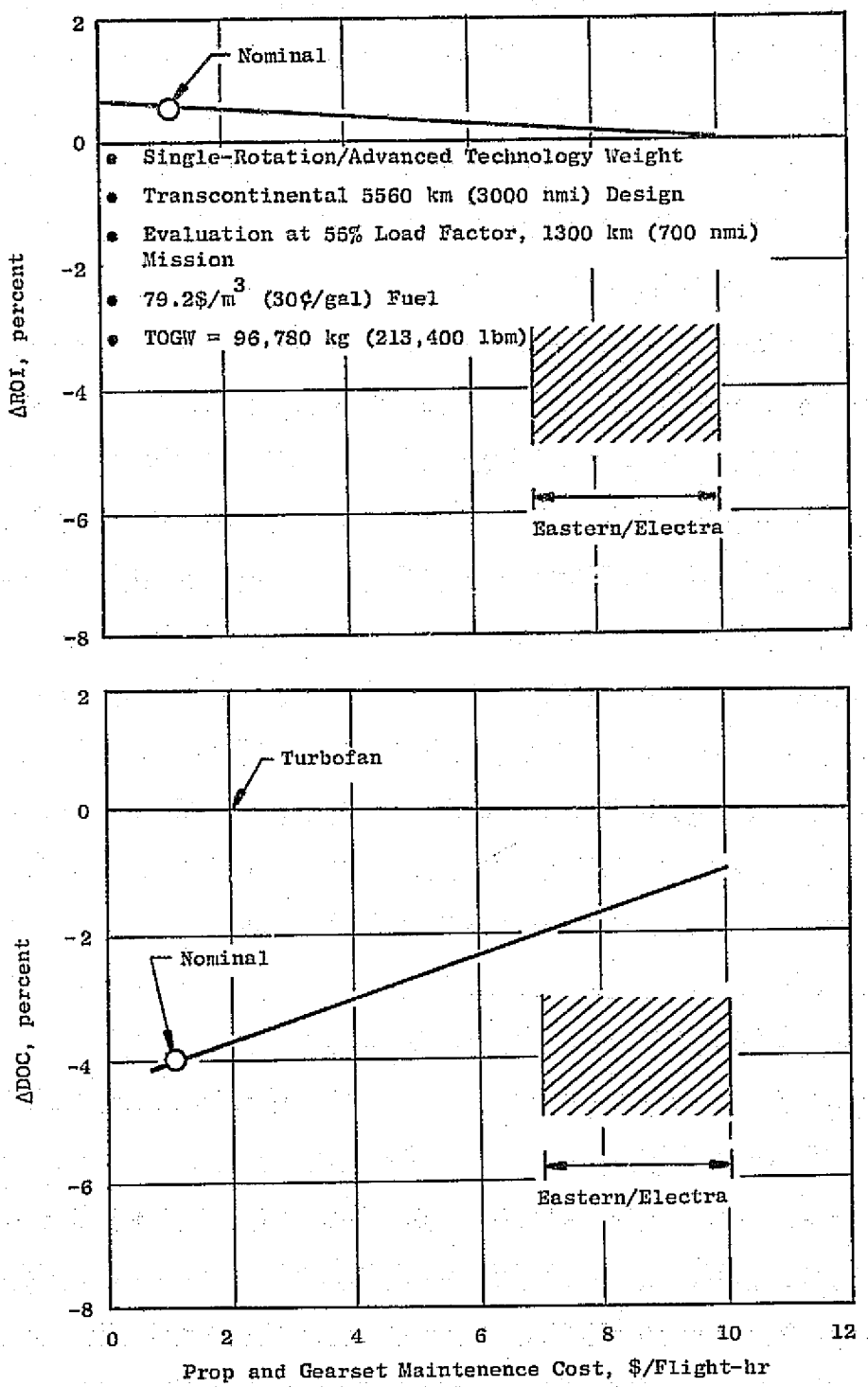

Figure 47. Sensitivity of Turboprop Engine Evaluation to Propeller and Gear, Labor, and Material Maintenence Cost.

- Transcontinental 5560 km (3000 nmi) Design
- Single-Rotation/Advanced-Technology Weight
- Evaluation at 55% Load Factor, 1300 km (700 nmi) Mission
- 79.2 $/m^3 (30 ¢/gal) Fuel
- TOGW = 96,780 kg (213,400 lbm)

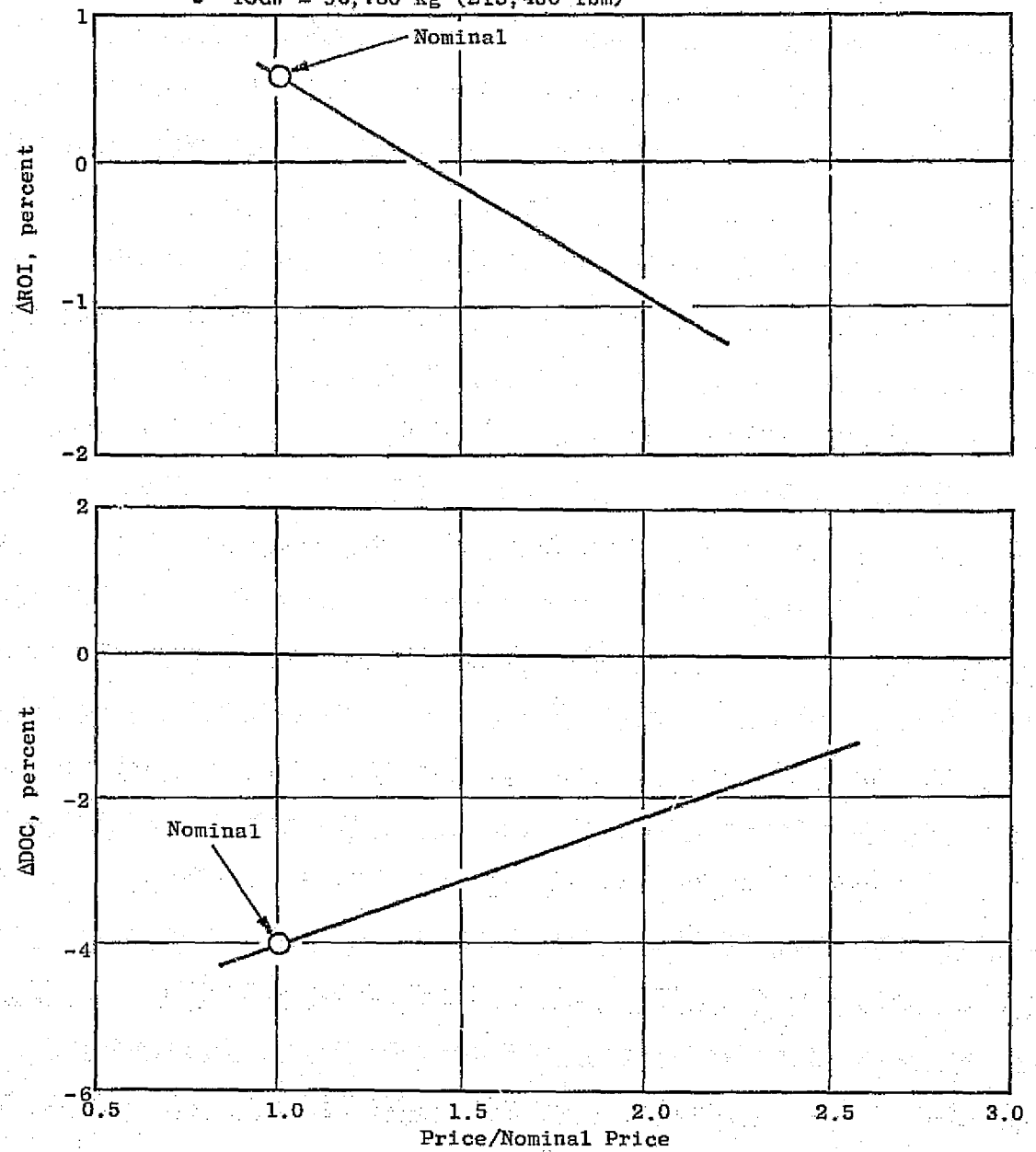

Figure 48. Sensitivity of Turboprop Engine Evaluation to Propeller and Gear Price.

- Single-Rotation /Advanced Technology Weight
- Transcontinental 5560 km (3000 nmi) Design
- Evaluation at 55% Load Factor, 1300 km (700 nmi) Mission
- TOGW = 96,780 kg (213,400 lbm)

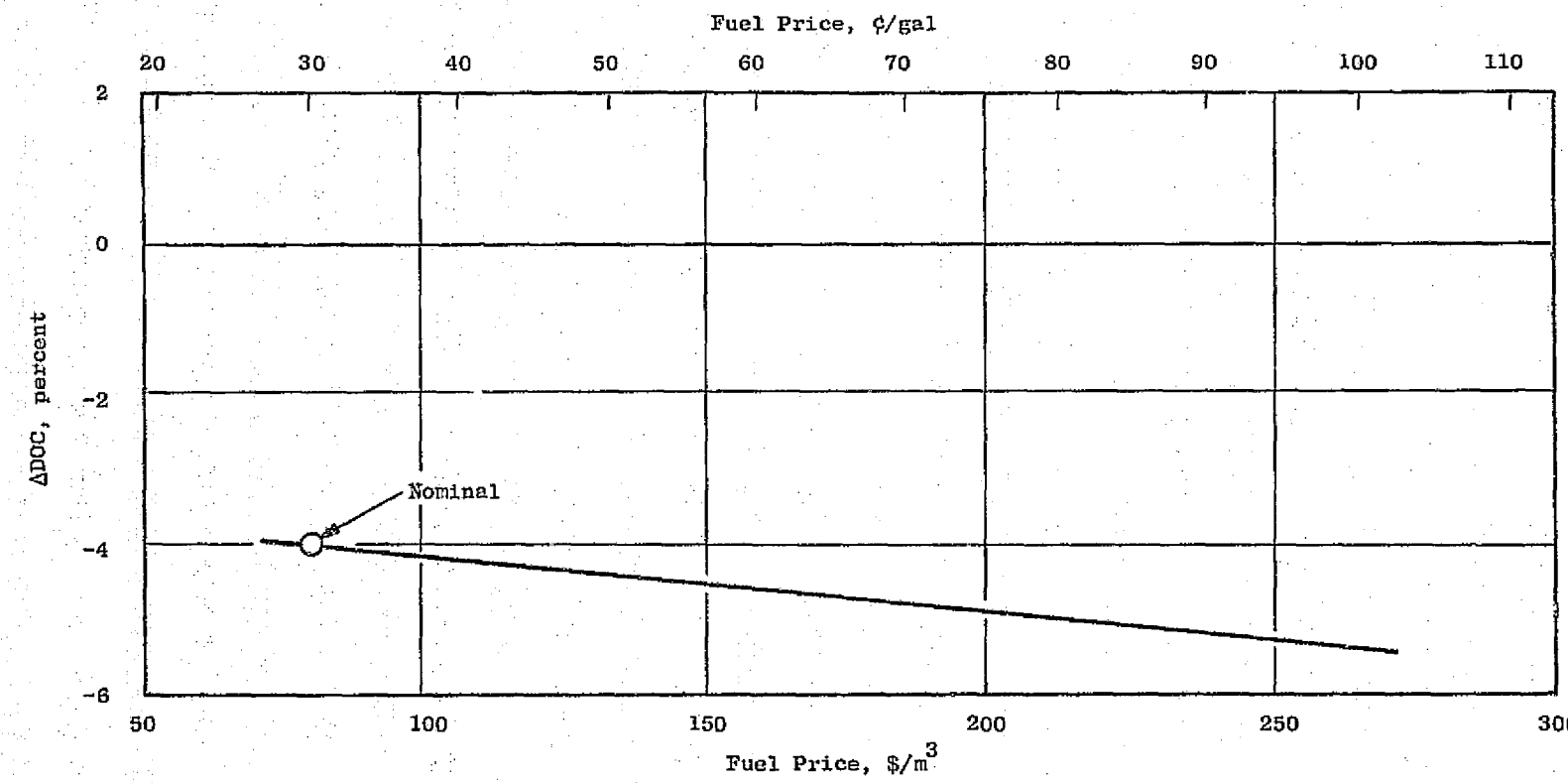

Figure 49. Sensitivity of Turboprop Engine Evaluation to Fuel Price.

Another area of uncertainty in evaluating the turboprop was the amount of cabin acoustic-shielding requirements. In this study 363 kg (800 lb) of shielding per aircraft was assumed based on the recommendation of Hamilton Standard as part of the subcontractor-supplied prop data. This penalty will be higher if the entire passenger compartment must be shielded. To give a "feel" for the impact, Figure 50 presents the sensitivity to variations in the shielding penalty.

5.4.6 Noise

Estimated noise levels for the turboprop are expected to meet FAR 36 with substantial margin. The estimated noise at takeoff is presented in Figure 51. Based on this figure, it is apparent that the dominant noise source is the propeller, with the turbine being second at a considerably lower level. The approach-noise data presented in Figure 52 indicates that, in terms of PNLT, the turbine is the dominant noise source. The combination of turbine-blade solidity and speed produces a high frequency source which, when converted to EPNL, was reduced to an acceptable level without treatment. Due to the high frequency of the booster noise, combined with the shielding effect of the inlet duct, inlet treatment was not required.

A noise source not included in the estimate was the effect of prop wash over the wing; this noise resulted from the added velocity behind the propeller. The ΔV due to the propeller would, however, have small effect on the total scrubbing noise; moreover, the isolated wing-scrubbing noise was a small contribution to the total-system, far-field noise at approach.

5.5 EVALUATION SUMMARY

Table LVI is a brief summary of the weight, cost, and maintenance cost per hour for each of the engines studied in Task II. The installed weights, costs, and maintenance are in the transcontinental mission size. Engines on the left are in the trijet aircraft; on the right, a quadjet aircraft. Engine size was defined so that an equitable comparison between the turbofan- and turboprop-powered aircraft could be made.

The summary shows that the installed weight, cost, and maintenance costs all increase for the three unconventional turbofans. The same is true for the turboprops, relative to the turbofan baseline, except for a modest maintenance-cost reduction. Installed sfc reductions were established for each of the engines in the refined evaluation.

The mission fuel, DOC, and ROI results obtained with the final design information of Table LVI are shown in Table LVII. The regenerative turbofan, at a fan pressure ratio of 1.55, is compared to the geared fan at the same fan pressure ratio (to factor-out propulsive efficiency effects). The results are given for the transcontinental and the intercontinental missions. Return of investment (ROI) is presented, in addition to DOC, according to standard economic procedures used in the STEDLEC study (Reference 1).

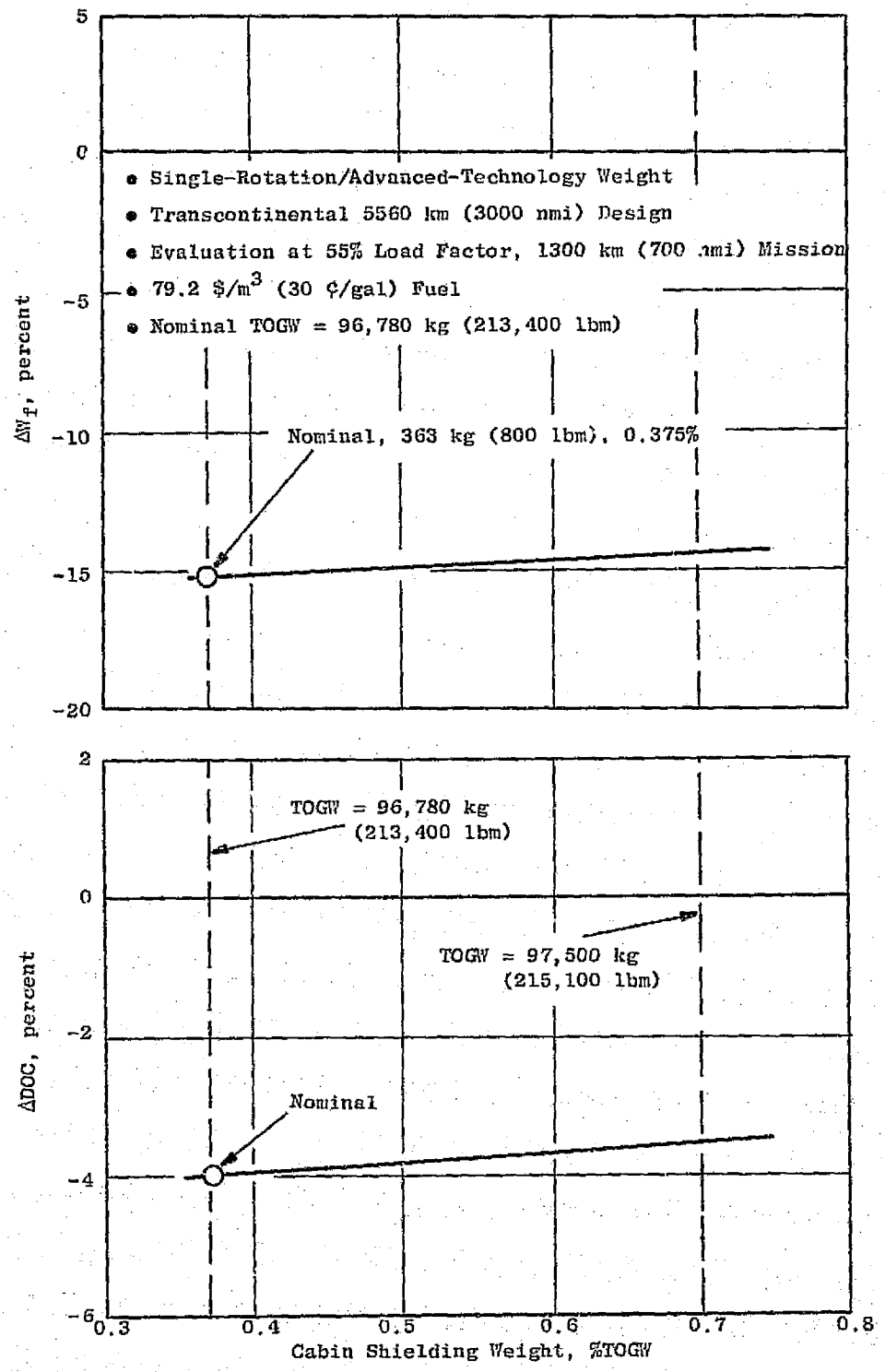

Figure 50. Sensitivity of Turboprop Engine Evaluation to Cabin Acoustic-Shielding Requirements.

- Four Engines, Transcontinental
- M = 0.26
- 488 m (1600 ft) Altitude at 6.5 km (3.5 nmi)
- TOGW = 102,060 kg (225,000 lbm)

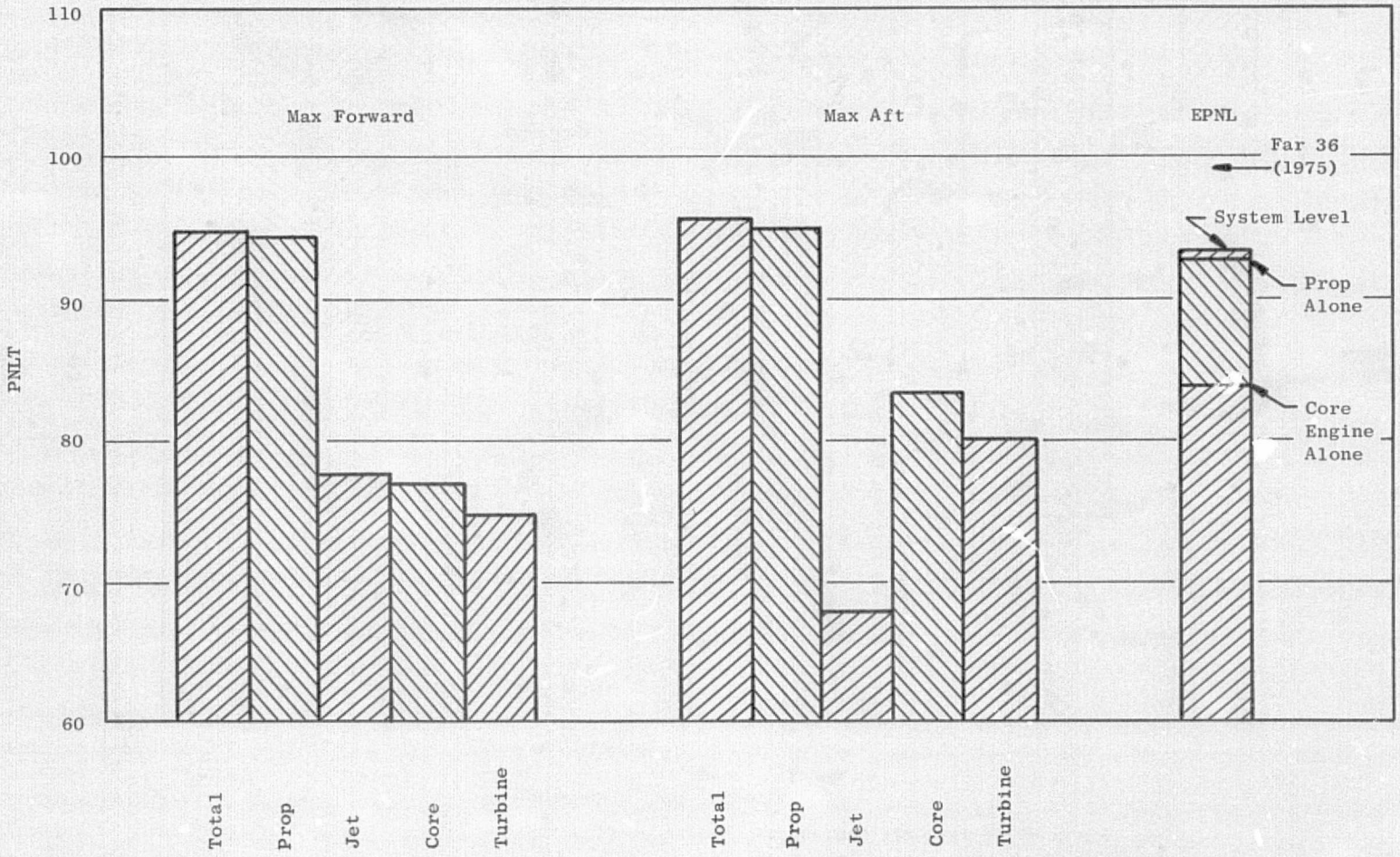

Figure 51. Turboprop Noise Levels: Takeoff Power (No Cutback).

- Four Engines, Transcontinental
- M = 0.22
- TOGW = 102,060 kg (225,000 lbm)
- Component Levels Do Not Include Aircraft-Alone Noise
- Approach F_n 32% Takeoff
- Flap Setting 35°

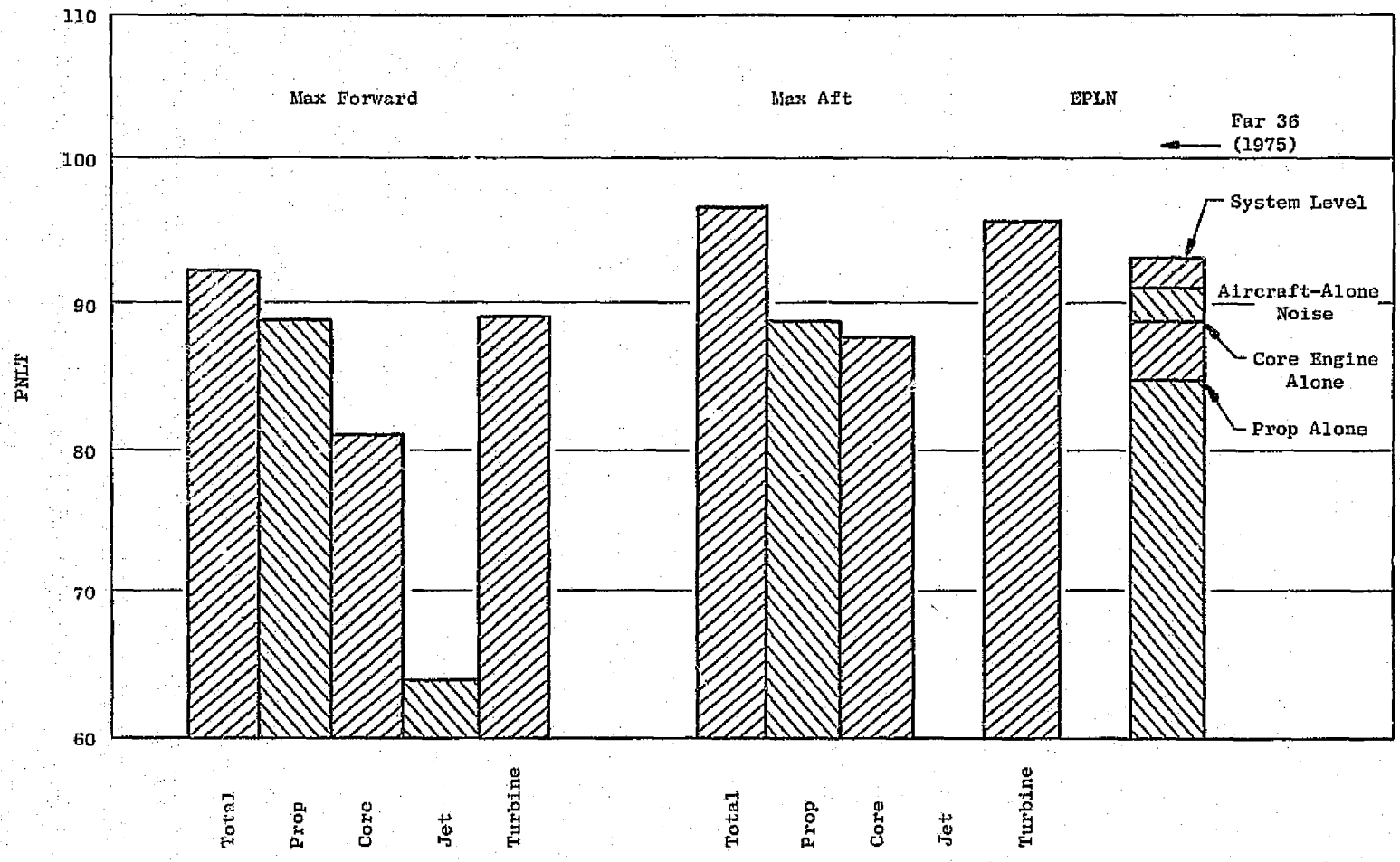

Figure 52. Turboprop Noise Levels: Approach Power.

Table LVI. Design Evaluation Summary.

Engine	Baseline Turbofan	Regenerative Direct-Drive Turbofan	Geared Turbofan	Geared Variable-Boost Turbofan	Baseline Turbofan	Turboprop	Variable-Boost Turboprop
Aircraft	Trijet	Trijet	Trijet	Trijet	Quadjet	Quadjet	Quadjet
Installed Engine Weight, kg (lbm)	1850 (4070)	3360 (7400)	2090 (4600)	2200 (4850)	1220 (2690)	1770 (3900)	1650 (3640)
% Installed Weight	100	182	113	119	100	145	135
% Installed Cost	100	139	109	112	100	108	108
% Maintenance Cost per hr	100	138	102	102	100	97	93
Installed sfc, Δ %	0	-8.2	-5.3	-6.6	0	-14.6	-15.6

Table LVII. Engine Evaluation Summary Results.

Unconventional Engine	Regenerator, Fan P/P 1.55		Geared Fan, Fan P/P 1.55		Variable-Boost[3] Geared Fan, Fan P/P 1.55		Turboprop, Single Rotation		Variable-Boost Turboprop, Single Rotation	
Reference Engine	Geared Fan Fan P/P 1.55		Direct Drive, Fan P/P 1.71		Geared Fan, Fan P/P 1.55		Direct Drive, Fan P/P/ 1.71		Turboprop, Single Rotation	
Mission	Trans-[1] continental	Inter-[2] continental	Trans-continental	Inter-continental	Trans-continental	Inter-continental	Trans-continental	Inter-continental	Trans-continental	Inter-continental
DOC, Δ %	+7.6	+8.7	-0.6	-1.9	-1.0	-1.4	-4.0	-5.2	-1.3	-2.0
ROI, Δ %	-2.9	-3.9	-0.1	+0.6	+0.3	+0.5	+0.6	+1.2	+0.5	+0.6
W_F, Δ %	+3.9	+5.2	-4.6	-6.1	-1.7	-2.2	-15.0	-13.7	-2.3	-3.1

(1) Transcontinental; 5560 km (3000 nmi)/200 PAX Design, 1300 km (700 nmi)/55% Load Factor, 79.2 $/m^3 (30 ¢/gal) Fuel

(2) Intercontinental; 10,190 km (5500 nmi)/200 PAX Design, 3700 km (2000 nmi)/55% Load Factor, 118.8 $/m^3 (45 ¢/gal) Fuel

(3) Cruise Sized

It is interesting to note that, for the geared fan, the ROI decreases slightly (undesirable direction) while the DOC is reduced. The reversal in the economic indicator can be explained by greater weighting of initial cost in the ROI versus fuel cost saved in later years.

The regenerator engine has fuel and DOC increases when compared to the 1.55 pressure ratio fan. The geared fan shows a fuel saving and a modest economic improvement. The turboprop has a large fuel saving and a DOC reduction. Because of the importance of the climb segment, where the turboprop sfc improvement is greater than at cruise, the turboprop fuel saving is greater for the transcontinental mission.

SECTION 6.0

SUMMARY OF TASK II RESULTS

A schematic layout of the interturbine rotary-regenerator engine and nacelle is shown in Figure 53, and the results of the evaluation are summarized in Table LVIII. As was the case in Task I, there was no significant benefit in fuel usage compared to the direct-drive turbofan and a penalty when compared to the geared turbofan of the same fan pressure ratio. It should also be pointed out that a significant advancement in technology is required to build such a regenerator.

A layout of the geared turbofan is shown in Figure 54 and the results of the evaluation, compared to the baseline engines, are summarized in Table LIX. An improvement in fuel usage of 4-1/2%, plus a small improvement in DOC, were estimated; therefore, this approach indicates sufficient potential for further consideration from a technology-development standpoint.

The results of the Task II evaluation of the variable-boost concept, as applied to both the geared turbofan and turboprop, are summarized on Table LX. The concept is of interest for aircraft which are sized by cruise-thrust requirements, rather than takeoff, since the variable-boost feature serves as a means of derating the engine at takeoff. Other methods of derating the engine at takeoff, such as reducing takeoff turbine inlet temperature, could also be considered; however, it is felt that the variable-boost approach is the more desirable in terms of sfc advantage.

A layout of the turboprop engine is illustrated in Figure 55, and a schematic layout of the installation is given in Figure 56. Results of the Task II turboprop evaluation are summarized in Table LXI. As in Task I, a large improvement in fuel usage was estimated for the 80% level of propeller efficiency. An improvement in DOC was also calculated, based on data available for the study; however, it should be pointed out that the turboprop evaluation results involve considerable uncertainty due to possible variations in the factors listed in Table LXII.

The overall conclusions of Study Unconventional Aircraft Engines Designed for Low Energy Consumption (SUAEDLEC) are summarized on Table LXIII. Technology-development effort is recommended to support the direct-drive turbofan, the geared turbofan, the turboprop, and variable-boost versions thereof. This approach retains the option to select any of these engines when such a selection becomes necessary.

- Scaled to Same F_n, 10,670 m (35,000 ft), Mach 0.8, +10° C (+18° F), Max. Climb

Bypass Ratio = 7
Fan Pressure Ratio = 1.55
Overall Cycle Pressure Ratio = 32
Effectivity = 0.9
Turbine Inlet Temperature = 1480° C (2700° F)
at Takeoff Power = 1540° C (2800° F)

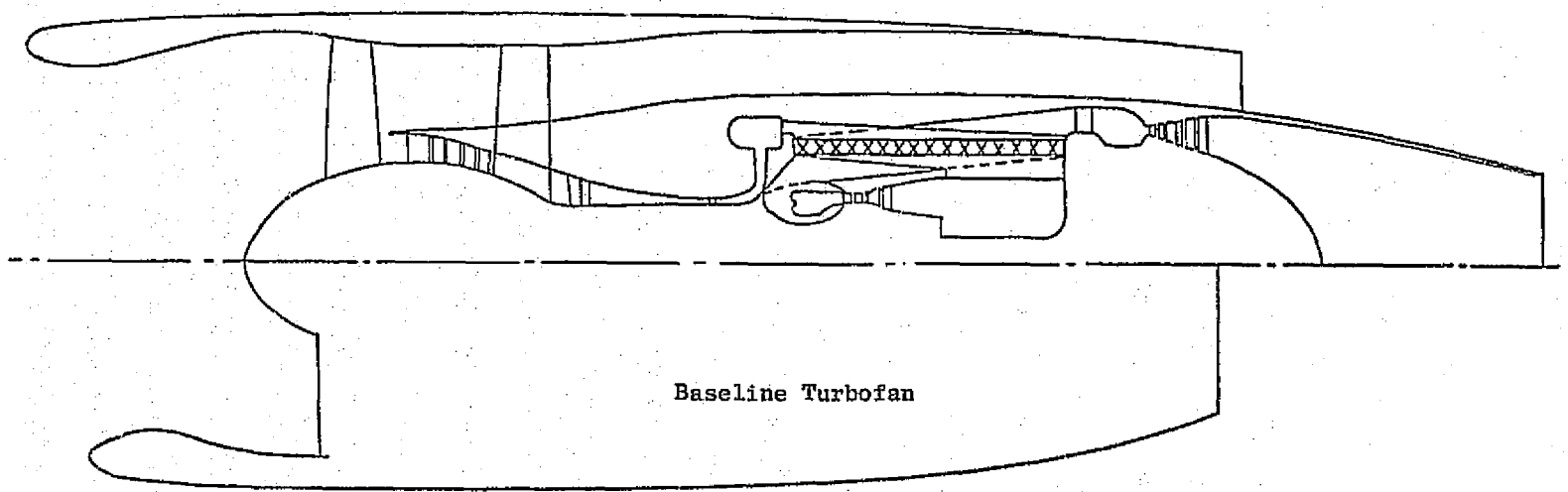

Figure 53. Installed Regenerator Engine Vs. Baseline Turbofan.

- 10,670 m (35,000 ft), Mach 0.8, +10° C (18° F), Max. Climb

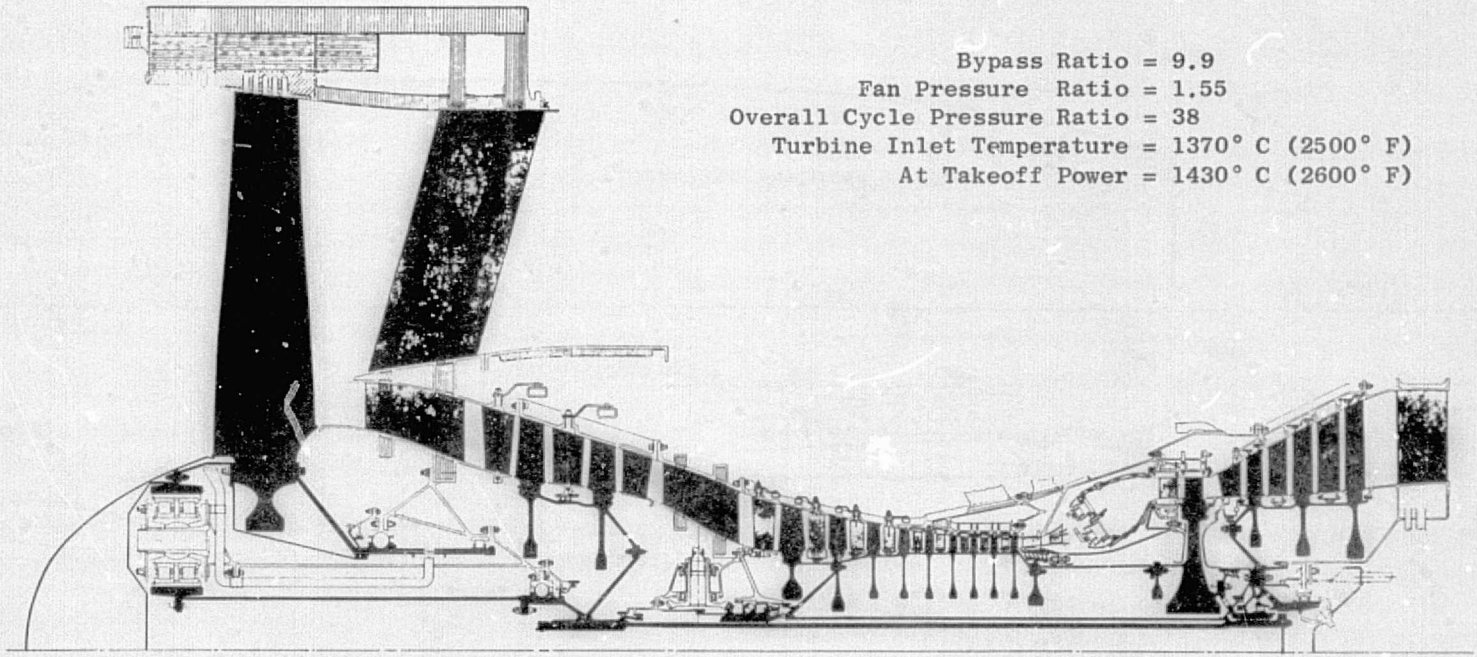

Figure 54. Geared Turbofan.

Table LVIII. Regenerative Turbofan Evaluation.

- Physical size of heat exchanger is limiting problem.
- Interturbine location is a way of circumventing size problem.
- Improvement in installed sfc: 8% vs. baseline turbofan.
- Weight increase: 46% vs baseline.
- Fuel usage: - 1/2% vs. baseline.
  +4% vs. geared turbofan at same fan pressure ratio.
- Economics: cost impact of regenerator and ducting results in increase in DOC compared to conventional turbofans.

Table LIX. Geared Turbofan Evaluation.

•	Performance	- Allows higher bypass ratio Without excessive LPT stages.
		- Provides high LP spool efficiencies.
		- Improvement in installed sfc: 5% versus baseline.
•	Installed	- Increase of 11%, primarily larger fan effect.
•	Fuel Usage	- Improvement of 4-12% (transcontinental mission).
•	Economics	- Improvement in DOC of 1/2% estimated.
•	Technical Risk	- Advanced bearings and gear material technology.
		- Mechanical design of gearset into engine.
		- LP aerodynamic components relatively straightforward.

Table LX. Variable Boost Evaluation.

•	Performance	- Allows higher cycle pressure ratio to be used at cruise without exceeding baseline-engine levels at takeoff. - Improvement in sfc of 1+% vs. nonvariable-boost turboprop. - Results in 12% lower takeoff thrust for given cruise thrust.
•	Engine Weight and Cost	- At least equal to nonvariable-boost engine sized to same cruise thrust.
•	Concept is advantageous for advanced aircraft which tend to require higher cruise-to-takeoff thrust ratios than current high bypass engines.	
•	Concept is appropriate for higher bypass turbofan and turboprop which have higher takeoff thrust than conventional turbofan (sized for given cruise thrust).	
•	Concept must be compared with other approaches of derating engines at takeoff.	

Table LXI. Turboprop Evaluation.

•	High disc-loading propeller has 20% propulsive efficiency advantage at M = 0.8.	
•	Installed sfc improvement*:	13% vs. baseline turbofan. 8% vs. geared turbofan.
•	Installed weight increase:	45% vs. baseline turbofan.
•	Fuel-usage advantage*:	15% vs. baseline, transcontinental. 10% vs. geared turbofan.
•	Economics:	Improvement in DOC estimated on simple basis but subject to large uncertainty.

*Using Hamilton Standard estimate of propeller efficiency: 0.815 at 95% max. cruise.

- 10,670 m (35,000 ft), Mach 0.8, +10° C (18° F), Max. Climb

Cycle Pressure Ratio = 38
Turbine Inlet Temperature = 1370° C (2500° F)
At Takeoff Power = 1430° C (2600° F)

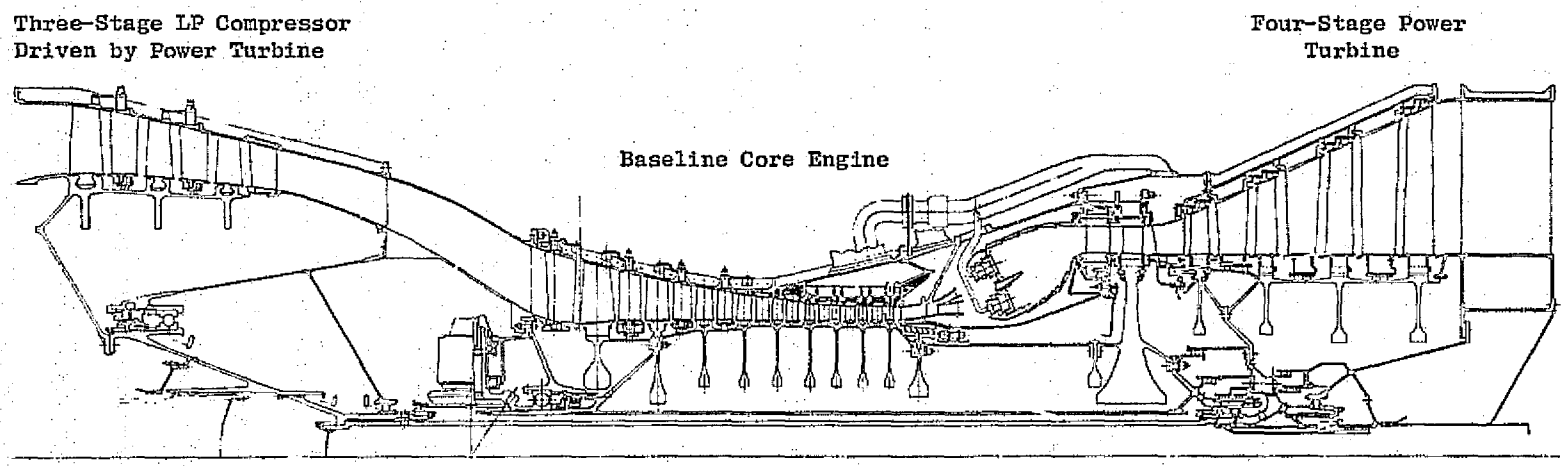

Figure 55. Turboprop Engine.

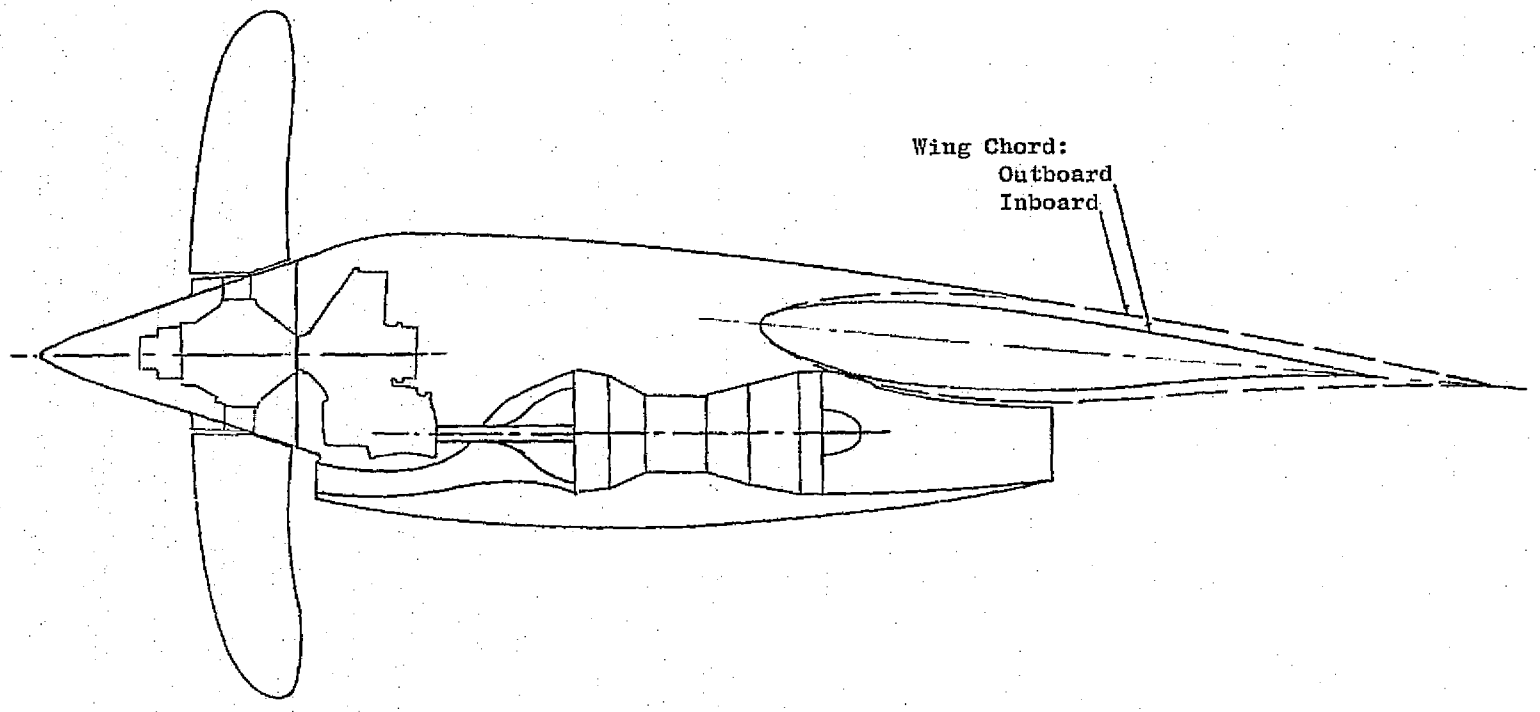

Figure 56. Turboprop Installation.

Table LXII. Turboprop Uncertainties.

- Level of efficiency achievable in a practical mechanical design of propeller.
- Integration between propeller installation and swept-wing aerodynamics.
- Design of propeller installation and wing; weight impact.
- Cabin noise suppression required.
- Level of turboprop propulsion system price (relative to turbofan).
- Maintenance costs of propeller, variable-pitch system, and gearset.

Table LXIII. Conclusions.

- Geared turbofans;
  - Advantage in fuel usage of 5% vs. direct-drive turbofan.
  - Economic advantage relatively small.
  - Further consideration recommended.
- Variable boost:
  - Advantageous for application requiring high cruise-to-takeoff thrust.
  - Further consideration recommended.
- Regeneration does not have a payoff for subsonic transport engines.
- Turboprops (for 0.8 Mach no.):
  - Fuel-usage advantage of 10 to 15% estimated, dependent upon successful development of 80% propeller efficiency.
  - Economic advantage subject to uncertainity.
  - Study by aircraft companies recommended.

SECTION 7.0

TASK III TECHNOLOGY RECOMMENDATIONS

Technology development is required across a broad front to achieve a substantial improvement in economics and energy consumption over current, high bypass turbofans. The technology requirements, and the corresponding mission payoff, of specific technology features were identified in Reference 1 and 2 for conventional turbofan engines. Although the specific designs may be different, most of the technology identified is applicable to the unconventional engines (the geared turbofan, the turboprop, and variable-boost versions of these engines) recommended for further consideration in this study.

The key core technology needs are summarized in Table LXIV. The core technology is directly applicable to all three of the engine concepts recommended herein; indeed, the identical core design could be used for a variety of engines with the resulting thrust size dependent upon the specific design and ratings. In any event, early attention to core technology is recommended. Much of this technology will also be applicable to new models of current engines.

The key technology needs for basic turbofan-engine design are summarized in Table LXV. The LP spool technology required for the geared turbofan is relatively straightforward except for the gearset itself. It is recommended that programs pertinent to both the geared and direct-drive fans be pursued in order to provide input to assist when the selection must be made.

The key technology needs in the area of turbofan systems and installations are summarized in Table LXVI. This technology is useful for a variety of engines, including new models of current engines, although the specific designs required will differ. This technology should be pursued as a part of a broad NASA air-breathing engine technology program.

Turboprops require large advancements in technology to provide the gains in aircraft economics and fuel usage indicated in this study; Table LXVII lists the most important technology items. Initial effort is recommended on the development of 80% propeller efficiency for a practical Mach 0.8 design. Since the propeller and its installation have a major effect upon the aircraft design, more detailed studies by aircraft companies are recommended in order to establish what technology levels are required of an advanced-turboprop system. If results from these initial programs are favorable, further effort would be justified. The development of lightweight acoustic shielding for cabins is also recommended as part of this initial effort.

Table LXIV. Key Core Technology Needs for Energy-Efficient Engines.

- Applicable to all Engines of Identified Interest

• Advanced Turbofan Compressor	- High Efficiency - Rugged Design - Simple, Compact Layout
• Single-Stage Core Turbine	- Improved Efficiency
• Combustor	- Emissions
• Materials and Processes	- Improved Blade Materials at Reasonable Cost - Ceramics Exploration - Low Cost Processes
• Clearance Control	- Low Expansion Materials - Improved Coatings and Shroud Materials - Active Cooling Concepts - Self-Acting Seals

Table LXV. Key Turbofan Technology Needs for Energy-Efficient Engines.

• Composites: Fan Blades, Frame, and Case	- Weight - Cost - Safety (Blades)
• High Tip-Speed Fan for Direct-Drive Turbofan	- Efficiency - Compatibility with Composites
• Highly Loaded LPT for Direct-Drive Turbofan	- Efficiency - Compatibility with Cooling
• Advanced Gear Technology*	- Bearing and Gear Materials - Integrated Design
• Boosters	- Variable-Boost Approach

*Input to Choice of Geared vs. Direct-Drive Fan

Table LXVI. Key Turbofan Installation and Systems Technology Needs for Energy-Efficient Engines.

• Long-Duct, Mixed Flow	- Improved, Low Loss Mixing
• Integrated Composite Nacelle	- Weight and Cost Reduction
• Advanced Reverser	- Cost and Weight Reduction
• Noise Reduction Technology	- More Effective Treatment
• Advanced Digital Control Systems	- Flexibility
• Preliminary Design and Systems Study	- Guidance and Evaluation

Table LXVII. Turboprop Technology for Mach 0.8 Transports.

Initial Programs

- Propeller: Basic Efficiency Level
- Studies of Aircraft Design and Economics (to Establish Technology Goals)
- Propeller Noise and Lightweight Cabin Shielding

Follow-on Programs

- Integration of Propeller with Aircraft Aerodynamics
- Propeller (Structural)
- Two-Stage Gear Technology

SECTION 8.0

NOMENCLATURE/SYMBOLS

AA	Annulus area
AR	Aspect ratio
B_{10}	Length of time in which 10% of the parts fail
C&A	Controls & Accessories
C_L	Lift coefficient
D	Diameter, meters (feet)
DHL, D_{HL}	Inlet highlight diameter, meters (feet)
$D_{Max.}$	Nacelle maximum diameter, meters (feet)
D_T	Fan tip diameter, meters (feet)
DOC	Direct operating cost
EPNL	Effective perceived noise level, dB
F	Thrust, newtons (lbf)
F_n	Net thrust, newtons (lbf)
F_{n_I}	Installed net thrust, newtons (lbf)
F_n/W_2	Specific thrust, newtons/kg (lbf/lbm)
HP	High pressure
HPC	High pressure compressor
HPT	High pressure turbine
L/D	Lift/drag ratio
L&M	Labor and material
LF	Load factor
LP	Low pressure
LPC	Low pressure compressor
LPT	Low pressure turbine

M	Mach number
Maint./M.H.	Maintenance in man hours
N_B	Number of blades
NO_x	Nitric oxide and nitrous oxide
P	Pressure, newtons/meter^2 (lbf/in.^{2})
P/P	Pressure ratio
PAX	Passenger
PI	Replacement parts/new parts ratio
PNLT	Perceived noise level total, dB
P_3	Compressor discharge pressure newtons/meter^2 (lbf/in.^{2})
r	Radius, meters (feet)
r_H	Hub radius, meters (feet)
r_T	Tip radius, meters (feet)
ROI	Return on investment
sfc	Specific fuel consumption, kg/newton-hr (lbm/lbf-hr)
sfc_I	Installed specific fuel consumption, kg/newton-hr (lbm/lbf-hr)
SLS	Sea level standard
T	Temperature, ° C (° F)
TF	Turbofan
TOBFL	Takeoff balance field length
TOGW	Takeoff gross weight
TP	Turboprop
To or T_o	Ambient Temperature, ° C (° F)
T_4, T_{41}	High pressure turbine inlet temperature ° C (° F)
U_T	Tip speed, m/sec (ft/sec)
$U_T/\sqrt{\theta}_2$	Corrected tip speed, m/sec (ft/sec)
VP	Variable pitch

W_f	Fuel flow, kg/sec (lbm/hr)
$W\sqrt{\theta}/\delta$, $W_2\sqrt{\theta}/\delta$	Engine inlet airflow, kg/sec
$W\sqrt{\theta}/\delta$ - AA	Corrected inlet airflow per annulus area, kg/sec-m^2 (lbm/hr-ft^2)
W_2	Engine inlet mass flow, kg/sec (lbm/sec)
W_{2C}	High pressure compressor inlet flow kg/sec (lbm/sec)
$W_{2C}\sqrt{\theta}/\delta$	Compressor inlet airflow kg/sec (lbm/hr)
W/W_{2C} HPT	HPT Cooling and leakage flow, %
W/W_{2C} LPT	LPT Cooling and leakage flow, %
W_{B1}	Intermediate compressr bleed, %
β	Bypass ratio
Δ	Delta, difference
ΔH	Enthalpy change, joules/kg (Btu/lb)
ΔT_o	Difference from ambient temperature, ° C (° F)
δ	P.14.696
ϵ	Effectiveness
η	Efficiency
η_{TT}	Turbine efficiency
θ	T/518.7
$\overline{\psi}$	Turbine blade loading parameter
$\overline{\psi}_P$	Mean loading of turbine stage.

SECTION 9.0

REFERENCES

1. Neitzel, R.E., Hirschkron, R., and Johnston, R.P., NASA CR135053, "Study of Turbofan Engines Designed for Low Energy Consumption." Prepared under contract No. NAS3-19251 by General Electric Co.

2. Neitzel, R.E., and Dugan, J., "Technology Requirements for Advanced Energy Conservative Turbofans," SAE Paper No. 751083, November 1975.

3. Rohrbach, C., and Metzger, F.B., "The Prop Fan - A New Look in Propulsion," AIAA Paper No. 75-1208, October 1975.

4. "Fuel Conservation Possibilities for Terminal Area Compatible Aircraft," NASA CR-132608, prepared under Contract No. NAS1-12018 by Boeing Commercial Airplane Co., March 1975.

5. QCSEE Preliminary Analysis and Design Report, Vol. I, NASA CR-134838, General Electric AEG, October 1974.